2009

Analysis of Cystic Kidney Disease-Related Genes in Caenorhabditis Elegans

Corey L. Williams
University Of Alabama At Birmingham

ANALYSIS OF CYSTIC KIDNEY DISEASE-RELATED GENES IN *CAENORHABDITIS ELEGANS*

by

COREY L. WILLIAMS

BRADLEY K. YODER, MENTOR
P. DARWIN BELL
GUILLERO MARQUES
MICHAEL A. MILLER, COMMITTEE CHAIR
ERIK M. SCHWIEBERT
ELIZABETH S. SZTUL

A DISSERTATION

Submitted to the graduate faculty of The University of Alabama at Birmingham,
in partial fulfillment of the requirements for the degree of
Doctor of Philosophy

BIRMINGHAM, ALABAMA

2009

ANALYSIS OF CYSTIC KIDNEY DISEASE-RELATED GENES IN CAENORHABDITIS ELEGANS

COREY L. WILLIAMS

CELL BIOLOGY

ABSTRACT

Cilia are evolutionarily conserved, membrane-bound, microtubule-based organelles found on a diverse array of cell types in eukaryotic organisms. Inherited diseases of cilia protein dysfunction include Nephronophthisis (NPHP), Joubert Syndrome (JBTS), Meckel-Gruber Syndrome (MKS), and Bardet-Biedl Syndrome (BBS). Important insight in the basic cell biological functions of BBS and NPHP proteins has been gained from analysis in the nematode *Caenorhabditis elegans*. My goal in this dissertation was to model MKS protein function in cilia biology utilizing the powerful genetic malleability of *C. elegans*. *mks-1* and *mks-3*, the *C. elegans* homologs of two MKS-associated proteins in humans, were selected for this analysis. MKS-3 is a transmembrane protein of unknown function, and MKS-1 is a protein comprised of an uncharacterized motif called the B9 domain. Because the B9 domain is found in only two other proteins in *C. elegans* (and most other eukaryotes), the B9 proteins TZA-1 and TZA-2 were also included in this analysis. Lastly, the *C. elegans* homologs of NPHP proteins NPHP-1 and NPHP-4 were also analyzed in conjunction with the MKS/TZA proteins. Utilizing mutations in each of the genes encoding these proteins, we were able to develop a model in which the MKS/B9 proteins and the NPHP proteins form independent but functionally related complexes at the base of *C. elegans* cilia. Disruption of either complex alone by genetic mutation did not hinder cilia formation. However, simultaneous disruption of both complexes resulted in severe ciliogenesis defects. This functional requirement of either the

MKS/B9 or the NPHP complex for cilia formation indicates that the two protein complexes serve similar yet distinct roles in maintaining cilia homeostasis. In the absence of a functional MKS/B9 complex, transmembrane proteins that normally localized only to the base of cilia (or just outside of the ciliary base) freely accessed the entire ciliary membrane. This data supports a model in which the MKS/B9 complex regulates ciliary membrane composition by selectively holding some transmembrane proteins at the base of cilia while blocking other transmembrane proteins from accessing the cilium. Overall, this dissertation provides insight into the related but distinct functions of MKS/B9 and NPHP proteins in cilia biology.

DEDICATION

My parents Carol C. Williams and Donald L. Williams

ACKNOWLEDGMENTS

I would first like to thank my graduate studies mentor, Dr. Bradley K. Yoder, for accepting me into his group and allowing me the time to figure out for myself what it takes to become a productive scientist. Our student-mentor relationship and our friendship has been outstanding. He has bestowed upon me almost as many scientific assets as he has dealt me defeats in darts.

I would also like to thank my committee members, Dr. Guillermo Marques, Dr. Michael A. Miller, Dr. Erik M. Schwiebert, Dr. Elizabeth S. Sztul, and Dr. P. Darwin Bell. I especially thank Dr. Bell and Dr. Tino Unlap for giving me the opportunity to develop a passion for academic research by hiring me as a technician. Through them, I was also first exposed to the research being conducted by Dr. Yoder's group.

I would like to thank current members of the Yoder lab, Dr. Nicolas F. Berbari, Dr. Neeraj Sharma, Dr. Zoe Verney, Svetlana Masyukova, Zak Kosan, Erica Hamby, Venus Roper, Mandy Croyle (who I believe is the smartest and hardest worker in the lab), and Amber O'Connor (who deserves extra special recognition for being the only person outside of my committee to actually read this dissertation).

I would like to thank former members of the Yoder lab, Dr. Courtney Haycraft, Dr. James Davenport, Dr. Jonathan M. Lehman, Dr. Boglarka Banizs, Dr. Jenny C. Schafer, and Dr. Marlene E. Winkelbauer. I especially thank Dr. Schafer for her guidance during my time as a rotation student. I also especially thank Dr. Winkelbauer, first for laying the groundwork that made my research project possible, and second, for being

my partner in crime on countless scientific misadventures. May we share many more successes and failures together in the future.

I would like to thank my friends and family for their support over these past four years. I thank Dr. Brian Siroky for demonstrating that being a graduate student could be fun. I thank my parents, the brilliant Carol and Don Williams, for supporting me as I made my own career choices. Even armed with a Ph.D., I doubt I'll ever beat either in a game of Scrabble. I thank my in-laws, Gene and Pam Smith, for their amazing generosity. Finally, I would like thank my wife, Candace Williams, for her unwavering support.

TABLE OF CONTENTS

Page

TABLE OF CONTENTS (Continued)

Page

LIST OF TABLES

Table *Page*

INTRODUCTION

FUNCTIONAL REDUNDANCY OF THE B9 PROTEINS AND NEPHROCYSTINS IN CAENORHABDITIS ELEGANS CILIOGENESIS

LIST OF FIGURES

Figure *Page*

INTRODUCTION

FUNCTIONAL REDUNDANCY OF THE B9 PROTEINS AND NEPHROCYSTINS IN CAENORHABDITIS ELEGANS CILIOGENESIS

LIST OF FIGURES (Continued)

REGULATION AND FUNCTION OF MKS-3 IN CAENORHABDITIS ELEGANS

LIST OF ABBREVIATIONS

3D	Three-dimensional
ACIII	adenylate cyclase III
ADP	adenosine diphosphate
ADPKD	Autosomal Dominant Polycystic Kidney Disease
AHI1	Abelson helper integration site 1
AP-1	activator protein 1
ARL	ADP-ribosylation factor-like
B9D	B9 domain
BBS	Bardet-Biedl Syndrome
BLAST	Basic Local Alignment Search Tool
CC2D2A	coiled-coil and C2 domains-containing protein 2A
cDNA	complementary DNA
C. elegans	*Caenorhabditis elegans*
CEP290	centrosomal protein 290
CFP	cyan fluorescent protein
CHE	abnormal chemotaxis
COACH	Cerebellar vermis hypo/aplasia, Oligophrenia, Congenital Ataxia, ocular Coloboma, and Hepatic fibrosis
CORS	Cerebello-Oculo-Renal Syndrome
CPK	congenital polycystic kidney
DAF	abnormal dauer formation
DNA	deoxyribonucleic acid

DsRed	Discosoma sp. red fluorescent protein
DYF	abnormal dye-filling
EMS	ethyl methanesulfonate
ER	endoplasmic reticulum
ESRD	end stage renal disease
GFP	green fluorescent protein
GLI	glioma-associated oncogene
GLIS2	GLI-similar 2
HGRS-1	Hepatocyte growth factor-regulated tyrosine kinase sub-strate 1
ICIS-1	involved in cilia stability 1
IFT	intraflagellar transport
IGF	insulin growth factor
INV	inversion of turning
IQCB1	IQ motif-containing protein B1
JBTS	Joubert Syndrome
JCK	juvenile congenital kidney
KAP3	kinesin associated protein 3
KIF3A	kinesin family member 3A
LOV	abnormal location of vulva
MKS	Meckel-Gruber Syndrome
MTOR	mammalian target of rapamycin

NEK8	never in mitosis kinase 8
NIH	National Institute of Health
NPHP	nephronophthisis
ORNL	Oak Ridge National Laboratory
ORPK	Oak Ridge Polycystic Kidney
OSM	osmotic avoidance abnormal
PCK	polycystic kidneys mouse
PCM	pericentriolar material
PCR	polymerase chain reaction
PCY	polycystic kidney disease mouse
PKD	polycystic kidney disease
P. tetraurelia	*Paramecium tetraurelia*
RCC1	regulator of chromosome condensation
RD16	retinal degeneration 16
RFX	regulatory factor binding to the X-box
RNA	ribonucleic acid
RNAi	RNA interference
RPGR	retinitis pigmentosa GTPase regulator
RPGRIP	retinitis pigmentosa GTPase regulator interacting protein 1
RPGRIP1L	retinitis pigmentosa GTPase regulator interacting protein 1-like
RT-PCR	reverse transcription PCR

SDS	sodium dodecyl sulfate
SEM	standard error of the mean
SH3	src homology 3
siRNA	small interfering RNA
SLSN	Senior Løken Syndrome
S. purpuratus	*Strongylocentrotus purpuratus*
STAM-1	signal-transducing adaptor molecule 1
tdTomato	tandem Tomato
TMEM67	transmembrane protein 67
TRAM-1	translocating chain-associating membrane protein transporter 1
TPR	tetratricopeptide
TZA	transition zone-associated
UNC	uncoordinated
WPK	Wistar polycystic kidney
XBX	X-box promoter regulated
YFP	yellow fluorescent protein

INTRODUCTION

Inherited Cystic Kidney Diseases

A significant number of clinically defined human disorders are characterized by the formation of cysts in the kidney. A subset of those disorders caused by genetic defects will be discussed here: Autosomal Dominant Polycystic Kidney Disease (ADPKD) and a group of related autosomal recessive diseases, Meckel-Gruber Syndrome (MKS), Nephronophthisis (NPHP), Senior-Løken Syndrome (SLSN), Joubert Syndrome Type B (JBTS), and Bardet-Biedl Syndrome (BBS) (see Figure 1). Among these disorders, which are caused by both overlapping and nonoverlapping loci, there is wide variability in renal and extrarenal pathologies. For example, some NPHP patients are not affected until young adulthood when renal cysts first emerge while MKS patients die soon after birth due to the combination of renal failure and developmental defects. The overlapping of loci across diseases also indicates that the severity of pathology in these patients depends on the particular nature of a given mutation. Additionally, variability in disease severity can be influenced by background mutations in an individual's genome that genetically modify the disease gene.

Autosomal Dominant Polycystic Kidney Disease. ADPKD is a disease that affects up to 1 in 400 individuals and is defined by pathologies associated with enlarged kidneys containing cysts of variable size between a few millimeters to 20 centimeters in diameter (Torres et al., 2007; Wilson, 2004). Symptoms of ADPKD emerge in adulthood, and these patients normally progresses to end stage renal disease (ESRD) in the third decade of life and later (Chapman, 2007). Two genes have been linked to ADPKD,

Pkd1 and *Pkd2*. Mutations in *Pkd1* are common as disruption of this gene is responsible for roughly 85% of all cases of ADPKD. *Pkd1* encodes polycystin-1, a transmembrane receptor, while *Pkd2* encodes polycystin-2, a calcium permeable ion channel. These two proteins colocalize to cilia on renal tubule epithelia (Yoder et al., 2002). Polycystin-1 and polycystin-2 are thought to function as a complex interacting through coiled-coil motifs in their c-terminal tails (Qian et al., 1997; Tsiokas et al., 1997). Mutations in the PKD genes do not disrupt cilia structure but do result in the loss of a flow-regulated mechano-sensitive calcium signal, and in the case of polycystin-1, altered AP-1 pathway activation and increased mTOR activity (Low et al., 2006; Shillingford et al., 2006). The mechanisms by which these disruptions ultimately lead to renal cyst formation are still under investigation. The current model holds that the polycystins function as mechanosensors that detect fluid movement through the renal tubules and regulate calcium signaling responses within the cell.

Meckel-Gruber Syndrome. MKS is an autosomal recessive perinatal lethal disorder defined by not only renal cysts but also by severe developmental defects including polydactyly and occipital encephalocele (Reviewed in Alexiev et al., 2006). Unlike ADPKD, the underlying genetic defect has not been identified in a large portion of MKS patients, but currently there are six loci associated with the disease, *MKS1* through *MKS6* (see Table 1). Of these six, all but the *MKS2* locus have been linked to a specific gene; however, the roles of the proteins encoded by these genes are not fully understood.

A broad spectrum of *MKS1* mutations have been identified in various families, many of which result in protein truncation (Dawe et al., 2007b; Frank et al., 2007; Kyt-

tala et al., 2006). Recently, several predicted hypomorphic *MKS1* mutations were found in BBS families (Leitch et al., 2008). Interestingly, Leitch et al. demonstrated with zebrafish morpholinos that these hypomorphic *MKS1* alleles could exacerbate the severity of BBS-related phenotypes. The *MKS1* gene product MKS1 contains a B9 domain that has not been investigated and is found in only two other human proteins, B9D1 and B9D2. MKS1 as well as the two other B9 proteins are found in the cilia/basal body proteome database (Gherman et al., 2006). Dawe et al. reported the localization of mouse MKS1 to centrosomes and basal bodies in cell culture (Dawe et al., 2007b). Recently, murine B9D2 was also visualized at basal bodies (Town et al., 2008). In the same study, Town et al. showed that disruption of *B9D2/stumpy* manifested cystic kidney and hydrocephalus phenotypes, suggesting that the B9 family of proteins may share similar functions.

Positional cloning of the *Wpk* locus in the Wistar Polycystic Kidney rat identified a mutation in the gene encoding TMEM67, a transmembrane protein with predicted topological similarity to the frizzled family of receptors (Smith et al., 2006b). Subsequent screening of human *TMEM67* in MKS families uncovered a variety of mutations and thus confirmed this gene as *MKS3* (Smith et al., 2006b). *MKS3* mutations most frequently disrupt the large n-terminal extracellular domain of the protein, but mutations affecting the transmembrane domains and the c-terminal cytoplasmic tail also exist (Frank et al., 2007). Unlike the majority of *MKS1* mutations, which are truncating, *MKS3* lesions include missense, nonsense, frameshift, and splice site mutations (Frank et al., 2007). Accordingly, disease severity widely varies across the population of *MKS3* patients. Interestingly, the breadth of mutations and phenotypes was made more evident

with the identification of *MKS3* mutations in patients diagnosed with Joubert Syndrome, and more recently, COACH Syndrome, two clinically distinct but phenotypically related diseases (Baala et al., 2007b; Brancati et al., 2008; Consugar et al., 2007). It was demonstrated by Dawe et al. that MKS3 localizes to basal bodies and cilia and is found in a protein complex also containing MKS1. In the same study, knockdown of either *MKS1* or *MKS3* message by siRNA inhibited cilia formation in inner medullary collecting duct cell culture (Dawe et al., 2007b).

Nine distinct mutations in the fourth MKS gene, *CEP290*, were first identified in a combined cohort of patients diagnosed with either JBTS, NPHP, or SLSN (NPHP plus retinal degeneration) (Sayer et al., 2006). Additional *CEP290* mutations were later discovered in MKS families, qualifying the gene as a *bona fide MKS* locus. (Baala et al., 2007a; Frank et al., 2008). *CEP290* mutations might also be responsible for some cases of BBS, but evidence supporting this claim by Leitch et al. was limited to one BBS family with a homozygous nonsense mutation that truncated the c-terminal end of the protein (Leitch et al., 2008). Interestingly, no strong correlation between the nature of *CEP290* mutation and phenotype has been identified, indirectly suggesting that genetic background may play an important part in modifying *CEP290*-associated disease pathology (Frank et al., 2008). *CEP290* encodes a protein that localizes to basal bodies, interacts with Retinitis Pigmentosa GTPase Regulator Interacting Protein 1 (RPGRIP1), and is in complex with dynactin subunits $p150^{Glued}$ and p50-dynamitin, kinesin subunit KIF3A, kinesin-associated protein (KAP3), γ-tubulin, PCM1, centrin, pericentrin, and ninein (Chang et al., 2006). Knockdown of *CEP290* message by siRNA compromised ciliogenesis in cell culture and abrogated Rab8 localization to the cilium (Kim et al., 2008).

In the *rd16* mouse, which harbors a hypomorphic *CEP290* mutation, morphology of olfactory cilia was unaltered, but ciliary localization of the G proteins $G_{\gamma 13}$ and G_{olf} was disrupted (McEwen et al., 2007).

The *MKS5* locus further connects MKS, JBTS, and NPHP as distinct mutations in this gene have been identified in all three diseases (Arts et al., 2007; Delous et al., 2007). *MKS5* encodes the basal body protein Retinitis Pigmentosa GTPase Regulator Interacting Protein 1-Like (RPGRIP1L) that interacts with nephrocystin-4/NPHP4 (Roepman et al., 2005).

Most recently, MKS-causing mutations were identified in *CC2D2A*, marking this gene as the sixth MKS locus (Tallila et al., 2008). Previously, *CC2D2A* was linked to autosomal recessive mental retardation and retinitis pigmentosa, implicating a potential role of the gene in inherited cystic kidney diseases (Noor et al., 2008). *CC2D2A* mutations were later identified in JBTS families (Gorden et al., 2008). *CC2D2A* encodes a protein that contains a coiled coil domain and a calcium-binding C2 domain and directly binds CEP290 (Gorden et al., 2008). Gorden et al. also demonstrated that fluorescent-tagged CC2D2A localized to basal bodies in retinal pigment epithelial cells. Tallila et al. showed in preliminary studies that *MKS6* fetuses may have cilium structure abnormalities (Tallila et al., 2008).

Nephronophthisis. Pathologies associated with the autosomal recessive disorder NPHP include the formation of corticomedullary cysts, disruption of tubular basement membrane, tubulointerstitial nephropathy, and sometimes retinal defects (reviewed in Hildebrandt and Zhou, 2007). Distinct from the cysts of variable size in the enlarged

kidneys of ADPKD patients, NPHP cysts are small and found only at the border between the cortex and the medulla of the kidneys (Hildebrandt and Omram, 2001; Hildebrandt and Otto, 2000). Onset of NPHP symptoms range from soon after birth through early adulthood, and patients eventually develop ESRD.

To date, nine genetic loci (*NPHP1-9*) have been identified in these patients (see Table 2). The *NPHP1* gene is disrupted in roughly 25% of NPHP patients and encodes an SH3 domain/coiled coil protein (NPHP1) that interacts with p130cas, tensin, filamin A and B, focal adhesion kinase 2, PACS-1, NPHP2, and NPHP4, and is in complex with NPHP3 (Benzing et al., 2001; Donaldson et al., 2000; Donaldson et al., 2002; Mollet et al., 2002; Mollet et al., 2005; Olbrich et al., 2003; Otto et al., 2000; Otto et al., 2003; Schermer et al., 2005). NPHP1 was originally localized to adherens junctions and focal adhesions of renal epithelial cells and has subsequently been found enriched at the basal bodies (Donaldson et al., 2000; Donaldson et al., 2002; Mollet et al., 2005; Otto et al., 2003). *NPHP1* is also mutated in some JBTS patients (corresponding to the *JBTS4* locus) and some SLSN patients (corresponding to the *SLSN1* locus) (Caridi et al., 1998; Parisi et al., 2004).

Whereas *NPHP1* mutations are responsible for roughly one quarter of all NPHP cases, only a small number of disease cases have been linked to the *NPHP2* locus and other *NPHP* loci. *NPHP2* encodes the protein inversin, which has 16 tandem ankyrin repeats, two IQ calmodulin binding domains, and a coiled coil domain. The protein localizes to cilia and basal bodies and binds β-tubulin in addition to NPHP1. Inversin plays a role in regulating the switch between canonical and non-canonical WNT signaling (Otto et al., 2003; Simons et al., 2005).

NPHP3 mutations were first identified in a cohort of South American NPHP families (Olbrich et al., 2003). Recently, additional *NPHP3* mutations were found in families with more severe forms of NPHP that featured MKS-like phenotypes such as *situs inversus*, polydactyly, and central nervous system malformations (Bergmann et al., 2008). However, Bergmann et al. did not formally announce *NPHP3* as an MKS locus. *Nphp3*$^{pcy/pcy}$ hypomorphic mice exhibit an NPHP-like renal phenotype but lack extrarenal defects like those observed in some human *NPHP3* patients (Olbrich et al., 2003; Takahashi et al., 1986). Interestingly, *Nphp3*$^{ko/ko}$ null mice die during gestation and exhibit left-right patterning defects and heart malformations, supporting the possibility that *NPHP3* mutations in MKS families may eventually be identified (Bergmann et al., 2008). In contrast to the majority of PKD mouse models, which exhibit shortened cilia, *Nphp3*$^{pcy/ko}$ mice have elongated renal epithelial cilia (Bergmann et al., 2008). Subcellular localization of NPHP3 has not been clearly determined although the protein interacts with both NPHP1 and NPHP2 (Bergmann et al., 2008; Olbrich et al., 2003).

Concurrent analyses in separate NPHP/SLSN cohorts initially identified 16 unique mutations in a novel gene at the *NPHP4/SLSN4* locus, making *NPHP4* the second mapped NPHP gene (Mollet et al., 2002; Otto et al., 2002). *NPHP4* encodes a protein (NPHP4) that localizes to cilia and basal bodies or to centrosomes in dividing cells and binds NPHP1, RPGRIP1, and RPGRIP1L (Mollet et al., 2005; Roepman et al., 2005). No functional domains have been identified in NPHP4 apart from an NPHP1 interaction region and a proline rich region.

The first identified *NPHP5* mutations were all truncations found in SLSN families. IQCB1/NPHP5 is a ciliary protein that binds calmodulin-2 through two IQ domains

and is in complex with Retinitis Pigmentosa GTPase Regulator (RPGR) (Otto et al., 2005). NPHP5 was recently shown to directly bind CEP290 (MKS4/NPHP6) (Schafer et al., 2008a). In the same study, Schafer et al. reported neural tube closure defects upon knockdown of *Xenopus laevis NPHP5* and pronephric cysts along with hydrocephalus upon knockdown of zebrafish *NPHP5*.

NPHP6 corresponds to the previously mentioned *MKS4* locus. The *NPHP7* locus corresponds to a gene (*GLIS2*) that encodes a Kruppel-like zinc finger transcription factor, Gli-similar protein 2 (GLIS2), that is found both at the cilium and within the nucleus (Attanasio et al., 2007; Zhang et al., 2002) GLIS2 binds to and is thought to negatively modulate beta catenin, linking its function to Wnt signaling (Kim et al., 2007). GLIS2 c-terminal cleavage is modulated by its binding partner p120, and a role of GLIS2 and p120 has been implicated in the neuronal patterning of chick embryos (Hosking et al., 2007). *NPHP8* corresponds to *JBTS7* and the previously discussed *MKS5* locus.

Following the identification of a missense mutation in the *NEK8* gene of autosomal recessive juvenile cystic kidney (*jck*) mice, three unique human *NEK8* mutations were found in an NPHP cohort, marking this gene as *NPHP9* (Liu et al., 2002; Otto et al., 2008). *NEK8* encodes never in mitosis A-related kinase 8 (NEK8), a protein comprised of a serine/threonine protein kinase catalytic domain and a regulator of chromosome condensation (RCC1) domain. Wild-type mouse NEK8 localizes to cilia and basal bodies while *jck* NEK8, which has a Gly-to-Val substitution at amino acid 448 (inside the RCC1 domain), localizes to basal bodies but does not enter the cilium (Trapp et al., 2008). Interestingly, Smith et al. demonstrated with scanning electron micrographs that *jck* mice possessed elongated renal epithelial cilia (Smith et al., 2006a). Smith et al. also reported

increased abundance of polycystin-1 and polycystin-2 along cilia axonemes of *jck* mice. In a more recent study, Sohara et al. reported increased mRNA expression of *Pkd1* and *Pkd2* and found that NEK8 and polycystin-2 could be coimmunoprecipitated (Sohara et al., 2008).

Joubert Syndrome. JBTS type B, also known as cerebello-oculo-renal syndrome (CORS), is an autosomal recessive disorder characterized by retinal dystrophy and renal anomalies as well as underdeveloped cerebellar vermis, brain stem abnormalities, and hypotonia (reviewed in Chen, 2007). JBTS can also be associated with polydactyly, situs inversus/isomerism, posterior encephalocele, and hepatic disease (Sepulveda et al., 1997). In addition to the four loci that are also linked to MKS and/or NPHP (and have already been discussed), there are two more mapped loci, *JBTS3* and *JBTS8*, and two loci causing JBTS that have not been linked to specific genes (see Table 3). These two incompletely mapped loci are *JBTS1* at chromosomal position 9q34.3 (Saar et al., 1999) and *JBTS2* at 11p12-11q13.3 (Keeler et al., 2003). Interestingly, the incompletely mapped *MKS2* locus is in the same genomic region as *JBTS2*, suggesting these loci may correspond to distinct alleles of the same gene.

JBTS3 (more commonly called *AHI1*) was the first gene directly linked to JBTS (Ferland et al., 2004). *AHI1* encodes Jouberin, a protein comprised of an n-terminal coiled coil domain, several WD40 domains, and a c-terminal SH3 domain. Until recently, very little was understood about the function or localization of Jouberin. A new report by Doering et al. demonstrated Jouberin localization to the stigmoid body, a generally uncharacterized structure found in the cytoplasm of some neurons, mostly those of

the hypothalamus (Doering et al., 2008). Concurrently, Elay et al. reported Jouberin-GFP localization to basal bodies and centrosomes in cultured cells and demonstrated with a yeast-2-hybrid assay that Jouberin could physically interact with NPHP1 (Eley et al., 2008).

Lastly, *Arl13b/JBTS8* mutations were recently identified in JBTS families (Cantagrel et al., 2008). The *Arl13b* gene product is a small GTPase that localizes to cilia and may be involved in cilia formation (Hori et al., 2008).

Bardet-Biedl Syndrome. Clinical pathology associated with BBS includes obesity, retinopathy, polydactyly, kidney and heart defects, genital malformations, and cognitive deficits (Green et al., 1989). Unlike the previously mentioned diseases, few BBS patients progress to ESRD. Mutations in a total of 14 genes have thus far been identified in BBS families, accounting for about 75% of all BBS cases (Leitch et al., 2008; Stoetzel et al., 2007; Tobin and Beales, 2007). In contrast to the considerable genetic overlap in the diseases mentioned previously, only two of the 14 genes reportedly mutated in BBS are also disrupted in the other autosomal recessive renal cystic disorders (see Table 4). These are *MKS1* and *CEP290* (Leitch et al., 2008). The BBS genes encode a diverse array of proteins that includes an ADP-ribosylation factor-like protein (BBS3/ARL6), TPR repeat proteins (BBS4 and BBS8/TTC8), chaperonin-like proteins (BBS6/MKKS, BBS10/C12ORF58, and BBS12/FLJ35630), an E3 ubiquitin ligase (BBS11/TRIM32), a B9 domain protein (BBS13/MKS1), a transmembrane, coiled coil domains, KID repeat, nuclear localization signal motif protein (BBS14/CEP290), and novel unrelated proteins (BBS1, BBS2, BBS5, BBS7/FLJ10715, and BBS9/PTHB1) (reviewed in Tobin and

Beales, 2007). Apart from BBS10, BBS11, and BBS12, in which subcellular localization has not yet been identified, each of the BBS proteins localize to basal bodies, cilia, and/or centrosomes. Interestingly, Nachury *et al*. utilized a tagged BBS4 protein expressed in retinal pigmented epithelial cell culture to isolate a stable protein complex comprised of BBS1, 2, 4, 5, 7, 8, and 9 as well as PCM1, tubulin, and Rabin8 (Nachury et al., 2007).

Overall, these genetic, cellular, and biochemical data indicate that MKS, NPHP, JBTS, SLSN, and BBS may represent a continuum of a common underlying ciliary/basal body disorder where the phenotypic outcome is determined by the nature of the mutation and the genetic background of the affected patient.

Cilia and Basal Bodies

Cilia are microtubule-based organelles that have multiple functions ranging from fluid and cell propulsion to sensory reception and signaling regulation (see Figure 2). Motile cilia, which are comprised of an axoneme ring of nine outer microtubule doublets and a central pair of microtubules (9+2), are present on tissues such as epithelial cells of the trachea and ependymal cells of the brain ventricles, and function in mucus clearance and cerebrospinal fluid movement, respectively. In the node of the developing mammalian embryo, a unique form of motile cilia exist which lack the central microtubule pair (9+0) yet are able to rotate, creating directional fluid movement that influences left-right axis determination (Nonaka et al., 1998). Immotile 9+0 primary cilia are found on most mammalian cells including photoreceptor cells of the eyes and neurons as well as on renal tubule epithelia. In the lumen of the nephron, the cilia of the tubule epithelia function

as mechanosensors to detect fluid flow and are necessary for mediating changes in intracellular calcium.

All cilia are associated with a basal body, which is a modified centriole that forms in nondividing cells. Prior to ciliogenesis, the mother centriole associates with vesicles that will form a phospholipid compartment surrounding the growing cilium and will later fuse with the plasma membrane. Following migration to the edge of the cell, the vesicle/plasma membrane fusion event anchors the mother centriole and cilium to the cell membrane (Sorokin, 1968). These processes of centriole migration and subsequent tethering to the membrane are not fully understood (Dawe et al., 2007a; Marshall, 2007). In addition to the role of basal bodies in initializing ciliogenesis, they also serve as the docking and assembly site for proteins involved in Intraflagellar Transport (IFT) as well as cargo targeted to the cilium (Deane et al., 2001).

Intraflagellar Transport (IFT)

IFT is essential for cilia formation and involves the bidirectional movement of large protein complexes (IFT particles) and associated cargo along the cilium microtubule axoneme (Cole et al., 1998; Kozminski et al., 1993; Orozco et al., 1999; Piperno et al., 1998). This occurs in the anterograde direction via kinesin motors and in the retrograde direction by a cytoplasmic dynein motor (Cole et al., 1998; Porter et al., 1999). The cilium is built from the base to the tip and begins at the site where the centriole docks with the cell membrane to become the basal body. It is here that the IFT motors, IFT particles (subcomplexes A and B), and associated cargo accumulate and incorporate prior to entry into the cilium axoneme. The mechanisms by which these components are traf-

ficked, assembled, and loaded at the basal body are poorly understood. Once the IFT complex is formed, the kinesin II motor travels along the microtubule axoneme carrying the IFT particles, cargo, and accessory motors. At the distal tip of the cilium, the IFT complex is remodeled such that kinesin II becomes cargo, and dynein is then used as the motor that drives the complex in the retrograde direction down the axoneme and back to the base where the complex is disassembled (see Figure 3) (Reviewed in Scholey, 2003).

Cilia and Cystic Kidney Disease

Many mutations that disrupt ciliary, basal body, or IFT proteins result in mild to lethal developmental and disease pathologies in mice and humans collectively referred to as ciliopathies (Badano et al., 2006b; Beales et al., 2007; Davenport et al., 2007; Haycraft et al., 2005; Moyer et al., 1994; Murcia et al., 2000; Pazour et al., 2000; Taulman et al., 2001). One of the first connections between cilia function and cystic kidney disease was made with the analysis of the Oak Ridge Polycystic Kidney (*Tg737*^{ORPK}) mouse. The *Tg737*^{ORPK} mouse was generated by random insertional mutagenesis that resulted in a hypomorphic disruption of the *Tg737* gene (Moyer et al., 1994; Yoder et al., 1995). The homozygous *Tg737*^{ORPK} mouse exhibited hydrocephalus, liver biliary dysplasia, and acinar cell atrophy of the pancreas in addition to polycystic kidneys. It was later shown that these mice had renal tubule epithelia cilia that were shorter than wild type (Pazour et al., 2000). Additionally, complete knockout of the *Tg737* gene in the *Tg737*$^{\Delta 2\text{-}3\beta Gal}$ mouse resulted in embryos that died in mid-gestation. These mice exhibited severe neural tube closure defects as well as left-right axis determination defects (Murcia et al., 2000). Furthermore, disruption of *Tg737* in *Chlamydomonas* and *C. elegans* resulted in flagella and

cilia morphology defects, respectively, indicating conserved function of the gene (Haycraft et al., 2001; Pazour et al., 2000). The *Tg737* gene was found to encode a protein (Polaris/IFT88) that is an integral component of the IFT particle that localizes to cilia and basal bodies (Taulman et al., 2001).

In addition to the $Tg737^{ORPK}$ mouse, many animal models of cystic kidney disease have been developed. Some were previously mentioned, and a subset will be briefly discussed here. The first murine case of inherited cystic kidney disease was reported in a phenotypic description of the congenital polycystic kidney (*cpk*) mutant mouse, which arose from a spontaneous mutation. Mapping of the *cpk* locus identified the gene encoding cystin, a protein that was subsequently found to localize to cilia (Hou et al., 2002; Yoder et al., 2002). *Pkd1* and *Pkd2* mutant mice, generated by targeted mutagenesis, have disrupted function of the polycystin-1 and polycystin-2 proteins, respectively, and develop cystic kidneys (Lu et al., 2001; Wu et al., 1998). Disruption of *NPHP2* in the inversion of embryonic turning (*inv*) and *NPHP3* in the polycystic kidney disease (*pcy*) mice resulted in cystic kidney phenotypes as well (Mochizuki et al., 1998; Nagao et al., 1995; Omran et al., 2001). Furthermore, the gene disrupted in the Wistar polycystic kidney (*wpk*) rat was recently identified as *MKS3* (Nauta et al., 2000; Smith et al., 2006b). All the proteins associated with these murine models localize to cilia and/or basal bodies.

Several mouse models of BBS have recently been generated by targeted mutagenesis. Interestingly, BBS mutant mice exhibit cell type-specific defects in cilia morphology; sperm flagella and olfactory cilia are malformed while motile tracheal and primary cilia structure is not altered (Fath et al., 2005; Kulaga et al., 2004; Mykytyn et al., 2004; Nishimura et al., 2004; Ross et al., 2005). Oddly, these mice still developed

renal cysts despite possessing properly formed renal epithelial cilia, indicating that BBS proteins may also function in cilia signaling pathways that modulate development and/or tissue homeostasis. Indeed, a recent study in cultured neurons harvested from BBS4 mutant mice demonstrated the loss of G protein-coupled receptor localization to the cilium (Berbari et al., 2008).

Cilia in C. elegans

Much of our understanding about IFT, ciliogenesis, and the function of proteins associated with ciliopathies has come from analyses conducted in invertebrates such as *Chlamydomonas* and *C. elegans*. Analysis of *C. elegans* mutants lacking properly formed cilia has uncovered many components of IFT that are conserved in most ciliated organisms. Unlike the ubiquitous nature of cilia in mammals, cilia are only present in *C. elegans* at the distal tips of neuron dendrites where they function as sensors of conditions in the external environment (Ward et al., 1975; Ware R. et al., 1975). Of the 302 neurons comprising the *C. elegans* hermaphrodite nervous system, 60 express cilia, and these include the amphid and labial (inner and outer) neurons in the head of the worm in addition to phasmid and PQR neurons in the tail. Cilia in *C. elegans* feature the 9+0 microtubule orientation and are separated from the distal tips of the dendrites by the transition zone, a region at the base of the cilium where the axonemal microtubules are anchored to the ciliary membrane. No identifiable centriole is attached to the base of *C. elegans* cilia; however, the homologs of several mammalian basal body proteins localize to the ciliary base, suggesting that some functional entity analogous to the basal body does exist in the worm. At the tips of dendrites extended from the cell bodies of neurons, the cilia either

fasciculate at pores in the cuticle and project into the external environment or invaginate the surrounding sheath cell. The neuronal dendrites and the surrounding sheath cell are physically connected by belt junctions found just proximal to the transition zones (see Figure 3). The molecular makeup of these belt junctions is not known although they are believed to be a form of adherens junctions. The cilia of *C. elegans* primarily function to sense the conditions in the external environment of the worm and initiate signals to the rest of the nervous system that cue responses in behavior. The processes regulated by cilia function in *C. elegans* include attraction or repulsion in response to chemicals, avoidance of regions of high osmolarity, and regulating foraging behavior in the presence of food. Additionally, *C. elegans* use cilia to sense dauer pheromone, a chemical secreted by the worm when living conditions are suboptimal. In response to this pheromone, *C. elegans* assume an alternative developmental pathway to adapt to the conditions. Finally, cilia are essential for the proper function of the DAF-2/Insulin-IGF-1-like receptor signaling pathway, which is responsible for regulating lifespan length in *C. elegans* (Apfeld and Kenyon, 1999). Because of this, the IGF1-like pathway is constitutively repressed in *C. elegans* mutants lacking cilia, resulting in a significant extension in lifespan.

Many of the genes encoding proteins necessary for IFT and cilia assembly in *C. elegans* were first identified in mutagenesis screens for worms defective in chemotaxis (*che-2*, *che-3*, *che-11*, and *che-13*) (Dusenbery et al., 1975; Fujiwara et al., 1999; Haycraft et al., 2003; Lewis and Hodgkin, 1977; Qin et al., 2001; Wicks et al., 2000), osmotic avoidance (*osm-1*, *osm-3*, *osm-5*, and *osm-6*) (Bell et al., 2006; Collet et al., 1998; Culotti and Russell, 1978; Haycraft et al., 2001; Orozco et al., 1999; Signor et al., 1999), and dauer formation (*daf-10* and *daf-19*) (Bell et al., 2006; Riddle et al., 1981; Swoboda et

al., 2000). More recently, additional genes were identified by screening for mutants defective in the ability to uptake fluorescent hydrophobic dye (DiI) into the dendrites and cell bodies of the amphid and phasmid neurons via cilia that are exposed to the external environment of the worm (De Riso et al., 1994; Starich et al., 1995). These include *dyf-1*, *dyf-2*, *dyf-3*, *dyf-5*, *dyf-6*, *dyf-11*, and *dyf-13* (Bell et al., 2006; Blacque et al., 2005; Burghoorn et al., 2007; Efimenko et al., 2006; Murayama et al., 2005; Ou et al., 2005). Finally, reverse genetic approaches have been utilized in *C. elegans* to analyze genes encoding proteins that are suspected components of the IFT machinery. These include *ift-74*, *ift-81*, *ifta-1*, and *xbx-1* (see Figure 4) (Blacque et al., 2006; Kobayashi et al., 2007; Schafer et al., 2003).

Research in *C. elegans* has also provided insight into the function of proteins associated with cystic kidney disorders such as BBS. The BBS protein homologs are found at the base of *C. elegans* cilia and in some cases along the cilium proper where they participate in IFT and are thought to play a role in stabilizing associations between the IFT A and B subcomplexes (Reviewed in Blacque and Leroux, 2006). It has also been demonstrated that cystic kidney disease proteins not directly linked to IFT such as polycystin-1 and polycystin-2 have conserved roles in *C. elegans*. The polycystin-1 and polycystin-2 homologs (LOV-1 and PKD-2, respectively) both localize to sensory ray cilia of the *C. elegans* male tail and male-specific CEM cilia in the head, and although these proteins are not required for cilia assembly, disruption of either results in male mating deficiencies associated with impaired cilia signaling activities (Barr et al., 2001). Analysis of the polycystins in *C. elegans* has also proved useful in understanding some of the mechanisms by which those proteins are trafficked and processed. Barr and colleagues have

demonstrated roles of AP-1 μ1 clathrin adaptor (UNC-101), signal transductor adaptor molecule 1 (STAM-1A), hepatocyte growth factor-regulated tyrosine kinase substrate (HGRS-1), and the process of IFT itself in modulating the polycystins inside cilia, along the dendrites, and within the neuronal cell bodies (Bae et al., 2006; Hu et al., 2007).

Additionally, the human NPHP proteins NPHP1 and NPHP4 have highly conserved homologs in *C. elegans* (NPHP-1 and NPHP-4, respectively) which colocalize specifically to the base of cilia where they appear to function as part of a protein complex. This is supported by the requirement of NPHP-4 for localization of NPHP-1 to the base of cilia (Winkelbauer et al., 2005). *nphp-1* and *nphp-4* mutant worms display several of the sensory behavior abnormalities typically associated with *C. elegans* mutants that have cilia morphology defects. These include altered chemotaxis responses toward attractants and increased lifespan in single *nphp* mutant worms as well as male mating defects in *nphp-1;nphp-4* double mutants (Jauregui and Barr, 2005; Winkelbauer et al., 2005). Although these mutants do not have overt abnormalities in cilia morphology based both on the ability of worms to absorb fluorescent dye and to properly localize an IFT protein along the length of cilia axonemes, recent transmission electron microscopy data indicates that *nphp* mutants have subtle yet distinctive ultrastructural cilia morphology defects including loss of cilia from a subset of amphid neurons in a subpopulation of worms (Jauregui et al., 2008).

In contrast to the extensive work conducted in *C. elegans* on the genes involved in human BBS, PKD, and NPHP, the homologs of the MKS-associated genes have largely been unexplored. Previous studies have shown that the *MKS1* homolog *xbx-7/mks-1* is expressed in ciliated sensory neurons of *C. elegans*; however the function or localization

of MKS-1 protein was not determined (Efimenko et al., 2005). MKS1 contains a B9 domain that has not been investigated and is found in only two other proteins in *C. elegans* (TZA-1 and TZA-2) or humans (B9D1 and B9D2). Like *mks-1*, the *MKS3* homolog *F35D2.4/mks-3* is expressed in ciliated sensory neurons, but no reports of MKS-3 protein function or localization have been made (Efimenko et al., 2005). *C09G5.8* may be a weak homolog of *MKS5,* and it has not been examined in *C. elegans*. *K07G5.3* is the homolog of the recently identified *MKS6* gene, and it is also expressed in ciliated sensory neurons (Blacque et al., 2005). Unpublished data indicate that the K07G5.3 protein localizes to the base of cilia (M. Leroux, personal correspondence). Finally, the *MKS4* protein CEP290 does not have a strong homolog in *C. elegans*.

Regulation of X-box Genes in C. elegans

Perkins et al. first reported that *daf-19* mutant worms completely lacked all cilia and transition zone structures (Perkins et al., 1986). Subsequently, the DAF-19 protein was described as the Regulatory Factor binding to an X-box (RFX) transcription factor. Homodimeric DAF-19 binds a regulatory promoter element called the X-box, a motif of 14 nucleotides typically found within 200 base pairs upstream of transcriptional start sites. DAF-19 drives expression of genes specifically in ciliated sensory neurons (Swoboda et al., 2000). It has been shown that several genes encoding the IFT machinery, the BBS proteins, and the NPHP proteins are all regulated by DAF-19 through their respective X-boxes. Using a computational genome search approach, Efimenko et al. identified roughly 750 X-box promoter motif-containing genes in *C. elegans* as candidates for regulation by DAF-19 (Efimenko et al., 2005). Included among those 750

genes were *mks-1*, *mks-3*, *tza-1*, *tza-2*, and *K07G5.3*. Thus, these genes are predicted to encode proteins that function in *C. elegans* specifically in the ciliated sensory neurons.

Purpose of Research

Given the strong evidence in support of a common molecular, cellular, and genetic basis for MKS, NPHP, and JBTS and the connection of the corresponding proteins with cilia and basal bodies, we believed it important to examine the mechanisms by which these proteins may function together and why their disruption can lead to a broad range of pathologies. *C. elegans* has proven its value as a tool for uncovering the basic function of cilia and basal body proteins, and we utilized the organism in this body of work to elucidate the roles of the MKS proteins and their potential connection to the NPHP proteins.

Chapter 2 describes the expression and localization profiles of the *C. elegans* B9 proteins MKS-1, TZA-1, and TZA-2, and provides basic insight into how these proteins are functionally related. Evidence is presented that suggests the B9 proteins function as part of a complex at the base of cilia in coordination with NPHP proteins to regulate cilia and dendrite morphology in sensory neurons. This chapter has been published in *Molecular Biology of the Cell*. Chapter 3 describes the expression and localization profile of the *C. elegans* transmembrane protein MKS-3 and provides insight into how MKS-3 localization is modulated by the B9 proteins. Coordinated function of MKS-3 and NPHP proteins is required for ciliogenesis and proper dendrite morphology. These findings suggest *mks-3* is in the same genetic pathway as *mks-1*, *tza-1*, and *tza-2*. This chapter will be submitted to a peer reviewed journal upon final revision.

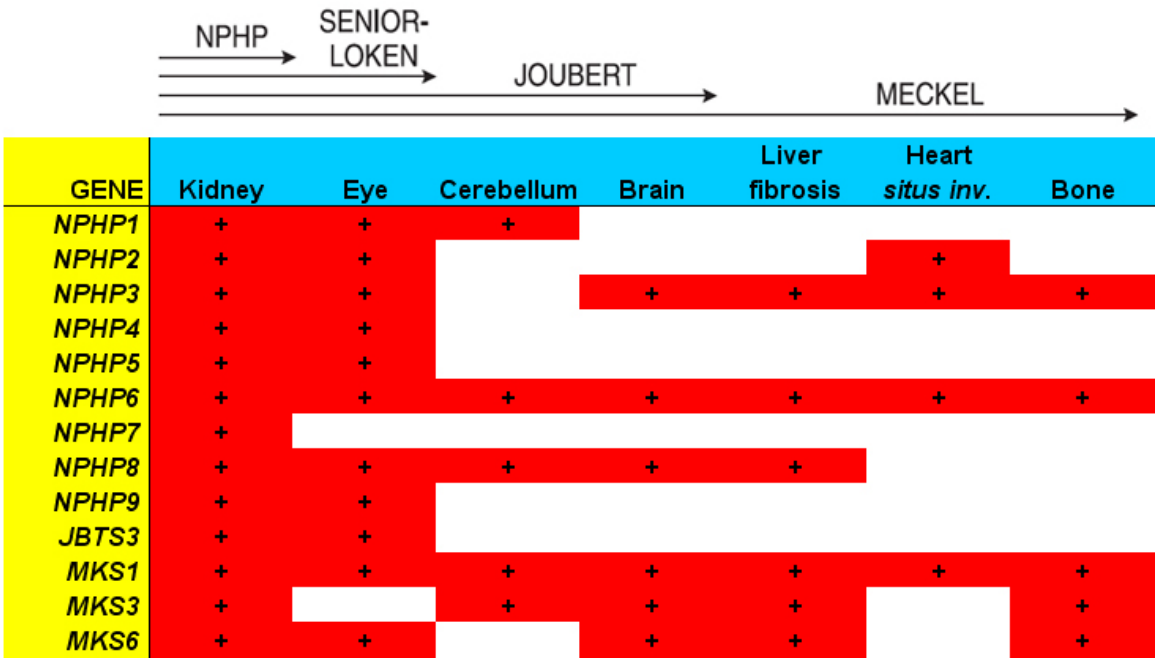

Figure 1. Genotype-phenotype comparisons of nephronophthisis-associated ciliopathies. Clinically, a nephronophthisis diagnosis is restricted to patients with only renal abnormalities. Patients with retinal degeneration in addition to renal abnormalities are diagnosed with Senior-Løken Syndrome. Diagnostic criteria for Joubert Syndrome extends to malformations in the cerebellum and brainstem. Additional organ involvement including neural tube closure defects, liver and hepatic anomalies, heart defects, and polydactyly, along with systemic deformities such as *situs inversus* are hallmarks for the most severe form of nephronophthisis-associated ciliopathies, Meckel-Gruber Syndrome. Both the nature of mutation in a patient and their genetic background can influence the severity of disease.

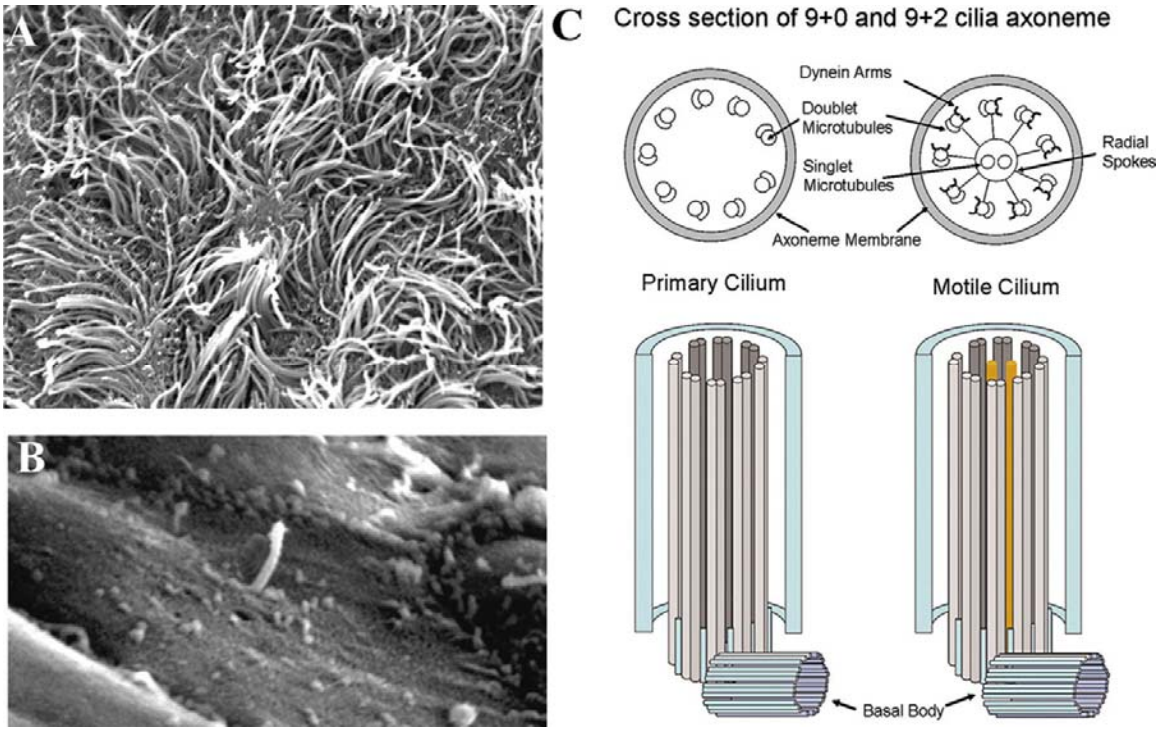

Figure 2. Motile or immotile (primary) cilia are located on the surface of nearly every cell within the mammalian body. (A) scanning electron microscopic (SEM) image of motile cilia present on wild-type mouse ependymal cells located in the lateral ventricles. (B) SEM image displaying a solitary primary cilium projecting from the surface of an ectodermal cell in the developing limb bud of an embryonic day 10.5 mouse embryo. (C) structural differences determine the motility of a cilium. Motile cilia (right) consist of 9 doublet microtubules surrounding 2 inner singlet microtubules used to conduct force. Primary cilia (left) are lacking both singlet microtubules and dynein arms.

Figure and legend used with permission from *American Journal of Physiology Renal Physiology*. 2005 Dec;289(6):F1159-69. Review. Davenport JR and Yoder BK.

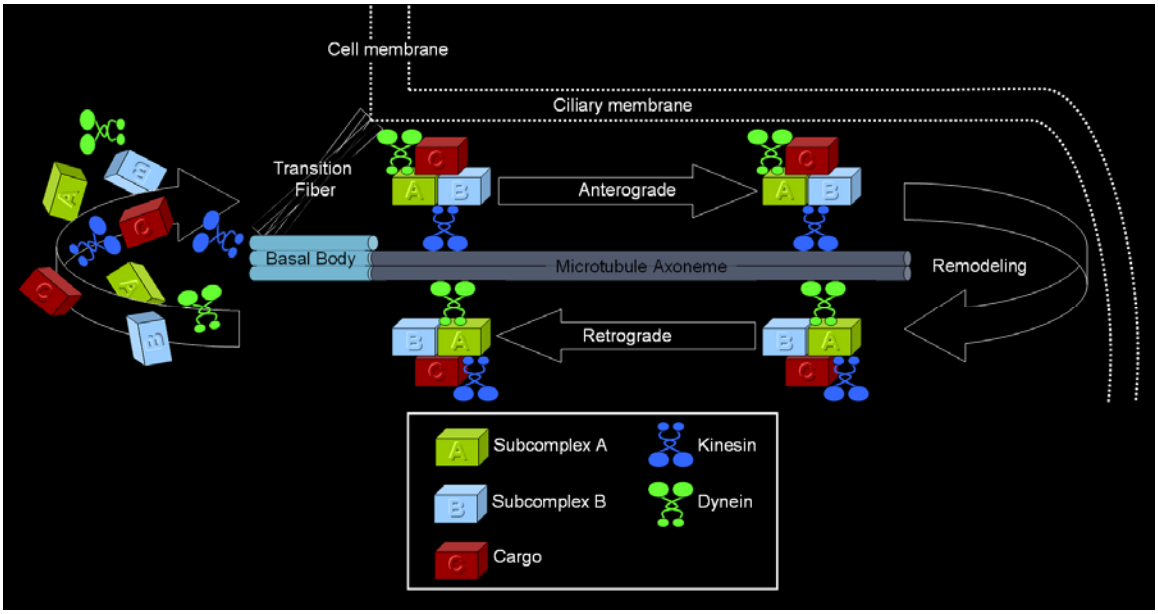

Figure 3. Intraflagellar Transport (IFT) in *C. elegans* cilia. Components required for cilia assembly accumulate at the base of the cilium (left) and are then loaded onto the cilium axoneme to form the IFT raft complex. (Top) The raft is transported in the anterograde direction along the cilium axoneme by the kinesin motor. The complex is remodeled at the distal tip of the cilium (right) and then (bottom) carried in the retrograde direction by the dynein motor. After arriving back at the base, the IFT raft is disassembled and/or recycled.

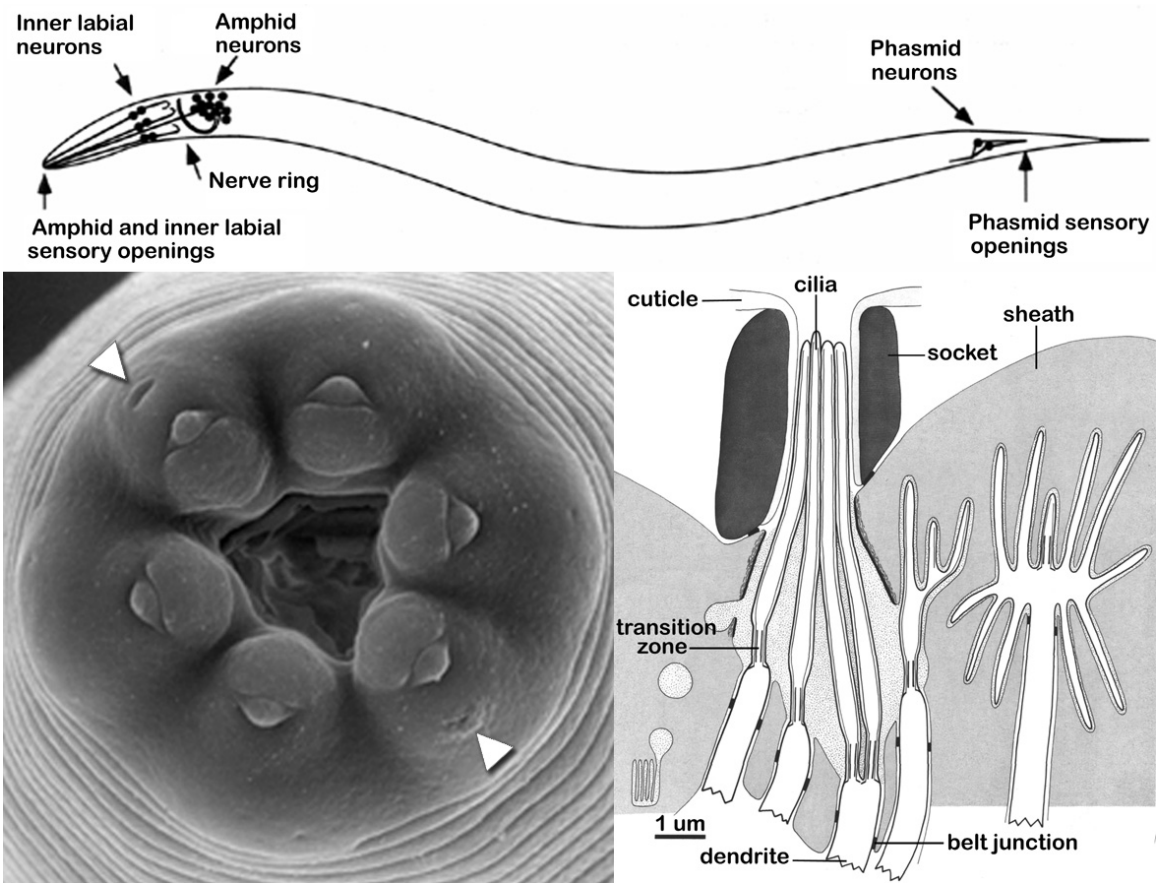

Figure 4. Cilia in *C. elegans*. (Top) Ciliated sensory neurons in *C. elegans* include the amphid and labial neurons in the head and the phasmid neurons in the tail. (Bottom, left) Scanning electron micrograph of the worm head. Arrows indicate the pores through which amphid cilia contact the environment. (Bottom, right) Schematic of cilia arrangement in the amphid bundle.

(Top) figure modified and used with permission from *Cold Spring Harbor Laboratory Press*. *C. elegans* II. 1997. 25: 723. Bargmann CI and Mori I. (Bottom) figure modified and used with permission from *Development*. 1986 Oct;117(2). Perkins LA, Hedgecock EM, Thomson JN, and Culotti JG.

Table 1: Meckel-Gruber Syndrome (MKS) Genes

Disease Locus	*Gene*	*Protein Sequence Characterization*	*Subcellular Localization*
MKS1 (17q23)	MKS1	B9 Domain	Centrosome
MKS2 (11q13)	Unknown	Unknown	Unknown
MKS3 (8q21)	TMEM67	Putative 7 transmembrane-spanning protein	Basal Body/Cilium
MKS4 (12q21)	CEP290	Coiled-coil domains/Bipartite nuclear localization sequence	Basal Body/Centrosome
MKS5 (16q)	RPGRIP1L	Coiled-coil domains/Bipartite nuclear localization sequence	Basal Body/Centrosome
MKS6 (4p15)	CC2D2A	C2 Calcium Binding Domain/Coiled Coil Domain	Basal Body

Table modified and used with permission from *Elsevier*. Current Topics in Developmental Biology. 2009. 13: 399. Sharma N, Berbari NJ, and Yoder BK.

Table 2: Nephronophthisis (NPHP) Genes

Disease Locus	*Gene*	*Protein Sequence Characterization*	*Subcellular Localization*
NPHP1 (2q13)	Nephrocystin-1	SH3 Domain/coiled-coil domain	Centrosome/Cilium/ Adherens Junctions
NPHP2 (9q31)	Inversin	IQ calmodulin binding domain/ankyrin repeats/D-box	Centrosome/Cilium
NPHP3 (3q22)	Nephrocystin-3	IQ calmodulin binding domain	Cilium
NPHP4 (1p36	Nephrocystin-4	Novel	Basal Body/ Centrosome/Cilium
NPHP5 (3q21)	IQCB1	IQ calmodulin binding domain	Cilium
NPHP6 (12q21)	CEP290	Coiled-coil domains/Bipartite nuclear localization sequence	Basal Body/Centrosome
NPHP7 (16p13)	GLIS2	Kruppel Like Zinc Finger	Nucleus/Cilium
NPHP8 (16q)	RPGRIP1L	Coiled-coil domains/Bipartite nuclear localization sequence	Basal Body/ Centrosome/Cilium
NPHP9 (17q11)	NEK8	Nima Kinase	Cilium

Table modified and used with permission from *Elsevier*. Current Topics in Developmental Biology. 2009. 13: 397. Sharma N, Berbari NJ, and Yoder BK.

Table 3: Joubert Syndrome (JBTS) Genes

Disease Locus	*Gene*	*Protein Sequence Characterization*	*Subcellular Localization*
JBTS1 (9q34)	Unknown	Unknown	Unknown
JBTS2 (11p12)	Unknown	Unknown	Unknown
JBTS3 (6q23)	AHI1/Jouberin	SH3 Domain/WD40 repeat domains/coiled-coil domain	Basal Body/Centrosome/ Stigmoid Body
JBTS4 (2q13)	Nephrocystin-1	SH3 Domain/coiled-coil domain	Centrosome/cilium/ Adherens Junctions
JBTS5 (12q21)	CEP290	Coiled-coil domains/Bipartite nuclear localization sequence	Basal Body/Centrosome
JBTS6 (8q21)	TMEM67	Putative 7 transmembrane-spanning Protein	Basal Body/Cilium
JBTS7 (16q12)	RPGRIP1L	Coiled-coil domains/Bipartite nuclear localization sequence	Basal Body/ Centro-some/Cilium
JBTS8 (3p12.3-q12.3)	Arl13b	Small GTPase	Cilium

Table modified and used with permission from *Elsevier*. Current Topics in Developmental Biology. 2009. 13: 407. Sharma N, Berbari NJ, and Yoder BK.

Table 4: Bardet-Biedl Syndrome (BBS) Genes

Disease Locus	*Gene*	*Protein Sequence Characterization*	*Subcellular Localization*
BBS1 (11q13)	BBS1	Novel	Basal Body/Cilium
BBS2 (16q22)	BBS2	Novel	Basal Body/Cilium
BBS3 (3p12)	ARL6	ADP-Ribosylation Factor-Like protein 6	Basal Body/Cilium
BBS4 (15q22)	BBS4	Novel, TPR Repeats	Basal Body/Cilium
BBS5 (2q31)	BBS5	Novel	Basal Body/Cilium
BBS6 (20p12)	MKKS	Chaperonin-like	Basal Body
BBS7 (4q27)	FLJ10715	Novel	Basal Body/Cilium
BBS8 (14q31)	TTC8	Novel, TPR Repeats	Basal Body/Cilium
BBS9 (7p14)	PTHB1	Novel	Basal Body/Cilium
BBS10 (12q21)	C12ORF58	Chaperonin-like	Unknown
BBS11 (9q31)	TRIM32	E3 Ubiquitin Ligase	Unknown
BBS12 (4q27)	FLJ35630	Chaperonin-like	Unknown
BBS13 (17q23)	MKS1	B9 Domain	Centrosome
BBS14 (12q21)	CEP290	Coiled-coil domains/Bipartite nuclear localization sequence	Basal Body/Centrosome

Table modified and used with permission from *Elsevier*. Current Topics in Developmental Biology. 2009. 13: 402. Sharma N, Berbari NJ, and Yoder BK.

FUNCTIONAL REDUNDANCY OF THE B9 PROTEINS AND NEPHROCYSTINS IN *CAENORHABDITIS ELEGANS* CILIOGENESIS

COREY L. WILLIAMS, MARLENE E. WINKELBAUER, JENNY C. SCHAFER, COURTNEY J. HAYCRAFT, PETER SWOBODA, AND BRADLEY K. YODER

Molecular Biology of the Cell Vol. 19, 2154-2168, May 2008

Format adapted and errata corrected for dissertation

SUMMARY

Meckel-Gruber Syndrome (MKS), Nephronophthisis (NPHP), and Joubert Syndrome (JBTS) are a group of heterogeneous cystic kidney disorders with partially overlapping loci. Many of the proteins associated with these diseases interact and localize to cilia and/or basal bodies. One of these proteins is MKS1, which is disrupted in some MKS patients and contains a B9 motif of unknown function that is found in two other mammalian proteins, B9D2 and B9D1. *Caenorhabditis elegans* also has three B9 proteins: XBX-7 (MKS1), TZA-1 (B9D2), and TZA-2 (B9D1). Herein, we report that the *C. elegans* B9 proteins form a complex that localizes to the base of cilia. Mutations in the B9 genes do not overtly affect cilia formation unless they are in combination with a mutation in *nph-1* or *nph-4*, the homologs of human genes (*NPHP1* and *NPHP4*, respectively) that are mutated in some NPHP patients. Our data indicate that the B9 proteins function redundantly with the nephrocystins to regulate the formation and/or maintenance of cilia and dendrites in the amphid and phasmid ciliated sensory neurons. Together, these data suggest that the human homologs of the novel B9 genes *B9D2* and *B9D1* will be strong candidate loci for pathologies in human MKS, NPHP, and JBTS.

INTRODUCTION

Meckel-Gruber Syndrome (MKS), Nephronophthisis (NPHP), and Joubert Syndrome (JBTS) are three genetically heterogeneous autosomal recessive disorders that exhibit renal cystic dysplasia in addition to several other phenotypes. MKS is a perinatal lethal disorder defined by not only renal cysts but also by severe developmental defects including polydactyly and occipital encephalocele (Alexiev *et al.*, 2006). In contrast, NPHP patients develop end-stage renal disease as children and young adults, but this disease is not associated with significant perinatal lethality. Phenotypes associated with NPHP include the formation of corticomedullary cysts, disruption of tubular basement membrane, tubulointerstitial nephropathy, and sometimes retinal defects (reviewed in Hildebrandt and Zhou, 2007). JBTS type B, also known as cerebello-oculo-renal syndrome (CORS), is characterized by retinal dystrophy and renal anomalies as well as underdeveloped cerebellar vermis, brain stem abnormalities, and hypotonia (reviewed in Chen, 2007). Genetic analysis has revealed that in some cases, MKS, NPHP, and JBTS share loci that are allelic in nature. These include *MKS3/JBTS6* (Baala *et al.*, 2007b), *NPHP1/JBTS4* (Parisi *et al.*, 2004), *MKS4/NPHP6/JBTS5* (Baala et al., 2007a; Sayer et al., 2006), and *MKS5/NPHP8/JBTS7* (Arts *et al.*, 2007; Delous *et al.*, 2007). Notably, the current known genes connected to MKS, NPHP, and JBTS have been linked to only a small percentage of afflicted individuals, suggesting that a large number of loci responsible for these disorders are yet to be identified (Hildebrandt and Otto, 2005; Khaddour *et al.*, 2007).

A common theme connecting most cystic kidney disorders is that the genes associated with the observed pathology encode cilia or basal body proteins. This is seen for

NPHP1, 2, and 4-8 (Attanasio et al., 2007; Delous et al., 2007; Fliegauf et al., 2006; Mollet et al., 2002; Morgan et al., 2002; Otto et al., 2002; Otto et al., 2005; Otto et al., 2003; Sayer et al., 2006) as well as MKS1 and MKS3 (meckelin) (Dawe et al., 2007b; Smith et al., 2006b). Furthermore, many of the NPHP proteins appear to function as part of a complex (Hildebrandt and Zhou, 2007; Mollet et al., 2005) that may also include RPGRIP1L (NPHP8), which was originally identified as a binding partner for NPHP4 (Roepman *et al.*, 2005). These genetic, cellular, and biochemical data together indicate that MKS, NPHP, and JBTS may represent a continuum of a common underlying ciliary/basal body disorder where the phenotypic outcome is determined by the nature of the mutation or genetic background of the affected patient.

Cilia are microtubule-based organelles that have multiple functions ranging from fluid and cell movement to sensory reception and signaling regulation. All cilia are associated with a basal body, which is a modified centriole that forms in nondividing cells. Prior to ciliogenesis, the centrioles migrate to the cell membrane where they form attachments and nucleate ciliary microtubule assembly (reviewed in Rosenbaum and Witman, 2002). The processes of centriole migration and subsequent tethering to the membrane are not fully understood (Dawe *et al.*, 2007a; Marshall, 2007). In addition to the role of basal bodies in initializing ciliogenesis, they also serve as the docking and assembly site for proteins involved in Intraflagellar Transport (IFT) as well as cargo targeted to the cilium (Deane *et al.*, 2001). IFT is essential for cilia formation and involves the bidirectional movement of large protein complexes (IFT particles) and associated cargo along the cilium axoneme (Cole et al., 1998; Kozminski et al., 1993; Orozco et al., 1999; Piperno et al., 1998). This occurs in the anterograde direction via kinesin motors and in

the retrograde direction by a cytoplasmic dynein motor (Cole *et al.*, 1998; Porter *et al.*, 1999). Mutations that disrupt IFT components compromise ciliogenesis and result in severe developmental and disease pathologies in mice and humans collectively referred to as ciliopathies (Badano et al., 2006b; Beales et al., 2007; Davenport et al., 2007; Haycraft et al., 2005; Moyer et al., 1994; Murcia et al., 2000; Pazour et al., 2000; Taulman et al., 2001).

Much of our understanding about IFT, ciliogenesis, and the function of proteins associated with ciliopathies has come from analyses conducted in invertebrates such as *Chlamydomonas* and *C. elegans*. Unlike the ubiquitous nature of cilia in mammals, cilia are present in *C. elegans* only at the distal tips of neuron dendrites where they function as sensors of conditions in the external environment. These ciliated cells include the amphid and labial (inner and outer) neurons in the head of the worm in addition to phasmid neurons in the tail. All cilia in *C. elegans* are immotile and are separated from the distal tips of the dendrites by a region called the transition zone, which is loosely analogous to the proximal end of the mammalian cilium where the basal bodies are located (Ward *et al.*, 1975; Ware R. *et al.*, 1975). While most animals possess basal bodies composed of nine triplet microtubules, *C. elegans* centrioles have a nine singlet microtubule arrangement yet are thought to have conserved function in cell division. There is no direct ultrastructural evidence that these centrioles are incorporated into the base of *C. elegans* cilia; however, in *daf-19* mutant worms lacking all ciliary structures, the centrioles are found at the distal tips of neuron dendrites where the cilia are normally formed (Perkins *et al.*, 1986). Thus, *C. elegans* centrioles are likely to have similar function in ciliogenesis as in mammalian systems.

Characterization of *C. elegans* and *Chlamydomonas* mutants where cilia are improperly formed or have defects in cilia-mediated signaling activity has uncovered many components of IFT that have evolutionarily conserved functions in mammals and has thus provided important insights into the molecular basis of the human ciliopathies (Ou et al., 2007; Scholey et al., 2004; Wang et al., 2006). This also includes analysis of the genes involved in Bardet-Biedl syndrome (BBS), another heterogeneous cystic kidney disorder involving proteins that localize to cilia or basal bodies (reviewed in Blacque and Leroux, 2006), as well as two genes linked to human polycystic kidney disease (PKD) (Barr *et al.*, 2001). Additionally, the human NPHP proteins neprocystin-1 (NPHP1) and nephrocystin-4 (NPHP4) have highly conserved homologs in *C. elegans* (NPH-1 and NPH-4, respectively) which colocalize specifically to transition zones where they appear to function in a common protein complex. This is supported by the requirement of NPH-4 for localization of NPH-1 to the transition zones (Winkelbauer *et al.*, 2005). *nph-1* and *nph-4* mutant worms display several of the sensory behavior abnormalities typically associated with *C. elegans* mutants that have cilia morphology defects. These include altered chemotaxis responses toward attractants and increased lifespan in the single *nph* mutants as well as male mating defects in *nph-1;nph-4* double mutants (Jauregui and Barr, 2005; Winkelbauer *et al.*, 2005). Although these mutants do not have overt abnormalities in cilia morphology based both on the ability of worms to absorb fluorescent dye and to properly localize an IFT protein along the length of cilia axonemes, recent transmission electron microscopy data indicate that a subpopulation of *nph* mutant worms occasionally exhibit ultrastructural and morphological defects in their cilia. These abnor-

malities include the loss or truncation of cilia from a subset of amphid neurons and open or lost B-tubules (Jauregui *et al.*, *in press* 2008).

In contrast to the extensive work conducted in *C. elegans* on the genes involved in human BBS, PKD, and NPHP, the homologs of the MKS-associated genes have largely been unexplored. Previous studies have shown that the *MKS1* homolog *xbx-7(R148.1)* is expressed in ciliated sensory neurons of *C. elegans*; however the function or localization of XBX-7 protein is unknown (Efimenko *et al.*, 2005). This protein contains a B9 domain that has not been investigated and is found in only two other proteins in *C. elegans* or humans. Herein we describe XBX-7 and the two other B9 proteins, TZA-1(Y38F2AL.2) and TZA-2(K03E6.4), and demonstrate that all three are part of a complex formed specifically at the base of cilia. TZA-1 is necessary for anchoring TZA-2 in this complex while XBX-7 requires both TZA-1 and TZA-2 for proper localization. Importantly, we have determined that the B9 proteins function redundantly with the transition zone proteins NPH-1 and NPH-4 to regulate the formation and/or maintenance of cilia and dendrites of the amphid and phasmid neurons. Mutations that disrupt the B9 proteins do not cause overt cilia morphology defects; however, simultaneous disruption of a single B9 protein along with disruption of a NPH protein results in malformed ciliated sensory neuron dendrites expressing shortened and laterally oriented cilia. Together, these data suggest the B9 proteins in combination with the NPH proteins have roles in mediating cilia assembly and provide insights into why disruption of basal body proteins leads to the broad range of overlapping ciliopathies associated with MKS, NPHP, and JBTS in humans. Moreover, our analyses indicate that the two B9 domain-encoding

genes in addition to *MKS1* are important candidate loci for MKS, NPHP, and JBTS patients in which the underlying genetic defect has not yet been identified.

MATERIALS AND METHODS

General molecular biology methods

Molecular biology procedures were performed according to standard protocols (Sambrook *et al.*, 1989). *C. elegans* genomic DNA, *C. elegans* cDNA, or cloned *C. elegans* DNA was used for PCR amplifications, for direct sequencing, or for subcloning (Sambrook *et al*., 1989). All PCR for cloning was performed with AccuTaq LA Polymerase (Sigma-Aldrich, St Louis, MO). Clones, primer sequences, and PCR conditions are available upon request. DNA sequencing was performed by the University of Alabama at Birmingham Genomics Core Facility of the Heflin Center for Human Genetics.

DNA and protein sequence analyses

Genome sequence information was obtained from the National Center for Biotechnology Information (http://www.ncbi.nlm.nih.gov/). Gene and protein sequences were identified using the *C. elegans* database Wormbase and references therein (http://www.wormbase.org). BLAST searches to identify homologs in human, mouse, and *S. purpuratus* were performed using the National Center for Biotechnology Information (NCBI) BLAST service (http://www.ncbi.nlm.nih.gov/BLAST/). Protein sequence alignments were performed and conserved motifs were identified using ClustalW (http://www.ebi.ac.uk/clustalw/).

Strains

Worm strains were obtained from the *Caenorhabditis* Genetics Center, *C. elegans* Knock-out Consortium, and National BioResource Project in Japan. Strains were grown

using standard *C. elegans* growth methods (Brenner, 1974) at 22°C unless otherwise stated. The wild-type strain was N2 Bristol. The following mutations were used: RB743 *nph-1(ok500)II*, JT6924 *daf-19(m86)II;daf-12(sa204)X*, FX2705 *xbx-7(tm2705)III*, FX2452 *tza-1(tm2452)IV*, FX925 *nph-4(tm925)V*, JT204 *daf-12(sa204)X*, RB1682 *tza-2(ok2092)X*, YH560 *nph-1(ok500)II;xbx-7(tm2705)III*, YH559 *nph-1(ok500)II;tza-1(tm2452)IV*, YH561 *nph-1(ok500)II;tza-2(ok2092)*,YH513 *xbx-7(tm2705)III;nph-4(tm925)V*, YH482 *tza-1(tm2452);nph-4(tm925)V*, and YH496 *nph-4(tm925)V;tza-2(ok2092)X*. RB743, FX2705, FX2452, FX925, and RB1682 were outcrossed three times and genotyped by PCR prior to analysis. The following extrachromosomal arrays were used: *yhEx279* and *yhEx281* were used for *xbx-7::YFP*, *tza-1::CFP*, and *tza-2::CFP* expression experiments; *yhEx240* and *yhEx288* were used for DAF-19 regulation of *xbx-7::YFP*, *tza-1::DsRed2*, and *tza-2::CFP* expression experiments; *yhEx232*, *yhEx285*, *yhEx290*, and *yhEx293* were used for TZA-2::CFP, XBX-7::YFP, and TZA-1::YFP localization analyses; *yhEx149* and *yhEx232* were used for localization of CHE-13::YFP in cilia of single mutants; *yhEx142*, *yhEx149*, *yhEx232*, *yhEx285*, and *yhEx290* were used for analysis of localization of NPH-1::CFP, NPH-4::YFP, TZA-2::CFP, XBX-7::YFP, and TZA-1::YFP in single mutants; *yhEx298*, *yhEx300*, *yhEx301*, *yhEx307*, *yhEx308*, and *yhEx309* were used for localization of CHE-13::YFP in double mutants; *yhEx281* and *yhEx297* were used for *xbx-7::YFP* expression experiments in double mutants; *yhEx149*, *yhEx232*, *yhEx298*, *yhEx300*, *yhEx301*, *yhEx307*, *yhEx308*, and *yhEx309* were used for CHE-13::YFP/CFP localization in cilia length measurements; *yhEx311* and *yhEx313* were used for *tza-1::DsRed2* and *f16f9.3::GFP* expression experiments.

Generation of constructs and strains

Vectors used for generating transcriptional and translational fusion constructs were modified from pPD95.81 (a gift from A. Fire). pCJF6 (CFP), pCJF7 (YFP), pCJ102 (DsRed2), pCJF36 (CHE-13::CFP), pCJF37 (CHE-13::YFP), pCJ146 (NPH-4::YFP), and pCJ148 (NPH-1::CFP) were generated as previously described (Winkelbauer *et al.*, 2005). pCJ309 (*xbx-7::YFP*), pCJ261.2 (*tza-1::DsRed2*), and pCJ257 (*tza-2::CFP*) were generated by inserting pCJF7, pCJ102, and pCJF6, respectively, with 1500 bp, 1200 bp, and 1000 bp promoter fragments amplified from N2 genomic DNA corresponding to the regions immediately upstream and slightly downstream of *xbx-7* ATG, *tza-1* ATG, and *tza-2* ATG, respectively. pCJ312 (*tza-1::CFP*) was generated by transferring the 1200 bp insert of pCJ261.2 into pCJF6. pCJ318 (XBX-7::YFP) and pCJ308 (TZA-1::YFP) were generated by inserting pCJF7 with a fragment consisting of the 1500 bp promoter and genomic region (covering the first 10 exons) of *xbx-7* or a fragment consisting of the 1200 bp promoter and genomic region of *tza-1*, respectively. pCJ271 (TZA-2::CFP) was generated by inserting pCJF6 with a fragment consisting of the 1000 bp promoter and genomic region of *tza-2*. pCP41 (*f16f9.3::GFP)* was generously provided by S. Shaham (The Rockefeller University). All PCR was performed using AccuTaq-LA DNA Polymerase (Sigma, St. Louis, MO, USA) according to the manufacturer's instructions. Transgenic worms were generated as previously described (Mello *et al.*, 1991).

Imaging

Worms were anesthetized using 10 mM Levamisole and immobilized on 2% agar

pads for imaging. Worms were examined using a Nikon Eclipse TE200 inverted microscope and images captured with a CoolSnap HQ camera (Photometrics, Tuscon, AZ, USA). Shutters and filters were computer driven. Images were processed using Metamorph software (Universal Imaging, Downingtown, PA, USA). Confocal analysis was performed on a Leica DMIRBE inverted epifluorescence / Nomarski microscope outfitted with Leica TCS NT SP1 Laser Confocal optics (Leica. Inc., Exton, PA, USA). Optical sections through the Z axis were generated using a stage galvanometer. Confocal images were processed with ImageJ (U. S. National Institutes of Health, Bethesda, Maryland, USA) and Voxx 2.09d (Indiana University School of Medicine, Indianapolis, IN, USA). Further processing of images was performed using Photoshop 7.0 (Adobe Systems, Inc., San Jose, CA, USA).

Yeast two-hybrid assay

Full-length *xbx-7*, *tza-1*, and *tza-2* cDNA was amplified from cDNA library using AccuTaq LA Polymerase (Sigma-Aldrich, St Louis, MO) and sequence-specific primers flanked by unique restriction enzyme sites. The resulting PCR fragments were cloned into the vectors pGBKT7 and pGADT7 (BD Biosciences Clontech). Interaction experiments were performed according to the MATCHMAKER 3 Yeast two-hybrid manual (BD Biosciences Clontech) as described previously (Haycraft *et al.*, 2003).

DAF-19 regulation

To asses DAF-19 regulation in vivo, the transgenic line YH493 was generated by injection of *xbx-7::YFP* into JT6924, and YH380 was generated by injection of *tza-*

1::DsRed2 and *tza-2::CFP* into JT6924. These strains were then crossed to JT204 to achieve *daf-19*(+) background. The strains used contain a mutation in *daf-12(sa204)X* to suppress the Daf-c phenotype of *daf-19(m86)II*.

RT-PCR

RNA was isolated as described previously (Haycraft *et al*., 2003) from *xbx-7(tm2705)*, *tza-1(tm2452)*, and *tza-2(ok2092)* mutants. Reverse transcribed RNA was generated using Superscript II Reverse Transcriptase (Invitrogen, Carlsbad, CA, USA) using the manufacturer's instructions. Fragments spanning the deleted region of each respective gene were then amplified by PCR and sequenced.

Assays

Dye-filling using DiI (Molecular Probes, Carlsbad, CA, USA) and osmotic avoidance assays were performed as described previously (Starich *et al*., 1995). The ability of *C. elegans* strains to form dauer stages was tested as described previously (Starich *et al*., 1995). Chemotaxis assays to volatile attractants were performed as described previously (Winkelbauer *et al*., 2005). Foraging behavior analysis was performed with slight modification of that described previously (Fujiwara *et al*., 2002). Briefly, a single young adult worm (rather than L4 stage worms) was placed in the center of a uniformly sized lawn of bacteria on a 6 cm plate and was allowed to move freely for 18 hours at 20°C before being removed from the plate by aspiration. Tracking was then quantified by counting the number of 3x3 mm squares on a grid the worm tracks touched.

RESULTS

xbx-7, tza-1, and tza-2 encode the B9 family of proteins in C. elegans

The B9 protein domain is present within only three human proteins, MKS1, B9D2 (B9 protein Domain 2), and B9D1 (B9 protein Domain 1). The function of this 104-amino acid motif is unknown. While the molecular role of B9D1 has not been explored, MKS1 as well as the B9D2 homolog in *P. tetraurelia* (ICIS-1) were recently described as proteins functioning in the process of ciliogenesis (Dawe *et al.*, 2007b; Ponsard *et al.*, 2007). To explore the possibility that the B9 domain proteins are functionally related in regards to cilia signaling activities and ciliopathies in MKS, we characterized the homologs of these proteins in *C. elegans*. As in mammals, *C. elegans* has three proteins with the B9 motif. These include the previously described XBX-7 (X-box promoter element regulated 7), which corresponds to mammalian MKS1, TZA-1 (Transition Zone-Associated 1), which corresponds to mammalian B9D2, and TZA-2 (Transition Zone-Associated 2), which corresponds to mammalian B9D1 (Figure 1, A).

To assess the conserved nature of the family of B9 proteins, we compared the putative homologs across several vertebrate and invertebrate species. Mammalian MKS1 and *C. elegans* XBX-7 are the most diverged of the B9 homologs and show the strongest similarities in the C-terminal regions of the proteins and within the B9 domains. In contrast, both TZA-1 and TZA-2 share homology with their mammalian counterparts, B9D2 and B9D1, respectively, throughout nearly their entire lengths.

xbx-7, tza-1, and tza-2 are coexpressed in ciliated sensory neurons and are dependant on DAF-19

Previous studies have shown that expression of several *C. elegans* genes associated with IFT and ciliogenesis, as well as homologs of genes involved in human cystic kidney disorders (e.g. BBS and NPHP associated genes), are regulated by the DAF-19 transcription factor (Blacque et al., 2005; Collet et al., 1998; Efimenko et al., 2005; Swoboda et al., 2000; Winkelbauer et al., 2005). DAF-19 is required for cilia formation and regulates expression of genes in ciliated sensory neurons through an X-box promoter element typically found within the first 200 nucleotides upstream of the translational start site (Efimenko et al., 2005; Swoboda et al., 2000). Genome sequence-based searches have identified *xbx-7*, *tza-1*, and *tza-2* as potential DAF-19 targets since they contain a conserved X-box motif in each of their respective promoters (Efimenko *et al.*, 2005). The X-boxes found in the promoters of these genes are located at position -69 of *xbx-7*, position -66 of *tza-1*, and position -84 of *tza-2,* relative to the start of translation (Figure 1, B). Previous data indicates that *xbx-7*, *tza-1*, and *tza-2* are all expressed in the ciliated amphid and labial neurons in the head and in the phasmid neurons at the tail of *C. elegans* (Blacque *et al.*, 2005; Efimenko *et al.*, 2005). Utilizing transgenic lines coexpressing transcriptional fusions *xbx-7::YFP* and *tza-1::CFP* or *xbx-7::YFP* and *tza-2::CFP*, we also observed expression of these genes specifically in ciliated sensory neurons and additionally found that their expression was overlapping (Supplementary Figure 1). Furthermore, our analyses revealed that expression of *tza-1::DsRed2* and *tza-2::CFP* in ciliated sensory neurons was dependant on DAF-19 as was previously shown for *xbx-7* (Efimenko *et al.*, 2005; Figure 2). This was demonstrated by generating transgenic lines with the transcriptional fusion constructs in the *daf-19(m86)* mutant background. Expres-

sion from these transgenes was abolished in the *daf-19(m86)* mutants but was recovered after a single outcross to *daf-19* wild-type worms (Figure 2).

XBX-7, TZA-1, and TZA-2 localize to the base of cilia

To determine the localization of the XBX-7, TZA-1, and TZA-2 proteins, we generated transgenic lines coexpressing B9 protein translational fusions with CFP or YFP under the control of their endogenous promoters (XBX-7::YFP, TZA-1::YFP, and TZA-2::CFP) and a translational fusion of the IFT protein CHE-13 with CFP or YFP, which we utilized as a cilia and transition zone marker. TZA-1::YFP, TZA-2::CFP, and XBX-7::YFP (corresponding to the 10-exon splice variant), were all detected specifically at the transition zones between cilia and the distal end of the dendrites of ciliated sensory neurons and were not detected in cilia axonemes as marked by CHE-13::CFP (Figure 3). This localization to the base of cilia is similar to that reported for MKS1 (Dawe *et al.*, 2007b). On closer inspection of TZA-1::YFP, we noted that it did not entirely colocalize with CHE-13::CFP in the head and tail neurons; TZA-1::YFP localized to a domain that extended beyond the transition zones into the dendrites away from the cilia and toward the cell bodies (Figure 3, C and G). The difference in the localization of TZA-1 was further examined in worms coexpressing both TZA-1::YFP and TZA-2::CFP (Figure 3, E and I). In addition to overlapping TZA-2::CFP at the transition zones, TZA-1::YFP was observed immediately posterior to TZA-2::CFP in the amphid dendrites of the head and anterior to TZA-2::CFP in the phasmid dendrites of the tail.

Analysis of xbx-7, tza-1, and tza-2 mutant alleles

Previous data in mammalian cells have indicated that disrupting MKS1 by siRNA results in defects in cilia formation. This appears to be due to abnormalities in cell polarization and in apical positioning of the centrosomes, which are required for basal body and cilia formation (Dawe *et al.*, 2007b). Similarly, disruption of the B9D2 homolog by RNAi in *P. tetraurelia* was found to interfere with cilia stability or formation (Ponsard *et al.*, 2007), but the mechanism by which this occurred was not determined.

To better assess the function of the B9 proteins and their potential role in ciliogenesis, we obtained genetic mutants FX2705 *xbx-7(tm2705)*, FX2452 *tza-1(tm2452)*, and RB1682 *tza-2(ok2092)* from the National Bioresource Project and the *C. elegans* Knockout Consortium. FX2705 *xbx-7(tm2705)* contains an internal genomic deletion of nucleotides 591-780 that begins in intron 2 and extends into exon 4, upstream of the region encoding the XBX-7 B9 domain (Figure 1, B). RT-PCR analysis of the *tm2705* transcript revealed that this deletion does not cause a shift in the reading frame and would encode a protein lacking amino acids 69-142 (Supplementary Figure 2, A). FX2452 *tza-1(tm2452)* is an internal deletion that removes nucleotides 446-724 of *tza-1*. This deletion, which spans through part of intron 1 into exon 3, disrupts much of the TZA-1 B9 domain coding region (Figure 1, B). RT-PCR analysis of the *tm2452* transcript revealed that this deletion does not cause a frameshift, and the predicted protein would lack 47 (30-77) out of 175 amino acids (Supplementary Figure 2, B). The RB1682 *tza-2(ok2092)* allele contains a deletion of nucleotides 574-1380. This deletion spans part of exon 2 through a portion of exon 3, directly disrupting the region encoding the TZA-2 B9 motif (Figure 1, B). RT-PCR of the *ok2092* transcript revealed that the allele contains a

frameshift producing a putative protein consisting of the first 42 correct amino acids followed by 49 altered amino acids (Supplementary Figure 2, C).

Disruption of the B9 genes does not overtly affect cilia morphology in C. elegans

To begin analyzing the *B9 gene* mutants and their potential effects on ciliogenesis, we first evaluated the ability of *xbx-7(tm2705)*, *tza-1(tm2452)*, and *tza-2(ok2092)* mutant worms to absorb fluorescent hydrophobic dye (DiI) into the dendrites and cell bodies of the amphid and phasmid neurons via cilia that are exposed to the external environment of the worm (Perkins *et al.*, 1986; Starich *et al.*, 1995). IFT mutants such as *osm-5*, *che-13*, and *xbx-1* cannot dye-fill due to gross cilia morphology defects, and likewise, mutants of BBS homologs such as *bbs-7* and *bbs-8* also have cilia structure and dye-filling deficiencies (Blacque et al., 2004; Haycraft et al., 2003; Haycraft et al., 2001; Schafer et al., 2003). In contrast, mutations in the NPHP homologs *nph-1* and *nph-4* reportedly do not compromise dye-filling (Jauregui and Barr, 2005; Winkelbauer *et al.*, 2005), although morphological defects in the cilia on a subset of the sensory neurons of these worms have recently been observed (Jauregui *et al*., *in press* 2008).

In contrast to the cilia null mutant *daf-19(m86)* worms, the *xbx-7(tm2705)*, *tza-1(tm2452)*, and *tza-2(ok2092)* mutant strains efficiently absorbed DiI into the amphid and phasmid neurons as was shown for the wild-type control (Figure 4, A; phasmid data is not shown). However, as seen in the *nph-4(tm925)* mutants, discrete regions of dye accumulation were evident along the dendrites of the *B9 gene* mutants. These pockets of dye accumulation were not reported in previous studies, and their cause is unknown. We additionally generated worm strains with all possible combinations of *B9 gene* mutations

including the *B9 gene* triple homozygous mutant. None of these compound mutants exhibited any discernable defects in DiI uptake apart from occasional accumulations of dye along the dendrites as seen in the single mutants (data not shown). To further analyze the possible effects that disruption of the B9 proteins may have on cilia morphology, we generated *xbx-7(tm2705)*, *tza-1(tm2452)*, and *tza-2(ok2092)* mutant strains each expressing CHE-13::YFP as a cilia marker. Consistent with their normal dye-filling phenotype, we could detect no alterations in CHE-13::YFP localization or signal in either *xbx-7(tm2705)*, *tza-1(tm2452)*, or *tza-2(ok2092)* mutant backgrounds (Figure 4, B).

In agreement with the absence of cilia morphological defects, none of the *B9 gene* mutants exhibited any defects in other processes linked to proper cilia structure such as chemotaxis toward a variety of attractants, osmotic avoidance, and dauer formation (data not shown) (Culotti and Russell, 1978; Dusenbery et al., 1975; Perkins et al., 1986; Riddle et al., 1981; Starich et al., 1995). Lifespan length and male mating behavior, additional processes dependant on cilia function in *C.* elegans, were not assayed in the *B9 gene* mutants (Apfeld and Kenyon, 1999; Liu and Sternberg, 1995).

At the level of analysis conducted here using the dye-filling assay and observing the expression and localization of an IFT protein in the mutant backgrounds of the *tm2705*, *tm2452*, and *ok2092* alleles, cilia appear to not be significantly affected by disruption of the B9 proteins. These data are in contrast to the siRNA results generated for MKS1 in mammalian cells and the RNAi data generated for ICIS-1 in *P. tetraurelia* (Dawe *et al.*, 2007b; Ponsard *et al.*, 2007).

TZA-1 is required for XBX-7 and TZA-2 localization at the base of cilia

Previously, TZA-1 and TZA-2 were identified as putative binding partners using yeast two-hybrid analysis as part of a large scale interactome study (Li *et al.*, 2004), and together with our finding that all the B9 proteins colocalize to the transition zones (Figure 3), we hypothesized they function at the base of cilia as part of a protein complex. This possibility was explored using a genetic approach to assess whether a mutation in one B9 protein has an effect on the localization of another B9 protein at the transition zones. We crossed wild-type worms expressing either XBX-7::YFP, TZA-1::YFP, or TZA-2::YFP into the other *B9 gene* mutants (i.e. XBX-7::YFP into *tza-1(tm2452)* or *tza-2(ok2092)*). In both *tza-1(tm2452)* and *tza-2(ok2092)* mutants, XBX-7::YFP failed to localize to the transition zones (Figure 5, A). In contrast, TZA-1::YFP localization at the base of cilia was not affected in the background of either *xbx-7(tm2705)* or *tza-2(ok2092)* (Figure 5, B). Additionally, TZA-2::CFP was not present at the transition zone in *tza-1(tm2452)* mutants (Figure 5, C).

To examine the possibility XBX-7 is anchored at the transition zones by either TZA-1 or TZA-2, we employed a yeast two-hybrid assay to test for direct protein-protein interactions. Although we were able to duplicate the interaction between TZA-1 and TZA-2 reported previously (Li *et al.*, 2004), we observed no growth on selective media of yeast strains expressing both XBX-7 and either TZA-1 or TZA-2 (Supplementary Figure 3). This data raises the possibility that XBX-7 associates with the B9 protein complex by an additional unidentified factor.

Since the NPHP1 and NPHP4 homologs in *C. elegans* (NPH-1 and NPH-4, respectively) associate with each other at the base of cilia (Winkelbauer *et al.*, 2005), we were interested in exploring the possibility that the B9 and NPH proteins function as part

of the same complex. However, in *nph-1(ok500)* and *nph-4(tm925)* mutant strains expressing either XBX-7::YFP, TZA-1::YFP, or TZA-2::CFP, localization of the fluorescent reporters to the base of cilia was unaffected (Figure 5, D; *nph-1(ok500)* data not shown). Likewise, *xbx-7(tm2705)*, *tza-1(tm2452)*, or *tza-2(ok2092)* mutant strains expressing NPH-1::CFP or NPH-4::YFP exhibited no delocalization of either reporter protein (Supplementary Figure 4). Together, these data indicate that the B9 proteins form part of a complex at the base of cilia independent of the function of the NPH proteins.

tza-1, tza-2, and nph-4 mutants exhibit defects in foraging behavior

Given our finding that the *B9 gene* mutants did not have overt cilia morphology defects or exhibit abnormalities in chemotaxis or osmotic avoidance, we further assayed these worms for behavioral phenotypes associated with cilia dysfunction. Previous reports indicate that mutants lacking cilia display abnormal foraging behavior and exhibit a dwelling phenotype in the presence of food (Fujiwara et al., 2002; Kobayashi et al., 2007; Murayama et al., 2005). We tested the *B9 gene* mutants and *nph-4(tm925)* mutants in an 18-hour tracking assay and found that *tza-1(tm2452)* and *tza-2(ok2092)* worms exhibited slight but significant defects in foraging behavior (Figure 6; Table 1). *xbx-7(tm2705)* worms were no different than the N2 wild-type controls. Interestingly, the *nph-4(tm925)* worms also displayed a foraging defect that was significantly more severe than that observed in the *B9 gene* mutants.

The fact that NPH and B9 proteins colocalize at the base of cilia, have homologs associated with human cystic kidney disorders (NPHP1, NPHP4, and MKS1), and mutants show similar defects regarding foraging behavior together suggests there may be a

functional connection between the NPH and B9 proteins. We addressed this possibility by generating *xbx-7;nph-4*, *tza-1;nph-4*, and *nph-4;tza-2* double mutant worms and evaluated them for foraging activity. The results show that the three double mutant strains all had significantly more severe dwelling phenotypes than any of the single mutants alone (Figure 6, B; Table 1). Furthermore, the severity of the double mutant phenotypes was similar to that seen in cilia mutants such as *che-2, che-13,* and *osm-5* (Fujiwara *et al.*, 2002; Kobayashi *et al.*, 2007). Particularly surprising was the pronounced dwelling phenotype observed in *xbx-7;nph-4* double mutant worms since the *xbx-7(tm2705)* single mutants alone were no different than wild-type controls. Together, these data suggest that the B9 proteins and NPH-4 may function in parallel at the transition zone to regulate foraging behavior.

Disruption of both a B9 protein and NPH-4 causes defects in dye-filling

Our finding that worms with compound *B9 gene;nph-4* mutations displayed foraging defects that were significantly more severe than the single mutants alone and were similar to that exhibited by cilia mutants raised the possibility that these double mutants had morphologically abnormal cilia. To begin addressing this question, we utilized the dye-filling assay. In contrast to the single mutants, all three *B9 gene;nph-4* double mutants had defects in their ability to absorb DiI (Figure 7). Although some fluorescence was typically detected in the heads of *xbx-7;nph-4* double mutants, there were far fewer amphid neurons able to uptake dye than expected (Figure 7, A; Table 2). Additionally, only 52.7% of *xbx-7;nph-4* double mutants examined were able to dye-fill the phasmid neurons. *tza-1;nph-4* double mutants were almost completely defective in dye-filling in

both the amphid and phasmid neurons; only 5.4% and 1.8% of the worms analyzed exhibited any dye-filling in the head and tail, respectively (Figure 7, B; Table 2). Of those 5.4% that dye-filled in the head, none exhibited more than a few amphid neurons uptaking DiI. The *nph-4;tza-2* double mutants exhibited dye-filling defects similar to those observed in *tza-1;nph-4* double mutants (Figure 7, C; Table 2). However, unlike the *tza-1;nph-4* double mutants, none of the *nph-4;tza-2* double mutants analyzed displayed dye-filling in the phasmid neurons. Together, these dye-filling data suggest that *B9 gene;nph-4* double mutant worms either have gross cilia morphology defects, have defects in access of cilia to the external environment, or have defects in the process by which the dye is transported into the ciliated sensory endings.

Cilia morphology is altered in B9 gene;nph gene double mutants

To explore the mechanism by which the *B9 gene;nph-4* double mutants exhibit a synthetic dye-filling deficiency, we generated transgenic strains expressing CHE-13::YFP as a cilia marker in each of the three double mutant backgrounds. We observed that *xbx-7;nph-4* double mutant worms, which exhibited a relatively mild dye-filling defect in comparison to *tza-1;nph-4* and *nph-4;tza-2* double mutants, possessed cilia but lacked properly organized amphid cilia bundles (Figure 8, C). Interestingly, the disorganized amphid bundles consisted of a variable combination of normally positioned cilia, cilia localized posterior in relation to the rest of the bundle, and transition zones that sometimes altogether lacked cilia axonemes (Figure 8, C). These worms also expressed significantly shortened phasmid cilia that were often positioned away from their expected

location near the cuticle where the cilia normally are housed in the sheath/socket channel (Figure 8, C; Table 3).

More severe ciliary defects were evident in *tza-1;nph-4* and *nph-4;tza-2* double mutant worms expressing the cilia marker CHE-13::YFP. The amphid cilia bundles of these worms failed to properly form, and the few cilia in the head that were observed appeared shortened, were sometimes misplaced, and were at times oriented in aberrant directions (Figure 8, E and G). Phasmid cilia of these double mutant worms were almost always shortened, mispositioned, and occasionally oriented laterally in comparison to wild type (Figure 8, F, H; Table 3).

Since NPH-4 is required for NPH-1 localization to the transition zones, we were interested in determining whether the ciliary defects observed in the *B9 gene;nph-4* double mutants were due directly to compromised function of the mutant NPH-4 protein or caused instead by the loss of NPH-1 from the transition zones. To address this question, we generated *nph-1;xbx-7*, *nph-1;tza-1*, and *nph-1;tza-2* double mutant worms expressing the cilia marker CHE-13::YFP. Remarkably, these worms exhibited ciliary defects closely resembling those observed in the *B9 gene;nph-4* double mutants (Figure 9). Much like *xbx-7;nph-4* double mutants, *nph-1;xbx-7* double mutants had the least severe ciliary defects of the three strains. Interestingly, the amphid cilia bundles of *nph-1;xbx-7* double mutants were nearly indistinguishable from wild type, apart from rare instances of single cilia being positioned away from the bundle (Figure 9, A and C). However, more distinct defects were observed in the phasmid neurons which most often expressed cilia of normal length and positioning but occasionally appeared both shortened and mispositioned (Figure 9, D; Table 3). Likewise, the phenotype of *nph-1;tza-1* double mutants

mimicked that of *tza-1;nph-4* double mutants; fewer amphid cilia were observed and those present were disorganized and had shortened or no ciliary axonemes. (Figure 9, E). In the phasmid neurons of the tail, cilia were both short and mispositioned relative to wild type (Figure 9, F; Table 3). Interestingly, the phenotype of *nph-1;tza-2* double mutants differed somewhat from *nph-4;tza-2* double mutants; unlike *nph-4;tza-2* worms, the amphid cilia of *nph-1;tza-2* double mutants retained some semblance of organized bundles although shortened and mispositioned cilia were still observed (Figure 9, G). Phasmid cilia in these worms exhibited typical defects observed in the other *B9 gene;nph gene* double mutants (Figure 9, H; Table 3).

Dendrites of ciliated sensory neurons are malformed in B9 gene;nph gene double mutants but associated sheath glia are intact

To further analyze the altered morphology of ciliated sensory neurons in *B9 gene;nph gene* double mutants, we generated transgenic mutant worms that expressed the transcriptional *xbx-7::YFP* fusion, which enabled us to visualize the dendrites of the neurons. In the *xbx-7;nph-4* double mutants, the dendrites of the phasmid neurons in the tail were sometimes not properly extended as compared to the phasmid dendrites of *xbx-7(tm2705)* single mutant worms (Figure 10, A and B). Predictably, *tza-1;nph-4,* and *nph-4;tza-2* double mutants expressing transcriptional *xbx-7::YFP* fusion displayed severely shortened phasmid dendrites in comparison to *tza-1(tm2452)* and *tza-2(ok2092)* single mutant worms (Figure 10, C-F). These data are reflective of our previous observations in *B9 gene;nph gene* double mutants that phasmid cilia were positioned at random locations

between the cell bodies of the neurons and the cuticle opening where the cilia are normally found.

In wild-type *C. elegans*, the ciliated sensory neurons in both the head and tail of the worm are associated with sheath glia cells that surround the cilia at the distal tips of the dendrites. Immediately adjacent to the transition zones, the dendrites form physical attachments with the surrounding sheath cell. This point of attachment is a form of an adherens junction known as a belt junction due to its ring-like appearance (Perkins *et al.*, 1986). To determine whether the *B9 gene;nph gene* double mutants had altered sheath cell morphology in addition to malformed dendrites of the ciliated sensory neurons, we generated transgenic wild-type and mutant worms that expressed the *tza-1::DsRed2* transcriptional fusion as a ciliated sensory neuron marker and the *f16f9.3::GFP* transcriptional fusion, which specifically stains amphid and phasmid sheath cells (gift of Dr. S. Shaham, The Rockefeller University, manuscript in preparation). In both the head and tail of *tza-1;nph-4* double mutant worms, sheath cell morphology was indistinguishable from wild type (Figure 10, G and H). Although the distal tips of the amphid neuron dendrites in *tza-1;nph-4* double mutants were properly surrounded and could potentially still be physically attached, it was evident in the tails of the double mutants that the shortened phasmid neuron dendrites were no longer associated with the distal ends of the sheath cells. Together, these data suggest that the B9 and NPH proteins function redundantly as part of a mechanism required for dendrite patterning and attachment to sheath cells and for ciliogenesis.

DISCUSSION

Ciliopathies in humans include the phenotypes seen in syndromes such as MKS, NPHP, JBTS, and BBS where most of the genes identified encode proteins that localize to cilia or basal bodies. One of the common phenotypes associated with defects in cilia signaling is the formation of renal cysts. This is seen for the cilia-localized proteins polycystin 1 and polycystin 2, which are affected in PKD. Mutations in the PKD genes do not disrupt cilia structure but do result in the loss of a flow-regulated mechano-sensitive calcium signal, and in the case of polycystin-1 altered AP-1 pathway activation and increased mTOR activity (Low *et al.*, 2006; Shillingford *et al.*, 2006). Proteins involved in the cystic renal pathology in NPHP patients localize to the base of cilia; however, the roles of many of the NPHP proteins are largely unknown. Mutations in *nph-1* and *nph-4* in *C. elegans* cause defects in morphology of a subset of cilia on a few amphid neurons in the hermaphrodite and in sensory neurons that are specific to the male (Jauregui *et al.*, *in press* 2008) and result in several phenotypes typically associated with disruption of cilia signaling pathways (Jauregui and Barr, 2005; Winkelbauer *et al.*, 2005). It is uncertain whether these phenotypes are due to loss of a specific signaling pathway mediated by the NPH proteins or due to ultrastructural ciliary defects that may disrupt multiple pathways. In contrast to PKD- and NPHP-associated proteins, evidence suggests that MKS1 and meckelin, which are involved in renal cyst formation in MKS, affect cell polarization, centriole migration, and severely disrupt cilia assembly, at least based on siRNA knockdown data (Dawe *et al.*, 2007b). An intriguing finding that is emerging with regards to MKS, NPHP, and JBTS is that genes associated with one of these syndromes are being identified as responsible for the phenotypes in one or both of

the other disorders. These data argue that the syndromes represent a spectrum of the same underlying defect and that the resulting phenotypes will be dictated by the nature of the mutation occurring in these genes. However, other than their colocalization to cilia or basal bodies, there is currently very little known about how proteins associated with MKS, NPHP, or JBTS are functionally related or how mutations in one of the genes may affect the localization and/or activity of another.

To begin addressing these questions, we are using C. *elegans* as a model system to elucidate the functional relationships between cilia and proteins associated with human cystic kidney disease syndromes. Here we analyzed the connection between the MKS1 homolog XBX-7 and its related B9 protein family members and the NPHP1 and NPHP4 homologs, NPH-1 and NPH-4. Intriguingly, we demonstrate that all three B9 genes in *C. elegans* are co-regulated by the same transcription factor in ciliated sensory neurons and that the B9 proteins localize to the transition zones at the base of the sensory cilia. Similar localization to basal bodies has been reported for the XBX-7 homolog in mammalian cells, suggesting conserved function (Dawe *et al.*, 2007b). However, siRNA mediated knockdown of MKS1 expression in mammalian cells or RNAi knockdown of the TZA-1 homolog in *P. tetraurelia* suggest these proteins are required for cilia assembly or formation (Dawe *et al*., 2007b; Ponsard *et al*., 2007). Additionally, during review of this manuscript a conditional mutant in the *tza-1* mouse homolog was described. These mutant mice had absent or truncated cilia and systemic phenotypes typically associated with disruption of cilia in mammals (Town *et al.*, 2008). In contrast, our analysis of single, double, or triple mutations in the B9 genes in *C. elegans* did not reveal cilia morphology defects unless these mutations were combined with mutations in either *nph-1* or *nph-4*. It

is plausible that the *B9 gene* single mutants exhibit ultrastructural abnormalities in cilia or subsets of cilia that would not be detectable by the methods used in this analysis. Alternatively, the discrepancy could be due in part to the nature of the alleles we analyzed. *xbx-7*(*tm2705*) and *tza-1*(*tm2452*) both result in internal deletions which do not cause frame shifts. Thus, the proteins encoded by *xbx-7(tm2705)* and *tza-1(tm2452)* may retain partial function with respect to their potential roles in ciliogenesis. In the case of the *xbx-7(tm2705)* mutants, this could explain the consistently milder phenotype relative to that seen in the other *B9 gene* mutants when crossed with an *nph gene* mutant. Although the *tza-1(tm2452)* mutation is an internal in-frame deletion, we show that this mutation results in loss of both XBX-7 and TZA-2 from the transition zones, which would thus be expected to acerbate the phenotype as was observed. In contrast, the *tza-2(ok2092)* allele results in deletion of most of the protein including the B9 domain and is thought to represent a null mutation.

Our genetic analyses in *C. elegans* indicate that the B9 proteins form part of a complex at the transition zone. This is supported by data showing that XBX-7 localization was dependent on the presence of both TZA-1 and TZA-2, and TZA-2 required only TZA-1 for proper localization. In contrast, disruption of TZA-2 or XBX-7 did not alter localization of TZA-1. We interpret these data to indicate that TZA-1 functions early in the assembly of a complex containing the B9 proteins followed by TZA-2 and subsequently by XBX-7. It is unknown whether the loss of fluorescent signal from the transition zones was due to the unincorporated proteins being diffused throughout the neurons or alternatively due to destabilization and degradation of these proteins. However, using a yeast two-hybrid assay, we observed a positive interaction between TZA-1 and TZA-2,

suggesting at least in the case of TZA-2 that the protein was mislocalized due to failure in assembly into the complex at the transition zone. In contrast, we did not observe a physical interaction between XBX-7 and the other B9 proteins, suggesting that there is an unknown factor that is responsible for anchoring XBX-7 in the complex. Whether there is a similar hierarchy of complex assembly with regards to the mammalian proteins remains to be determined.

Since the NPHP protein homologs NPH-1 and NPH-4 are part of a complex that localizes similarly to the B9 proteins at the transition zone (Winkelbauer *et al.*, 2005), and mutations in the NPHP proteins result in cystic renal disease in humans and mice, we explored the possibility that the *C. elegans* B9 and NPH proteins were functionally related or perhaps components of the same complex. However, our analysis of the localization of NPH-1 and NPH-4 in the *B9 gene* mutants revealed there were no effects on their localization to the transition zones nor were the B9 proteins affected by mutations in *nph-1* or *nph-4*. Thus, there does not appear to be a direct link between the B9 proteins and the NPH proteins with regards to complex formation at the base of cilia.

Cilia mutants in *C. elegans* exhibit numerous behavioral and sensory defects including abnormalities in chemotaxis, osmotic avoidance deficiencies, altered dauer formation, and a marked reduction in foraging activity in the presence of food. In the *B9 gene* mutants, we did not observe defects in osmotic avoidance, chemotaxis, or dauer formation, in agreement with the presence of overtly normal cilia morphology. However, both the *tza-1(tm2452)* and *tza-2(ok2092)* mutants did exhibit subtle yet significant reductions in foraging behavior, which was not evident in the *xbx-7(tm2705)* mutants. Interestingly, we also found that *nph-4(tm925)* mutants had defects in foraging activity that

was significantly more severe than either *tza-1(tm2452)* or *tza-2(ok2092)* mutants. These observations led us to evaluate whether the foraging behavior defects in the *B9 gene* mutants were due to disruption of the same pathway affected in the *nph-4(tm925)* mutants. We analyzed this in *B9 gene;nph-4* double mutants and found that mutations affecting both the B9 proteins and NPH-4 resulted in a markedly more severe dwelling phenotype than either mutation alone. This phenotype was similar to that seen in worms completely lacking cilia, suggesting redundant functions of the B9 proteins and NPH-4 at the base of cilia.

The *B9 gene;nph-4* double mutants were also unable to normally dye-fill. This was due to abnormalities in bundling, orientation, or length of the cilia along with gross cilia positioning defects caused by dendrite malformation. Additionally, we observed the same altered morphology in *B9 gene;nph-1* double mutants, suggesting that since NPH-4 is critical for the proper localization of NPH-1 to the transition zones, the defects observed in the *B9 gene;nph-4* double mutants can be attributed to the loss of NPH-1. The complex phenotype observed in these worms is unique among mutants defective in dye-filling. *daf-19* mutant worms exhibit phasmid neuron dendrites of varying lengths similar to those seen in the *B9 gene;nph gene* double mutants, but *daf-19* mutants lack all ciliary and transition zone structures (Swoboda *et al.*, 2000). Notably, centrioles positioned at the distal tips of the dendrites are detected by electron microscopy in *daf-19* mutants (Perkins et al., 1986). Since each of the B9 and nephrocystin genes are strongly regulated by the DAF-19 transcription factor and are therefore not expressed in *daf-19* mutant worms, it seems likely that the B9 proteins and nephrocystins will not be critical for positioning the centrioles at the distal tips of the dendrites. Disruption of the forkhead do-

main transcription factor gene *fkh-2* results in shortened dendrites and cilia morphology defects, but this phenotype is specific to AWB neurons alone (Mukhopadhyay *et al.*, 2007). *B9 gene;nph gene* double mutants may most closely resemble *mec-8* mutants in which amphid cilia fail to fully penetrate the sheath glia, are sometimes misoriented laterally, and do not fasciculate at the sheath/socket channel (Perkins *et al.*, 1986). However, gross dendrite morphology defects have not been reported in *mec-8* mutants. Although we observed grossly normal sheath cells in *B9 gene;nph gene* double mutants, we have not directly determined whether these cells cooperate with the socket cells to properly form the channels through which the cilia normally project. It is likely, however, that the channels do properly form since the *B9 gene;nph gene* mutants are still able to uptake DiI to some extent, indicating that on occasion some cilia are correctly formed and exposed to the external environment.

The additive effects seen in the *B9 gene;nph gene* double mutants indicate that the B9 proteins and NPH proteins likely function redundantly to coordinate how cilia and dendrites will form. It is possible that the phenotypes we see in these double mutants are related to those observed when the B9 proteins are singularly disrupted in other biological systems. Together, our findings provide insights into the allelic nature of the genes that can be involved in multiple syndromes and more importantly indicate that the mammalian homologs of the B9 domain proteins TZA-1 and TZA-2 are strong candidates as loci involved in the pathology of MKS, NPHP, or JBTS patients for which the underlying genetic defects have not yet been identified.

AKNOWLEDGEMENTS

We gratefully acknowledge Drs. M. Barr, C. Haycraft, N. Katsanis, and M. Leroux for valuable discussions and critical reading of the manuscript. We thank A. Tousson of the UAB Imaging Facility and J. Lehman for assistance in imaging. We thank J. Davenport for assistance in statistical analysis. We thank M. Croyle and V. Roper for technical assistance. The *C. elegans* Genome Sequencing Consortium provided sequence information, and the *Caenorhabditis* Genetics Center, which is funded by the National Institutes of Health, provided some of the C. elegans strains used in this study. We thank the *C. elegans* Knockout Consortium and the National BioResource Project in Japan for the *xbx-7(tm2705)*, *tza-1(tm2452)*, and *tza-2(ok2092)* deletion mutants. This work was supported by NIH R01 DK65655 to B.K.Y. and sponsored by the Laboratory Directed Research and Development Program of Oak Ridge National Laboratory (ORNL), managed by UT-Battelle, LLC for the U. S. Department of Energy under Contract No. DE-AC05-00OR22725 to E.J.M. Additional support was provided by the P30 DK074038 UAB Recessive Polycystic Kidney Disease Research and Translational Core Center.

REFERENCES

Alexiev, B. A., Lin, X., Sun, C. C. and Brenner, D. S. (2006). Meckel-Gruber syndrome: pathologic manifestations, minimal diagnostic criteria, and differential diagnosis. *Arch Pathol Lab Med* **130**, 1236-8.

Apfeld, J. and Kenyon, C. (1999). Regulation of lifespan by sensory perception in Caenorhabditis elegans. *Nature* **402**, 804-9.

Arts, H. H., Doherty, D., van Beersum, S. E., Parisi, M. A., Letteboer, S. J., Gorden, N. T., Peters, T. A., Marker, T., Voesenek, K., Kartono, A. et al. (2007). Mutations in the gene encoding the basal body protein RPGRIP1L, a nephrocystin-4 interactor, cause Joubert syndrome. *Nat Genet* **39**, 882-8.

Attanasio, M., Uhlenhaut, N. H., Sousa, V. H., O'Toole, J. F., Otto, E., Anlag, K., Klugmann, C., Treier, A. C., Helou, J., Sayer, J. A. et al. (2007). Loss of GLIS2 causes nephronophthisis in humans and mice by increased apoptosis and fibrosis. *Nat Genet* **39**, 1018-24.

Baala, L., Audollent, S., Martinovic, J., Ozilou, C., Babron, M. C., Sivanandamoorthy, S., Saunier, S., Salomon, R., Gonzales, M., Rattenberry, E. et al. (2007a). Pleiotropic effects of CEP290 (NPHP6) mutations extend to Meckel syndrome. *Am J Hum Genet* **81**, 170-9.

Baala, L., Romano, S., Khaddour, R., Saunier, S., Smith, U. M., Audollent, S., Ozilou, C., Faivre, L., Laurent, N., Foliguet, B. et al. (2007b). The Meckel-Gruber syndrome gene, MKS3, is mutated in Joubert syndrome. *Am J Hum Genet* **80**, 186-94.

Badano, J. L., Mitsuma, N., Beales, P. L. and Katsanis, N. (2006). The Ciliopathies: An Emerging Class of Human Genetic Disorders. *Annu Rev Genomics Hum Genet* **7**, 125-148.

Barr, M. M., DeModena, J., Braun, D., Nguyen, C. Q., Hall, D. H. and Sternberg, P. W. (2001). The Caenorhabditis elegans autosomal dominant polycystic kidney disease gene homologs lov-1 and pkd-2 act in the same pathway. *Curr Biol* **11**, 1341-6.

Beales, P. L., Bland, E., Tobin, J. L., Bacchelli, C., Tuysuz, B., Hill, J., Rix, S., Pearson, C. G., Kai, M., Hartley, J. et al. (2007). IFT80, which encodes a conserved intraflagellar transport protein, is mutated in Jeune asphyxiating thoracic dystrophy. *Nat Genet* **39**, 727-9.

Blacque, O. E. and Leroux, M. R. (2006). Bardet-Biedl syndrome: an emerging pathomechanism of intracellular transport. *Cell Mol Life Sci* **63**, 2145-61.

Blacque, O. E., Perens, E. A., Boroevich, K. A., Inglis, P. N., Li, C., Warner, A., Khattra, J., Holt, R. A., Ou, G., Mah, A. K. et al. (2005). Functional genomics of the cilium, a sensory organelle. *Curr Biol* **15**, 935-41.

Blacque, O. E., Reardon, M. J., Li, C., McCarthy, J., Mahjoub, M. R., Ansley, S. J., Badano, J. L., Mah, A. K., Beales, P. L., Davidson, W. S. et al. (2004). Loss of C. elegans BBS-7 and BBS-8 protein function results in cilia defects and compromised intraflagellar transport. *Genes Dev* **18**, 1630-42.

Brenner, S. (1974). The genetics of Caenorhabditis elegans. *Genetics* **77**, 71-94.

Chen, C. P. (2007). Meckel syndrome: genetics, perinatal findings, and differential diagnosis. *Taiwan J Obstet Gynecol* **46**, 9-14.

Cole, D. G., Diener, D. R., Himelblau, A. L., Beech, P. L., Fuster, J. C. and Rosenbaum, J. L. (1998). Chlamydomonas kinesin-II-dependent intraflagellar transport

(IFT): IFT particles contain proteins required for ciliary assembly in Caenorhabditis elegans sensory neurons. *Journal of Cell Biology* **141**, 993-1008.

Collet, J., Spike, C. A., Lundquist, E. A., Shaw, J. E. and Herman, R. K. (1998). Analysis of osm-6, a gene that affects sensory cilium structure and sensory neuron function in Caenorhabditis elegans. *Genetics* **148**, 187-200.

Culotti, J. G. and Russell, R. L. (1978). Osmotic avoidance defective mutants of the nematode Caenorhabditis elegans. *Genetics* **90**, 243-56.

Davenport, J. R., Watts, A. J., Roper, V. C., Croyle, M. J., van Groen, T., Wyss, J. M., Nagy, T. R., Kesterson, R. A. and Yoder, B. K. (2007). Disruption of intraflagellar transport in adult mice leads to obesity and slow-onset cystic kidney disease. *Curr Biol* **17**, 1586-94.

Dawe, H. R., Farr, H. and Gull, K. (2007a). Centriole/basal body morphogenesis and migration during ciliogenesis in animal cells. *J Cell Sci* **120**, 7-15.

Dawe, H. R., Smith, U. M., Cullinane, A. R., Gerrelli, D., Cox, P., Badano, J. L., Blair-Reid, S., Sriram, N., Katsanis, N., Attie-Bitach, T. et al. (2007b). The Meckel-Gruber Syndrome proteins MKS1 and meckelin interact and are required for primary cilium formation. *Hum Mol Genet* **16**, 173-86.

Deane, J. A., Cole, D. G., Seeley, E. S., Diener, D. R. and Rosenbaum, J. L. (2001). Localization of intraflagellar transport protein IFT52 identifies basal body transitional fibers as the docking site for IFT particles. *Current Biology* **11**, 1586-90.

Delous, M., Baala, L., Salomon, R., Laclef, C., Vierkotten, J., Tory, K., Golzio, C., Lacoste, T., Besse, L., Ozilou, C. et al. (2007). The ciliary gene RPGRIP1L is mutated in cerebello-oculo-renal syndrome (Joubert syndrome type B) and Meckel syndrome. *Nat Genet* **39**, 875-81.

Dusenbery, D. B., Sheridan, R. E. and Russell, R. L. (1975). Chemotaxis-defective mutants of the nematode Caenorhabditis elegans. *Genetics* **80**, 297-309.

Efimenko, E., Bubb, K., Mak, H. Y., Holzman, T., Leroux, M. R., Ruvkun, G., Thomas, J. H. and Swoboda, P. (2005). Analysis of xbx genes in C. elegans. *Development* **132**, 1923-34.

Fliegauf, M., Horvath, J., von Schnakenburg, C., Olbrich, H., Muller, D., Thumfart, J., Schermer, B., Pazour, G. J., Neumann, H. P., Zentgraf, H. et al. (2006). Nephrocystin specifically localizes to the transition zone of renal and respiratory cilia and photoreceptor connecting cilia. *J Am Soc Nephrol* **17**, 2424-33.

Fujiwara, M., Sengupta, P. and McIntire, S. L. (2002). Regulation of body size and behavioral state of C. elegans by sensory perception and the EGL-4 cGMP-dependent protein kinase. *Neuron* **36**, 1091-102.

Haycraft, C. J., Banizs, B., Aydin-Son, Y., Zhang, Q., Michaud, E. J. and Yoder, B. K. (2005). Gli2 and Gli3 localize to cilia and require the intraflagellar transport protein polaris for processing and function. *PLoS Genet* **1**, e53.

Haycraft, C. J., Schafer, J. C., Zhang, Q., Taulman, P. D. and Yoder, B. K. (2003). Identification of CHE-13, a novel intraflagellar transport protein required for cilia formation. *Exp Cell Res* **284**, 251-63.

Haycraft, C. J., Swoboda, P., Taulman, P. D., Thomas, J. H. and Yoder, B. K. (2001). The C. elegans homolog of the murine cystic kidney disease gene Tg737 functions in a ciliogenic pathway and is disrupted in osm-5 mutant worms. *Development* **128**, 1493-1505.

Hildebrandt, F. and Otto, E. (2005). Cilia and centrosomes: a unifying pathogenic concept for cystic kidney disease? *Nat Rev Genet* **6**, 928-40.

Hildebrandt, F. and Zhou, W. (2007). Nephronophthisis-associated ciliopathies. *J Am Soc Nephrol* **18**, 1855-71.

Jauregui, A. R. and Barr, M. M. (2005). Functional characterization of the C. elegans nephrocystins NPHP-1 and NPHP-4 and their role in cilia and male sensory behaviors. *Exp Cell Res* **305**, 333-42.

Jauregui, A. R., Nguyen, K. C. Q., Hall, D. H. and Barr, M. M. (*in press* 2008). The C. elegans nephrocystins act as global modifiers of cilium structure. *Journal of Cell Biology*.

Khaddour, R., Smith, U., Baala, L., Martinovic, J., Clavering, D., Shaffiq, R., Ozilou, C., Cullinane, A., Kyttala, M., Shalev, S. et al. (2007). Spectrum of MKS1 and MKS3 mutations in Meckel syndrome: a genotype-phenotype correlation. Mutation in brief #960. Online. *Hum Mutat* **28**, 523-4.

Kobayashi, T., Gengyo-Ando, K., Ishihara, T., Katsura, I. and Mitani, S. (2007). IFT-81 and IFT-74 are required for intraflagellar transport in C. elegans. *Genes Cells* **12**, 593-602.

Kozminski, K. G., Johnson, K. A., Forscher, P. and Rosenbaum, J. L. (1993). A motility in the eukaryotic flagellum unrelated to flagellar beating. *Proceedings of the National Academy of Sciences of the United States of America* **90**, 5519-23.

Li, S., Armstrong, C. M., Bertin, N., Ge, H., Milstein, S., Boxem, M., Vidalain, P. O., Han, J. D., Chesneau, A., Hao, T. et al. (2004). A map of the interactome network of the metazoan C. elegans. *Science* **303**, 540-3.

Liu, K. S. and Sternberg, P. W. (1995). Sensory regulation of male mating behavior in Caenorhabditis elegans. *Neuron* **14**, 79-89.

Low, S. H., Vasanth, S., Larson, C. H., Mukherjee, S., Sharma, N., Kinter, M. T., Kane, M. E., Obara, T. and Weimbs, T. (2006). Polycystin-1, STAT6, and P100 function in a pathway that transduces ciliary mechanosensation and is activated in polycystic kidney disease. *Dev Cell* **10**, 57-69.

Marshall, W. F. (2007). What is the function of centrioles? *J Cell Biochem* **100**, 916-22.

Mello, C. C., Kramer, J. M., Stinchcomb, D. and Ambros, V. (1991). Efficient gene transfer in C.elegans: extrachromosomal maintenance and integration of transforming sequences. *EMBO Journal* **10**, 3959-70.

Mollet, G., Salomon, R., Gribouval, O., Silbermann, F., Bacq, D., Landthaler, G., Milford, D., Nayir, A., Rizzoni, G., Antignac, C. et al. (2002). The gene mutated in juvenile nephronophthisis type 4 encodes a novel protein that interacts with nephrocystin. *Nat Genet* **32**, 300-5.

Mollet, G., Silbermann, F., Delous, M., Salomon, R., Antignac, C. and Saunier, S. (2005). Characterization of the nephrocystin/nephrocystin-4 complex and subcellular localization of nephrocystin-4 to primary cilia and centrosomes. *Hum Mol Genet* **14**, 645-56.

Morgan, D., Eley, L., Sayer, J., Strachan, T., Yates, L. M., Craighead, A. S. and Goodship, J. A. (2002). Expression analyses and interaction with the anaphase promoting complex protein Apc2 suggest a role for inversin in primary cilia and involvement in the cell cycle. *Hum Mol Genet* **11**, 3345-50.

Moyer, J. H., Lee-Tischler, M. J., Kwon, H. Y., Schrick, J. J., Avner, E. D., Sweeney, W. E., Godfrey, V. L., Cacheiro, N. L., Wilkinson, J. E. and Woychik, R. P. (1994). Candidate gene associated with a mutation causing recessive polycystic kidney disease in mice. *Science* **264**, 1329-33.

Mukhopadhyay, S., Lu, Y., Qin, H., Lanjuin, A., Shaham, S. and Sengupta, P. (2007). Distinct IFT mechanisms contribute to the generation of ciliary structural diversity in C. elegans. *Embo J* **26**, 2966-80.

Murayama, T., Toh, Y., Ohshima, Y. and Koga, M. (2005). The dyf-3 gene encodes a novel protein required for sensory cilium formation in Caenorhabditis elegans. *J Mol Biol* **346**, 677-87.

Murcia, N. S., Richards, W. G., Yoder, B. K., Mucenski, M. L., Dunlap, J. R. and Woychik, R. P. (2000). The Oak Ridge Polycystic Kidney (orpk) disease gene is required for left-right axis determination. *Development* **127**, 2347-55.

Orozco, J. T., Wedaman, K. P., Signor, D., Brown, H., Rose, L. and Scholey, J. M. (1999). Movement of motor and cargo along cilia. *Nature* **398**, 674.

Otto, E., Hoefele, J., Ruf, R., Mueller, A. M., Hiller, K. S., Wolf, M. T., Schuermann, M. J., Becker, A., Birkenhager, R., Sudbrak, R. et al. (2002). A gene mutated in nephronophthisis and retinitis pigmentosa encodes a novel protein, nephroretinin, conserved in evolution. *Am J Hum Genet* **71**, 1161-7.

Otto, E. A., Loeys, B., Khanna, H., Hellemans, J., Sudbrak, R., Fan, S., Muerb, U., O'Toole, J. F., Helou, J., Attanasio, M. et al. (2005). Nephrocystin-5, a ciliary IQ domain protein, is mutated in Senior-Loken syndrome and interacts with RPGR and calmodulin. *Nat Genet* **37**, 282-8.

Otto, E. A., Schermer, B., Obara, T., O'Toole, J. F., Hiller, K. S., Mueller, A. M., Ruf, R. G., Hoefele, J., Beekmann, F., Landau, D. et al. (2003). Mutations in INVS encoding inversin cause nephronophthisis type 2, linking renal cystic disease to the function of primary cilia and left-right axis determination. *Nat Genet* **34**, 413-20.

Ou, G., Koga, M., Blacque, O. E., Murayama, T., Ohshima, Y., Schafer, J. C., Li, C., Yoder, B. K., Leroux, M. R. and Scholey, J. M. (2007). Sensory ciliogenesis in Caenorhabditis elegans: assignment of IFT components into distinct modules based on transport and phenotypic profiles. *Mol Biol Cell* **18**, 1554-69.

Parisi, M. A., Bennett, C. L., Eckert, M. L., Dobyns, W. B., Gleeson, J. G., Shaw, D. W., McDonald, R., Eddy, A., Chance, P. F. and Glass, I. A. (2004). The NPHP1 gene deletion associated with juvenile nephronophthisis is present in a subset of individuals with Joubert syndrome. *Am J Hum Genet* **75**, 82-91.

Pazour, G. J., Dickert, B. L., Vucica, Y., Seeley, E. S., Rosenbaum, J. L., Witman, G. B. and Cole, D. G. (2000). Chlamydomonas IFT88 and its mouse homologue, polycystic kidney disease gene Tg737, are required for assembly of cilia and flagella. *Journal of Cell Biology* **151**, 709-18.

Perkins, L. A., Hedgecock, E. M., Thomson, J. N. and Culotti, J. G. (1986). Mutant sensory cilia in the nematode Caenorhabditis elegans. *Developmental Biology* **117**, 456-87.

Piperno, G., Siuda, E., Henderson, S., Segil, M., Vaananen, H. and Sassaroli, M. (1998). Distinct mutants of retrograde intraflagellar transport (IFT) share similar morphological and molecular defects. *Journal of Cell Biology* **143**, 1591-601.

Ponsard, C., Skowron-Zwarg, M., Seltzer, V., Perret, E., Gallinger, J., Fisch, C., Dupuis-Williams, P., Caruso, N., Middendorp, S. and Tournier, F. (2007). Identification of ICIS-1, a new protein involved in cilia stability. *Front Biosci* **12**, 1661-9.

Porter, M. E., Bower, R., Knott, J. A., Byrd, P. and Dentler, W. (1999). Cytoplasmic dynein heavy chain 1b is required for flagellar assembly in Chlamydomonas. *Mol Biol Cell* **10**, 693-712.

Riddle, D. L., Swanson, M. M. and Albert, P. S. (1981). Interacting genes in nematode dauer larva formation. *Nature* **290**, 668-71.

Roepman, R., Letteboer, S. J., Arts, H. H., van Beersum, S. E., Lu, X., Krieger, E., Ferreira, P. A. and Cremers, F. P. (2005). Interaction of nephrocystin-4 and RPGRIP1 is disrupted by nephronophthisis or Leber congenital amaurosis-associated mutations. *Proc Natl Acad Sci U S A* **102**, 18520-5.

Rosenbaum, J. and Witman, G. (2002). Intraflagellar transport. *Nat Rev Mol Cell Biol* **3**, 813-25.

Sambrook, J., Fritsch, E. F. and Maniatis, T. (1989). *Molecular Cloning: A Laboratory Manual*. Cold Spring Harbor, NY: Cold Spring Harbor Laboratory.

Sayer, J. A., Otto, E. A., O'Toole, J. F., Nurnberg, G., Kennedy, M. A., Becker, C., Hennies, H. C., Helou, J., Attanasio, M., Fausett, B. V. et al. (2006). The centrosomal protein nephrocystin-6 is mutated in Joubert syndrome and activates transcription factor ATF4. *Nat Genet* **38**, 674-81.

Schafer, J. C., Haycraft, C. J., Thomas, J. H., Yoder, B. K. and Swoboda, P. (2003). XBX-1 encodes a dynein light intermediate chain required for retrograde intraflagellar transport and cilia assembly in Caenorhabditis elegans. *Mol Biol Cell* **14**, 2057-70.

Scholey, J. M., Ou, G., Snow, J. and Gunnarson, A. (2004). Intraflagellar transport motors in Caenorhabditis elegans neurons. *Biochem Soc Trans* **32**, 682-4.

Shillingford, J. M., Murcia, N. S., Larson, C. H., Low, S. H., Hedgepeth, R., Brown, N., Flask, C. A., Novick, A. C., Goldfarb, D. A., Kramer-Zucker, A. et al. (2006). The mTOR pathway is regulated by polycystin-1, and its inhibition reverses renal cystogenesis in polycystic kidney disease. *Proc Natl Acad Sci U S A* **103**, 5466-71.

Smith, U. M., Consugar, M., Tee, L. J., McKee, B. M., Maina, E. N., Whelan, S., Morgan, N. V., Goranson, E., Gissen, P., Lilliquist, S. et al. (2006). The transmembrane protein meckelin (MKS3) is mutated in Meckel-Gruber syndrome and the wpk rat. *Nat Genet* **38**, 191-6.

Starich, T. A., Herman, R. K., Kari, C. K., Yeh, W. H., Schackwitz, W. S., Schuyler, M. W., Collet, J., Thomas, J. H. and Riddle, D. L. (1995). Mutations affecting the chemosensory neurons of Caenorhabditis elegans. *Genetics* **139**, 171-88.

Swoboda, P., Adler, H. T. and Thomas, J. H. (2000). The RFX-type transcription factor DAF-19 regulates sensory neuron cilium formation in C.elegans. *Mol. Cell* **5**, 411-421.

Taulman, P. D., Haycraft, C. J., Balkovetz, D. F. and Yoder, B. K. (2001). Polaris, a protein involved in left-right axis patterning, localizes to basal bodies and cilia. *Molecular Biology of the Cell* **12**, 589-99.

Town, T., Breunig, J. J., Sarkisian, M. R., Spilianakis, C., Ayoub, A. E., Liu, X., Ferrandino, A. F., Gallagher, A. R., Li, M. O., Rakic, P. et al. (2008). The stumpy

gene is required for mammalian ciliogenesis. *Proceedings of the National Academy of Sciences* **105**, 2853-2858.

Wang, Q., Pan, J. and Snell, W. J. (2006). Intraflagellar transport particles participate directly in cilium-generated signaling in Chlamydomonas. *Cell* **125**, 549-62.

Ward, S., Thomson, N., White, J. G. and Brenner, S. (1975). Electron microscopical reconstruction of the anterior sensory anatomy of the nematode Caenorhabditis elegans. *Journal of Comparative Neurology* **160**, 313-37.

Ware R., W., Clark, D., Crossland, K. and Russell, R., L. (1975). The nerve ring of the neamtode Caenorhabditis elegans: sensory input and motor out. *Journal of Comparative Neurology* **162**, 71-110.

Winkelbauer, M. E., Schafer, J. C., Haycraft, C. J., Swoboda, P. and Yoder, B. K. (2005). The C. elegans homologs of nephrocystin-1 and nephrocystin-4 are cilia transition zone proteins involved in chemosensory perception. *J Cell Sci* **118**, 5575-87.

TABLES

Table 1. Tracking assay statistics

Genotype	*n*	Mean % of N2	SEM	*P* values compared with N2	*xbx-7*	*tza-1*	*nph-4*	*tza-2*
Wild Type	28	100	2.82					
xbx-7(tm2705)	28	98.5	2.59	0.3547				
tza-1(tm2452)	29	87.2	3.01	0.0016*				
tza-2(ok2092)	29	85.3	2.88	0.0003*				
nph-4(tm925)	26	65.3	5.57	<0.0001*				
xbx-7;nph-4	29	28.9	1.74	<0.0001*	<0.0001*		<0.0001*	
tza-1;nph-4	27	40.4	4.37	<0.0001*		<0.0001*	0.0005*	
nph-4;tza-2	29	23.7	1.7	<0.0001*			<0.0001*	0.0006*

P <0.05 was deemed significant (indicated by asterisks).

Table 2. % dye-filling in mutant strains

Genotype	Head	Tail	*n*
Wild Type	100	97.2	72
xbx-7(tm2705)	100	97.2	108
tza-1(tm2452)	100	98.6	71
tza-2(ok2092)	100	98.9	96
nph-4(tm925)	100	100	91
xbx-7;nph-4	94.3	52.7	74
tza-1;nph-4	5.4	1.8	112
nph-4;tza-2	10.8	0	93

Table 3. Phasmid cilia length statistics

Genotype	*n*	Mean Length (μm) ± SEM	*P* values compared with N2	*xbx-7*	*tza-1*	*nph-4*	*tza-2*
Wild Type	33	7.04 ± 0.09					
xbx-7(tm2705)	27	7.03 ± 0.15	0.486				
tza-1(tm2452)	40	6.97 ± 0.13	0.3478				
tza-2(ok2092)	36	7.15 ± 0.09	0.1957				
nph-4(tm925)	24	6.87 ± 0.27	0.2766				
xbx-7;nph-4	38	4.39 ± 0.24	<0.0001*	<0.0001*		<0.0001*	
tza-1;nph-4	33	2.88 ± 0.20	<0.0001*		<0.0001*	<0.0001*	
nph-4;tza-2	33	2.88 ± 0.15	<0.0001*			<0.0001*	<0.0001*
nph-1;xbx-7	53	6.68 ± 0.17	0.0346*	0.0644			
nph-1;tza-1	30	3.43 ± 0.26	<0.0001*		<0.0001*		
nph-1;tza-2	58	3.96 ± 0.23	<0.0001*				<0.0001*

P <0.05 was deemed significant (indicated by asterisks).

FIGURE LEGENDS

Figure 1. B9 protein family conservation and schematic gene representations. (A) Homology with other organisms presented as % amino acid identity / % amino acid similarity. (B) Schematic representation of *xbx-7*, *tza-1*, and *tza-2* genomic regions. Promoter X-box location, gene region encoding each B9 domain, gene region deleted in each mutant allele, and in the case of *xbx-7*, splice isoforms are shown. *xbx-7(tm2705)* and *tza-1(tm2452)* both contain internal in-frame deletions while *tza-2(ok2092)* contains an internal frameshift deletion that results in a truncated protein. Exons are represented as black boxes. Diamond signifies site of *xbx-7* alternative splicing.

Figure 2. DAF-19 regulation of *xbx-7*, *tza-1*, and *tza-2* in *C. elegans*. Expression analysis of (A) *xbx-7::YFP*, (B) *tza-1::DsRed2*, and (C) *tza-2::CFP* in the head ciliated sensory neurons in (left panels) *daf-19(m86)* mutant and (right panels) *daf-19(+)* backgrounds. The expression of each transgene was absent in *daf-19(m86)* mutants while outcrossing to *daf-19(+)* background restored expression to wild-type levels. (Arrowhead) Position of the amphid neuron cell bodies from which the dendrites extend to the anterior of the worm. Cilia project from the (arrow) distal tips of the dendrites. For this and subsequent figures, anterior is toward the left.

Figure 3. Localization of XBX-7, TZA-1, and TZA-2 proteins to transition zones at the base of cilia in *C. elegans.* (A) An illustration depicting the anatomical positions of (left) amphid cilia bundles in the head and (right) phasmid cilia bundles in the tail. Cilia axonemes are represented by blue, transition zones by green, and the dendritic processes

by red. (B-D) Transgenic lines were generated that expressed XBX-7::YFP, TZA-1::CFP, or TZA-2::CFP along with cilia/transition zone markers CHE-13::CFP or CHE-13::YFP, each under the control the endogenous promoter of the corresponding gene. (B) XBX-7::YFP localized to the transition zones at the base of cilia in the (top) amphid neurons of the head and (bottom) phasmid neurons of the tail but not along cilia axonemes. (C) TZA-1::YFP localized to the transition zones at the base of cilia in the (top) amphid neurons of the head and (bottom) phasmid neurons of the tail but not along cilia axonemes. In contrast to CHE-13::CFP localization, which was restricted to the cilia axonemes and transition zones, TZA-1::YFP was found at the transition zones and (top, brackets) extended slightly into the dendrites of the amphid neurons. In the (bottom) phasmid neurons, the (brackets) extension of TZA-1::YFP into the dendrites versus the restriction of CHE-13::CFP to the transition zones and cilia axonemes was more distinctive. (D) TZA-2::CFP localized to the transition zones at the base of cilia in the (top) amphid neurons of the head and (bottom) phasmid neurons of the tail but not along cilia axonemes. (E) Analysis of TZA-1::YFP and TZA-2::CFP colocalization at the base of cilia. In contrast to TZA-2::CFP localization, which was restricted to the transition zones, TZA-1::YFP was found at the transition zones and (brackets) extended into the dendrites of both the (top) amphid and (bottom) phasmid neurons. (F-I) Enlargement of phasmid cilia regions from B-E, respectively. (G) TZA-1::YFP and CHE-13::CFP and (I) TZA-1::YFP and TZA-2::CFP colocalized largely to the transition zones but not to (arrowheads) a small domain at the distal ends of the dendrites which contained TZA-1::YFP only.

Figure 4. Cilia morphology analysis of transition zone protein mutants. (A) Potential cilia defects were analyzed in *xbx-7(tm2705), tza-1(tm2452), tza-2(ok2092),* and *nph-4(tm925)* mutants by evaluating their ability of to absorb DiI into the ciliated sensory neurons. The ability of *xbx-7(tm2705), tza-1(tm2452), tza-2(ok2092),* and *nph-4(tm925)* mutants to absorb DiI was not affected compared to wild-type controls. However, in these mutant worms, the dye appeared to (arrowheads) concentrate in aggregates along the dendrites. This was (arrows) particularly evident in the *nph-4(tm925)* mutants and was not seen in the wild-type controls. N2 wild-type worms and *daf-19(m86)* mutants, which lack cilia, were used as positive and negative controls, respectively. (B) Cilia morphology was more directly analyzed in *xbx-7(tm2705), tza-1(tm2452), tza-2(ok2092),* and *nph-4(tm925)* mutants expressing the cilia marker CHE-13::YFP. (Left) head and (right) tail cilia morphology appeared overtly normal in these strains.

Figure 5. TZA-1 protein is required for proper localization of XBX-7 and TZA-2 to the transition zone. To analyze the effect of *tza-1(tm2452)*, *tza-2(ok2092)*, or *nph-4(tm925)* mutations on XBX-7::YFP localization, strains were generated by passing an extrachromosomal array encoding XBX-7::YFP from wild-type worms into the mutant backgrounds. Similarly, the TZA-1::YFP array was passed into *xbx-7(tm2705)*, *tza-2(ok2092)*, or *nph-4(tm925)* mutant background from wild-type, and the TZA-2::CFP array was passed into *xbx-7(tm2705)*, *tza-1(tm2452)*, or *nph-4(tm925)* mutant background from wild-type. (A) In contrast to (left) wild type, XBX-7::YFP was not detected at the transition zone in the (middle) *tza-1(tm2452)* or (right) *tza-2(ok2092)*mutants. (B) Compared to (left) wild type, TZA-1::YFP localization was unaltered in the background of

(middle) *xbx-7(tm2705)* and (right) *tza-2(ok2092)* mutants. (C) TZA-2::CFP localization was not affected in (middle) *xbx-7(tm2705)* mutant background; however, it failed to localize correctly to the transition zone in (right) *tza-1(tm2452)* mutant background. (D) In the *nph-4(tm925)* mutant background, (left) XBX-7::YFP, (middle) TZA-1::YFP, and (right) TZA-2::CFP localization was not affected.

Figure 6. *tza-1*, *tza-2*, and *nph-4* mutants exhibit defects in foraging behavior. Single worms were allowed to roam freely for 18 hours on a bacteria lawn of 3.0 cm diameter, and area covered by the worm was quantified by overlaying the lawn with a grid and counting the number of squares of the grid that contained tracks. (A) Representative tracking patterns of (left) N2 wild-type, (middle) *nph-4(tm925)*, and (right) *tza-1;nph-4* worms. Wild-type worms roamed across the entire area of the bacteria lawns while *nph-4(tm925)* mutants restricted movement to a smaller portion of the lawn. Exploratory behavior in *xbx-7;nph-4, tza-1;nph-4*, and *nph-4;tza-2* double mutants was even more limited. (B) Graph of quantified tracking data for N2 wild type, *xbx-7(tm2705)*, *tza-1(tm2452)*, *tza-2(ok2092)*, *nph-4(tm925)*, *xbx-7;nph-4*, *tza-1;nph-4*, and *nph-4;tza-2*. Data are given as percent area units covered compared with N2 (set to 100%). Error bars indicate SEM. **P* <0.005; ***P* <0.0001, compared to N2.

Figure 7. *B9 gene;nph-4* double mutants exhibit dye-filling defects. Potential cilia abnormalities were analyzed in *xbx-7;nph-4, tza-1;nph-4,* and *nph-4;tza-2* double mutants by evaluating their ability to absorb DiI into the ciliated sensory neurons. (A) *xbx-7;nph-4* mutants displayed either (top) partial or (bottom) complete inability to dye-fill (left)

amphid neurons and (right) phasmid neurons. (B) *tza-1;nph-4* mutants displayed either (top) partial or (bottom) complete inability to dye-fill (left) amphid neurons and (right) phasmid neurons. (C) *nph-4;tza-2* displayed either (top) partial or (bottom) complete inability to dye-fill (left) amphid neurons but were completely defective in dye-filling (right) phasmid neurons.

Figure 8. *B9 gene;nph-4* double mutants exhibit cilia morphology and positioning defects. Cilia were analyzed in *xbx-7;nph-4, tza-1;nph-4,* and *nph-4;tza-2* double mutant worms expressing CHE-13::YFP as a cilia/transition zone marker. (A) A representative amphid cilia bundle in the head of an N2 wild-type worm. (B) A representative pair of phasmid cilia in the tail of an N2 wild-type worm. These cilia are positioned near the cuticle of the worm where they are exposed to the external environment. See Figure 3A for schematic representation of the N2 wild-type amphid and phasmid cilia bundles. (C) Amphid cilia bundle morphology was altered in *xbx-7;nph-4* double mutant background. In many of the *xbx-7;nph-4* double mutants, some of the cilia were (arrow) positioned posterior to the rest of the bundle. In other *xbx-7;nph-4* double mutants, cilia failed to extend off the (arrowhead) transition zones at the distal ends of the dendrites. (D) Phasmid cilia in *xbx-7;nph-4* double mutants appeared (top) almost normal in some mutant worms but in others they were (bottom) shortened and mispositioned relative to wild type. (E) Amphid cilia bundle morphology was (top and bottom) grossly abnormal in *tza-1;nph-4* double mutants. The head region contained few cilia axonemes and lacked typical bundle arrangement. (F) *tza-1;nph-4* double mutants exhibited stunted phasmid cilia that were observed (top) slightly or (bottom) severely mispositioned. (G, H) *nph-*

4;tza-2 double mutants exhibited ciliary defects similar to those in *tza-1;nph-4* double mutants, including (arrowhead) laterally oriented phasmid cilia in comparison to wild type.

Figure 9. *B9 gene;nph-1* double mutants exhibit cilia morphology and positioning defects. Cilia were analyzed in *nph-1;xbx-7, nph-1;tza-1,* and *nph-1;tza-2* double mutant worms expressing CHE-13::YFP as a cilia/transition zone marker. (A) A representative amphid cilia bundle in the head of an N2 wild-type worm. (B) A representative pair of phasmid cilia in the tail of an N2 wild-type worm. These cilia are positioned near the cuticle of the worm where they are exposed to the external environment. See Figure 3A for schematic representation of the N2 wild-type amphid and phasmid cilia bundles. (C) Amphid cilia bundle morphology was largely unaltered in *nph-1;xbx-7* double mutant background. *nph-1;xbx-7* double mutants occasionally exhibited cilia positioned (arrowhead) posterior to the rest of the bundle but otherwise resembled wild-type worms. (D) Phasmid cilia in *nph-1;xbx-7* double mutants most often appeared (top) normal but in some cases were observed (bottom) shortened and mispositioned relative to wild type. (E) Amphid cilia bundle morphology was (top and bottom) grossly abnormal in *nph-1;tza-1* double mutants. The head region contained (arrow) few cilia, consisted mostly of (arrowhead) transition zones lacking axonemes, and had no discernable amphid bundle arrangement. (F) *nph-1;tza-1* double mutants exhibited stunted phasmid cilia that were observed (top) slightly or (bottom) severely mispositioned and often oriented laterally. (G) *nph-1;tza-2* double mutants exhibited amphid ciliary defects more severe than *nph-1;xbx-7* double mutants but less severe than *nph-1;tza-1* double mutants. Although not

perfectly arranged, (top and bottom) some bundling of multiple cilia was typically observed amongst (arrowhead) shortened and mispositioned cilia and (arrowhead) transition zones lacking axonemes. (H) In contrast to the relatively mild defects observed in the amphid bundles, the phenotype of phasmid cilia in *nph-1;tza-2* double mutant worms mimicked the severity of defects seen in the phasmid cilia of *nph-1;tza-1* double mutant worms.

Figure 10. The dendrites of ciliated sensory neurons in *B9 gene;nph gene* double mutants are malformed although the surrounding sheath cells are intact. (A-F) Transgenic *B9 gene* single mutants and *B9 gene;nph-4* double mutants were generated that expressed the *xbx-7::YFP* transcriptional fusion to visualize the ciliated sensory neurons. (A, C, E) Expression of *xbx-7::YFP* revealed that the (arrow) phasmid dendrites are properly extended from the (arrowhead) cell bodies in the background of single *B9 gene* mutations. (B, D, F) The phasmid dendrites of *B9 gene;nph-4* double mutant worms were shortened at variable lengths and sometimes (arrow) misdirected. (G, H) Morphological analysis of (left) amphid and (right) phasmid sheath cells in wild-type and *tza-1;nph-4* double mutant worms. Transgenic worms were generated that coexpressed the *tza-1::DsRed2* transcriptional fusion to visualize the ciliated sensory neurons and the *f16f9.3::GFP* transcriptional fusion to visualize the associated sheath cells. (G) In wild-type worms, the amphid and phasmid sheath cells fully surrounded the dendrites of the ciliated sensory neurons at (arrows) their distal tips where the cilia are formed. (H) Sheath cell morphology was unaffected in *tza-1;nph-4* double mutants. The amphid sheath cells were properly extended to surround the distal tips of the associated neurons. Likewise, phasmid sheath cells in

the tail were appeared normally extended while the phasmid neuron dendrites were (arrows) shortened and clearly dissociated from (arrowhead) the distal ends of the sheath cells.

SUPPLEMENTARY FIGURE LEGENDS

Supplementary Figure 1. Expression of *xbx-7*, *tza-1*, and *tza-2* in *C. elegans*. (A) *xbx-7::YFP* and *tza-1::CFP* and (B) *tza-2::CFP* and *xbx-7::YFP* transgenes were expressed in an overlapping pattern the ciliated sensory neurons of the worm including the (left) amphid and labial neurons in the head as well as the (right) phasmid neurons in the tail.

Supplementary Figure 2. Sequencing of the *tm2705*, *tm2452*, and *ok2092* mutant transcripts. RNA isolated from mutant worms was reverse transcribed, amplified by PCR, and then sequenced. Nucleotide numbering corresponds to the position in the wild-type gene. (A) The *xbx-7(tm2705)* deletion causes the resulting transcript to splice exon 2 (ending at nucleotide 535) with exon 5 (beginning at nucleotide 1724). The original reading frame (solid vertical lines) is not altered by this mutation. (B) The *tza-1(tm2452)* deletion results in a transcript that splices exon 1 with a cryptic splice acceptor in exon 3 created by the fusion of nucleotides 445 and 725. The original reading frame is not altered by this mutation. (C) The *tza-2(ok2092)* deletion fuses nucleotide 573 in exon 1 with nucleotide 1381 in exon 4. This causes a shift of reading frame (dashed lines) in the resulting transcript.

Supplementary Figure 3. Yeast two-hybrid analysis of possible interactions between the B9 proteins. Yeast expression constructs were generated containing full length XBX-7, TZA-1, or TZA-2 cDNA and cotransformed into yeast. (Top row) Low stringency selective media lacking Trp and Leu was used to isolate yeast colonies containing both co-transformed constructs. (Bottom row) Colonies expressing the fusion proteins were then

tested for possible interactions on high stringency selective media containing X-α-Gal and lacking Trp, Leu, His, and Ade. (First column) The positive controls p53 and large T-Antigen grew on selective media and expressed the α-galactosidase reporter gene. (Second column) Yeast strains cotransformed with XBX-7 and TZA-1 grew on low stringency selective media but failed to grow when plated on high stringency selective media, suggesting that XBX-7 does not physically bind TZA-1. (Third column) Yeast strains cotransformed with XBX-7 and TZA-2 grew on low stringency selective media but failed to grow when plated on high stringency selective media, suggesting that XBX-7 does not physically bind TZA-2. (Fourth column) Yeast strains cotransformed with TZA-1 and TZA-2 grew on low stringency selective media and also grew when plated on high stringency selective media and expressed the α-galactosidase reporter gene, confirming the positive interaction between TZA-1 and TZA-2 reported previously (Li *et al.*, 2004).

Supplementary Figure 4. NPH-1 and NPH-4 localization is not affected by mutations in the B9 genes. To analyze the effect of *xbx-7(tm2705)*, *tza-1(tm2452)*, or *tza-2(ok2092)* mutations on NPH-1::CFP or NPH-4::YFP localization, strains were generated by passing extrachromosomal arrays encoding NPH-1::CFP or NPH-4::YFP from wild-type worms into the mutant backgrounds. The cilia/transition zone region of one amphid cilia bundle is shown in each panel. Compared to wild type, (top) NPH-1::CFP localization and (bottom) NPH-4::YFP localization to the transition zones of amphid neurons was not altered in the *xbx-7(tm2705)*, *tza-1(tm2452)*, or *tza-2(ok2092)* mutant backgrounds.

A

	C. elegans	*S. purpuratus*	*M. musculus*	*H. sapiens*
*Ce*XBX-7	100/100			
S. purpuratus	22/39	100/100		
Mus musculus	22/40	43/62	100/100	
*Hs*MKS1	28/46	44/63	89/95	100/100
*Ce*TZA-1	100/100			
S. purpuratus	44/61	100/100		
Mus musculus	42/63	62/81	100/100	
*Hs*B9D2	43/63	64/81	96/97	100/100
*Ce*TZA-2	100/100			
S. purpuratus	32/47	100/100		
Mus musculus	30/50	68/79	100/100	
*Hs*B9D1	29/50	67/79	94/95	100/100

B

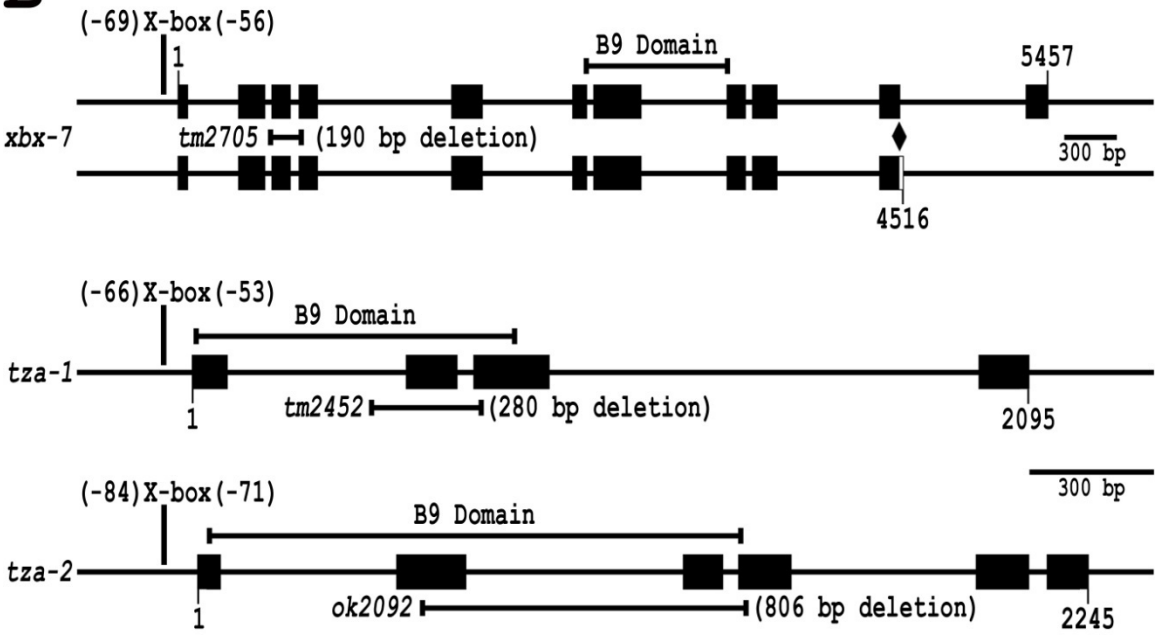

Figure 1. B9 protein family conservation and schematic gene representations.

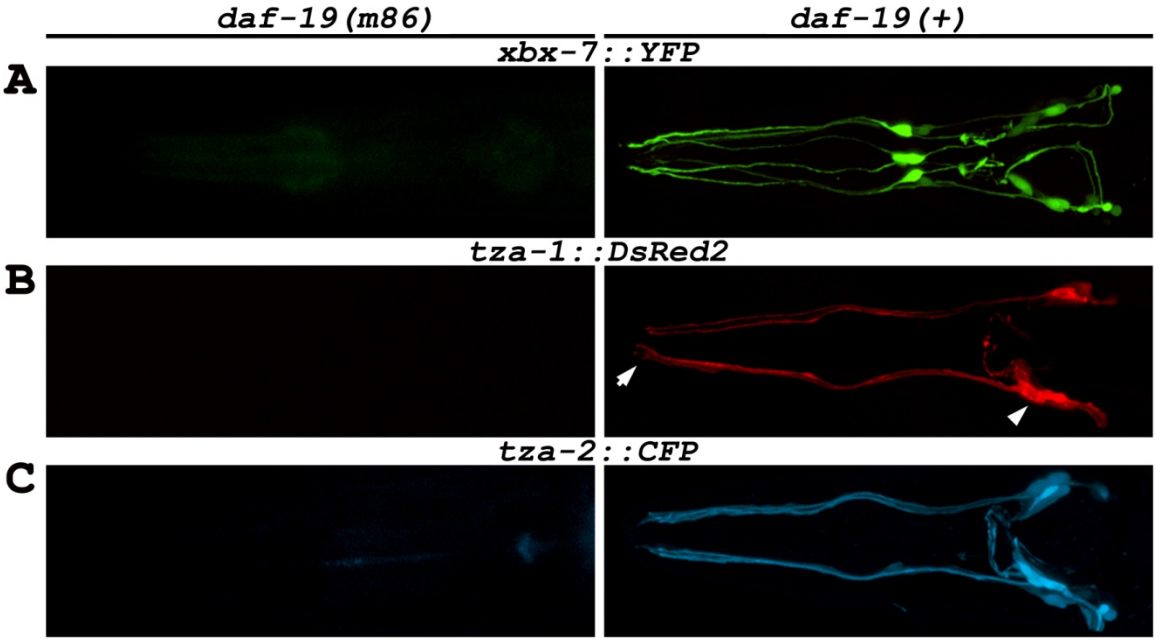

Figure 2. DAF-19 regulation of *xbx-7*, *tza-1*, and *tza-2* in *C. elegans*.

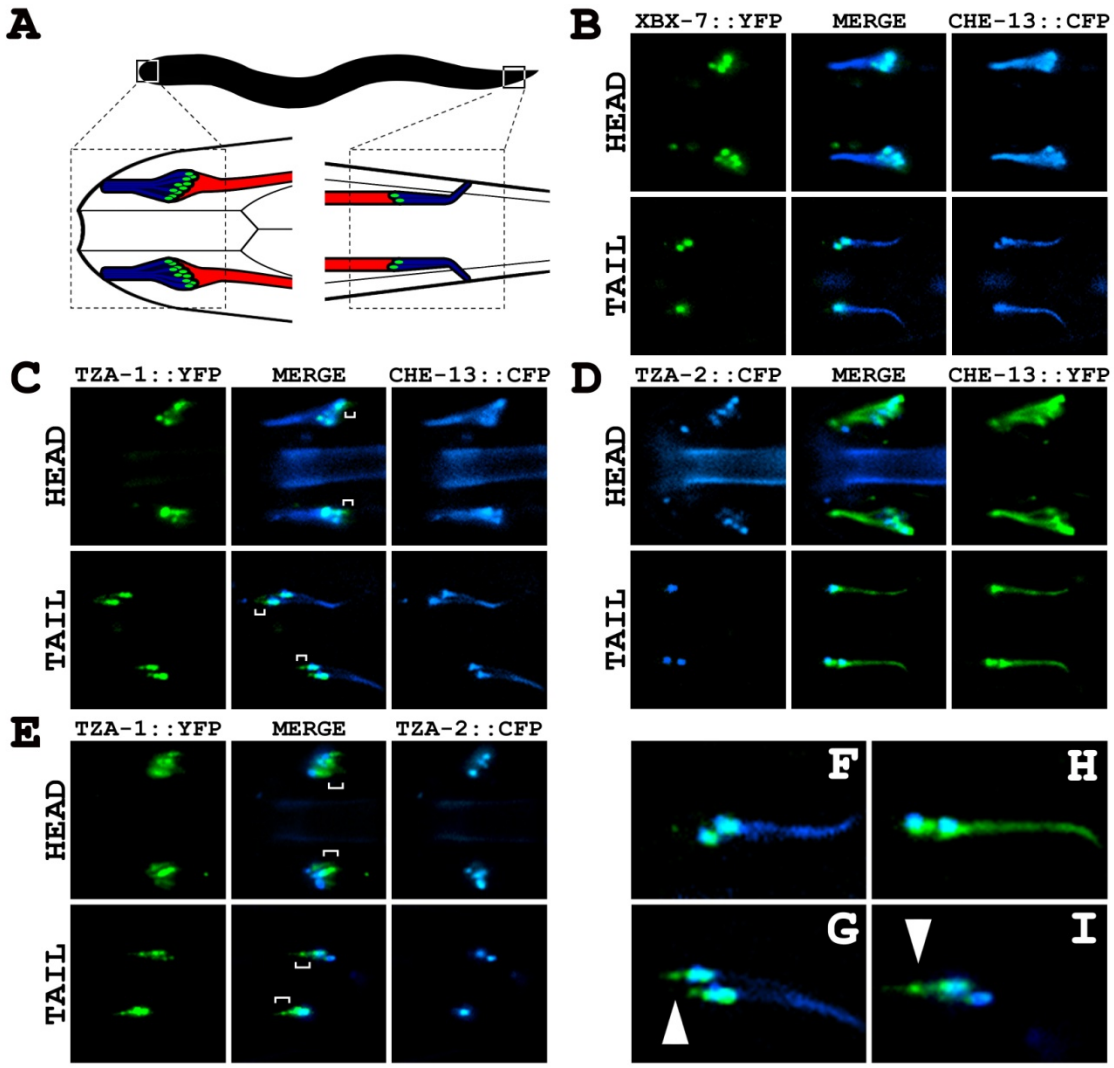

Figure 3. Localization of XBX-7, TZA-1, and TZA-2 proteins to transition zones at the base of cilia in *C. elegans.*

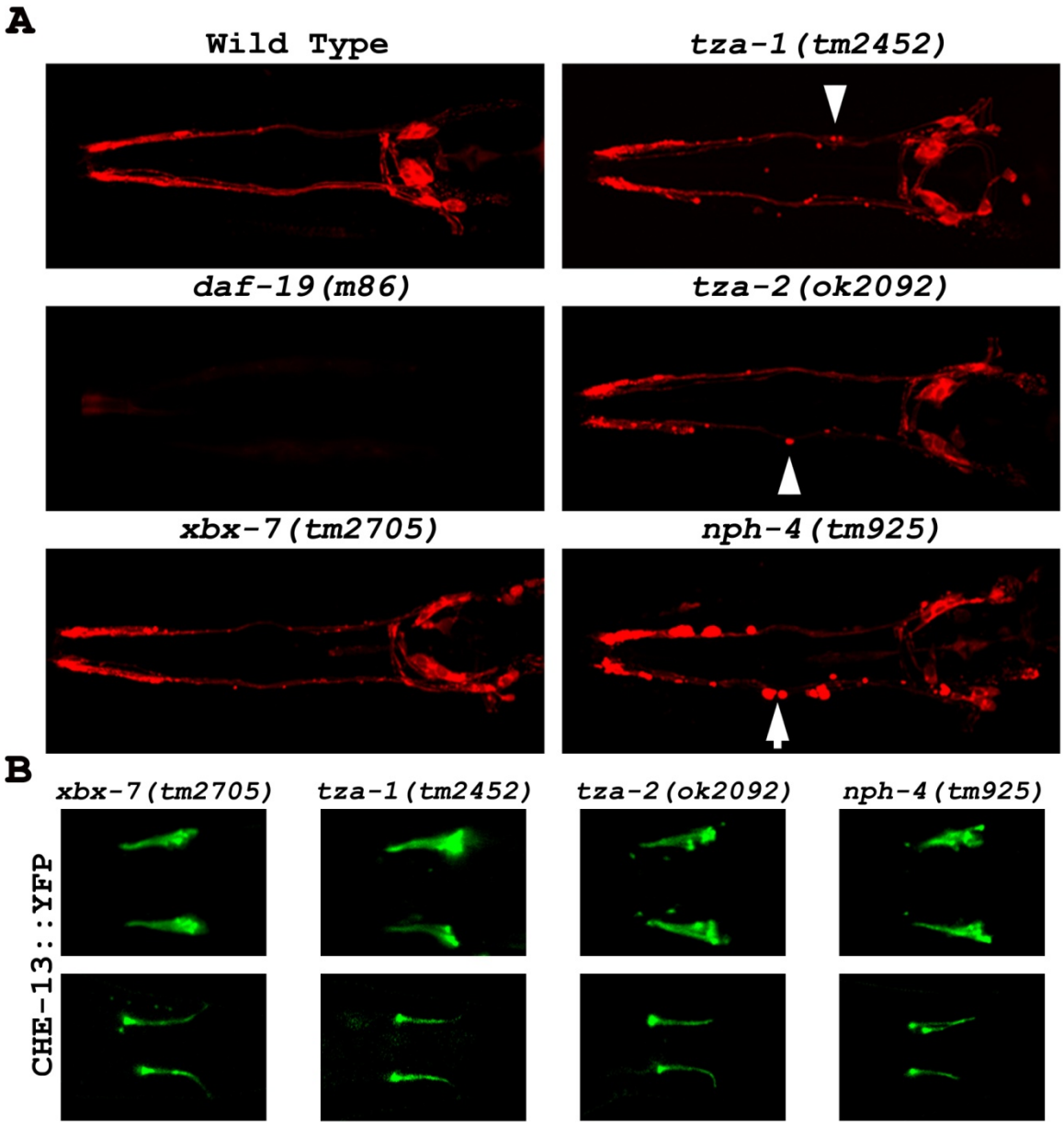

Figure 4. Cilia morphology analysis of transition zone protein mutants.

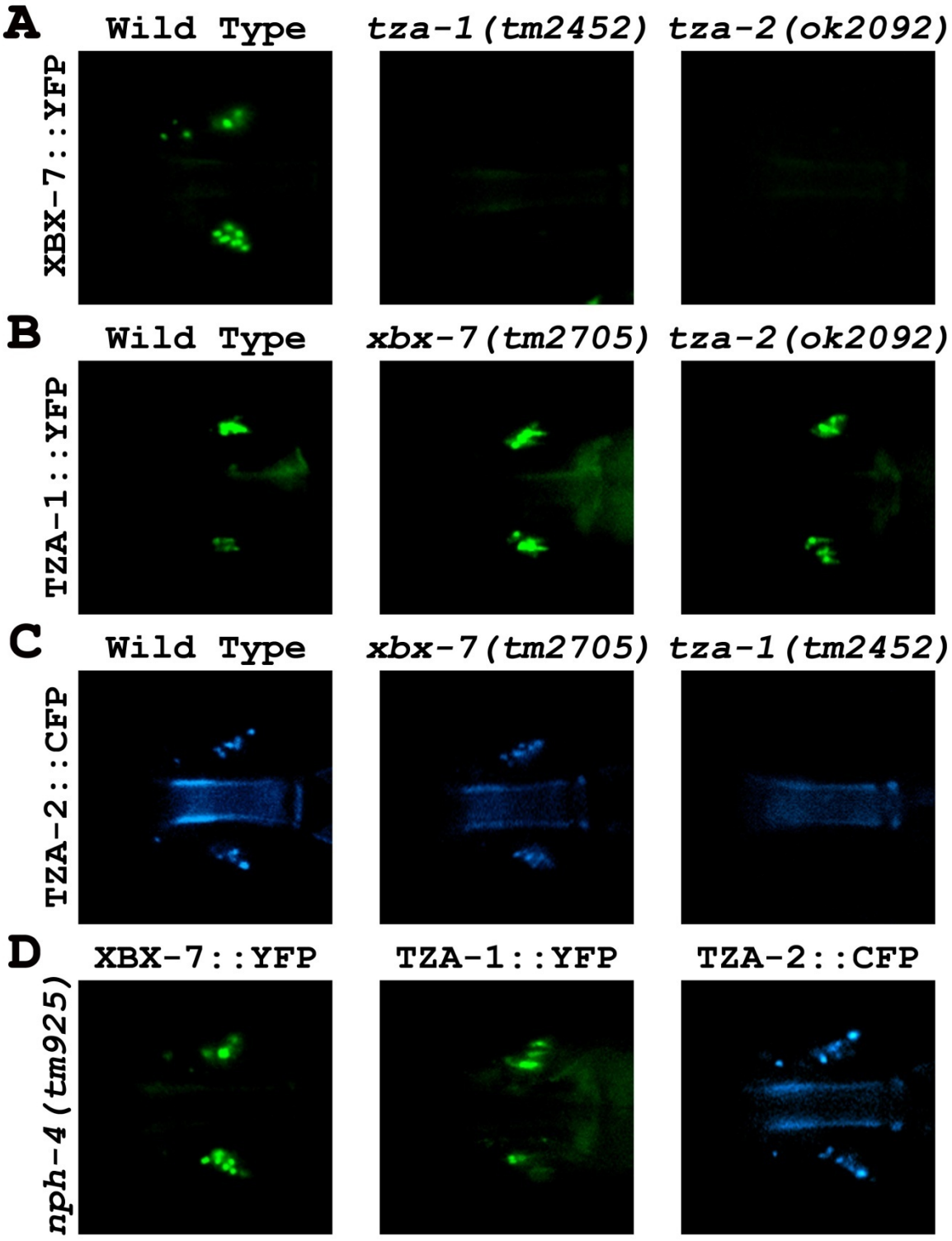

Figure 5. TZA-1 protein is required for proper localization of XBX-7 and TZA-2 to the transition zone.

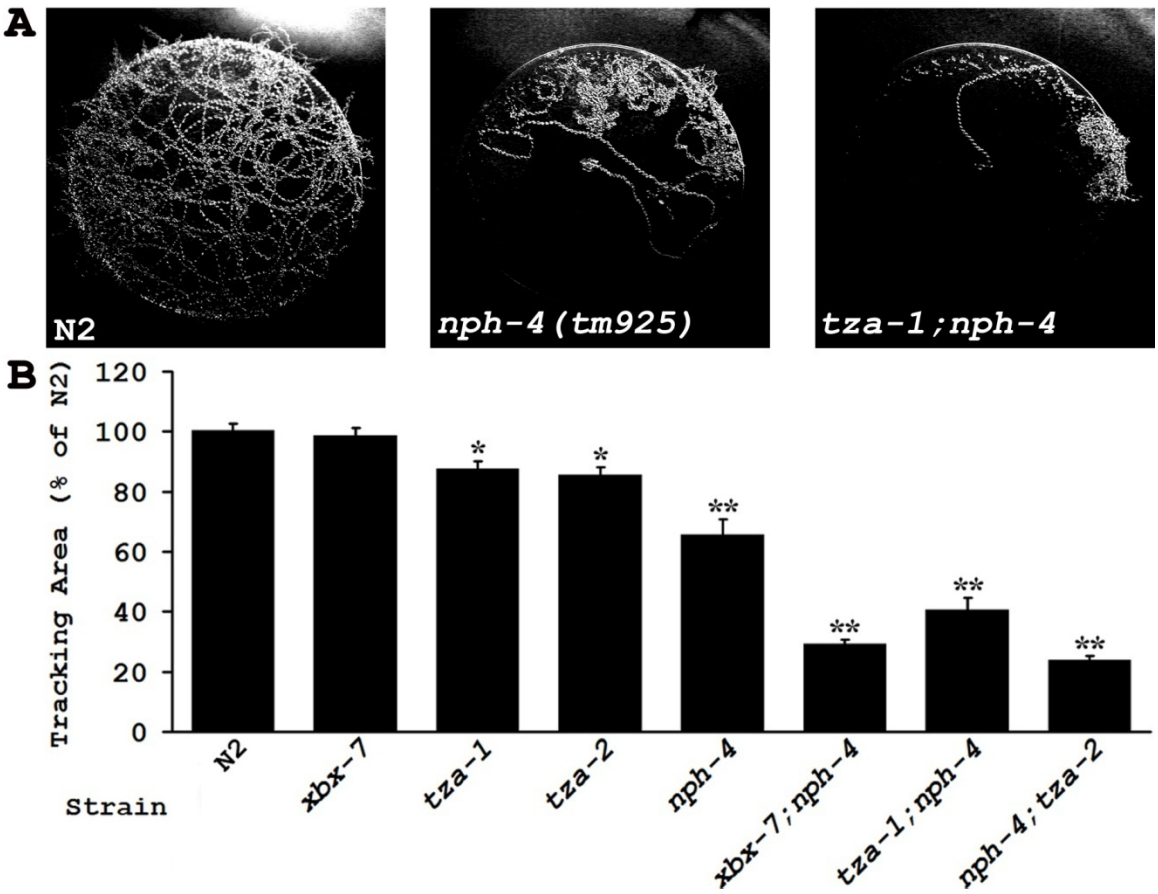

Figure 6. *tza-1*, *tza-2*, and *nph-4* mutants exhibit defects in foraging behavior.

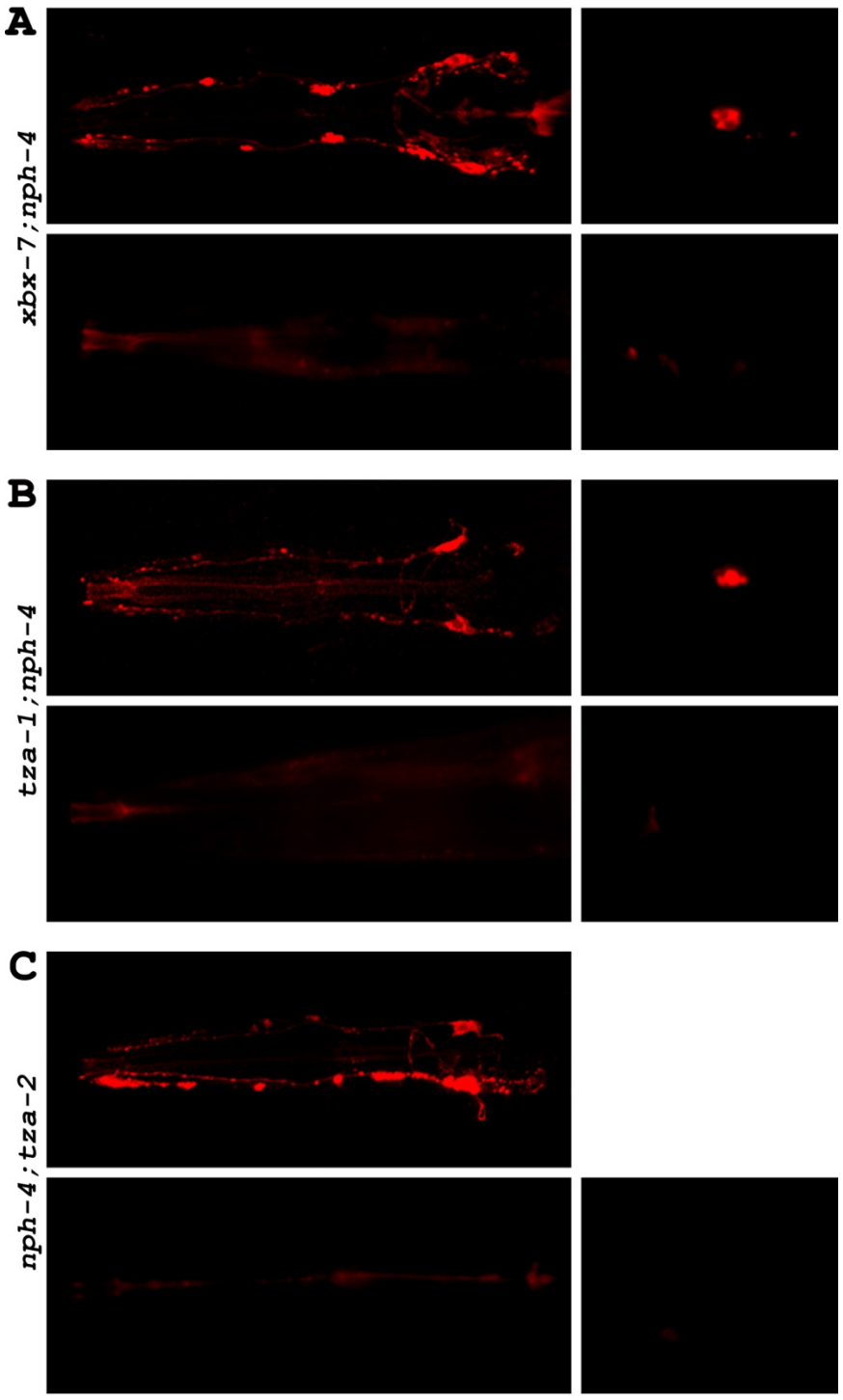

Figure 7. *B9 gene;nph-4* double mutants exhibit dye-filling defects.

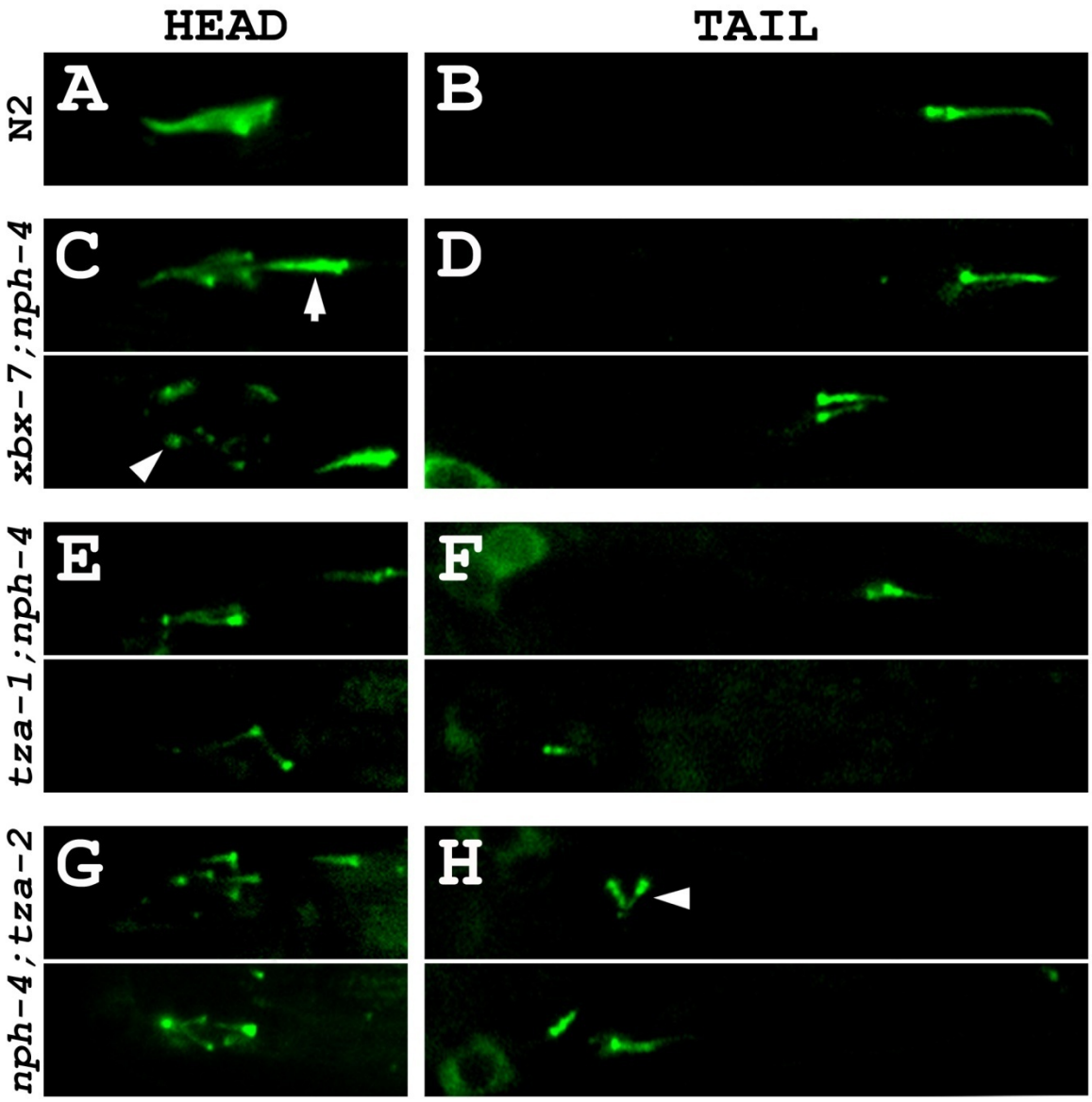

Figure 8. *B9 gene;nph-4* double mutants exhibit cilia morphology and positioning defects.

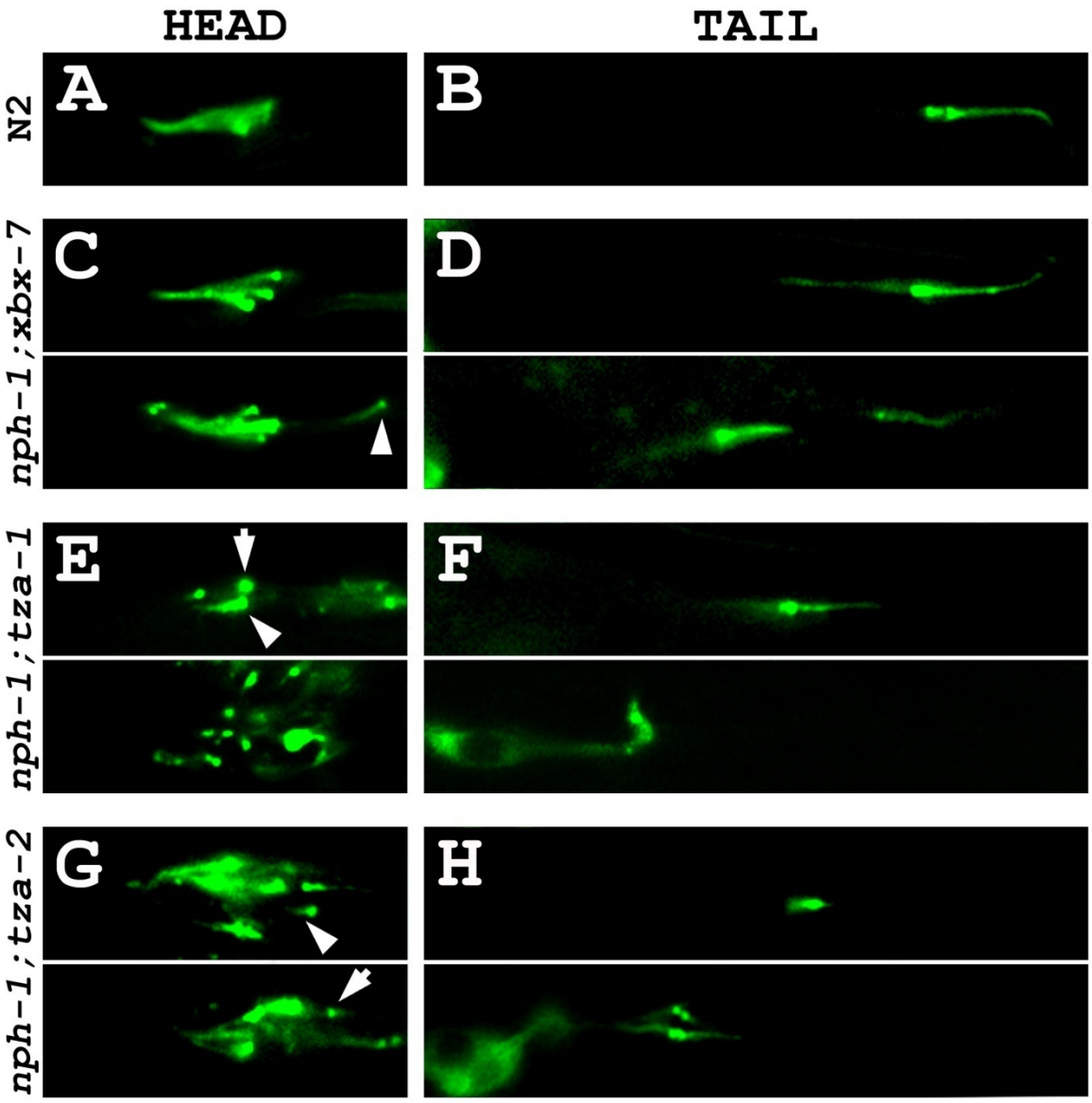

Figure 9. *B9 gene;nph-1* double mutants exhibit cilia morphology and positioning defects.

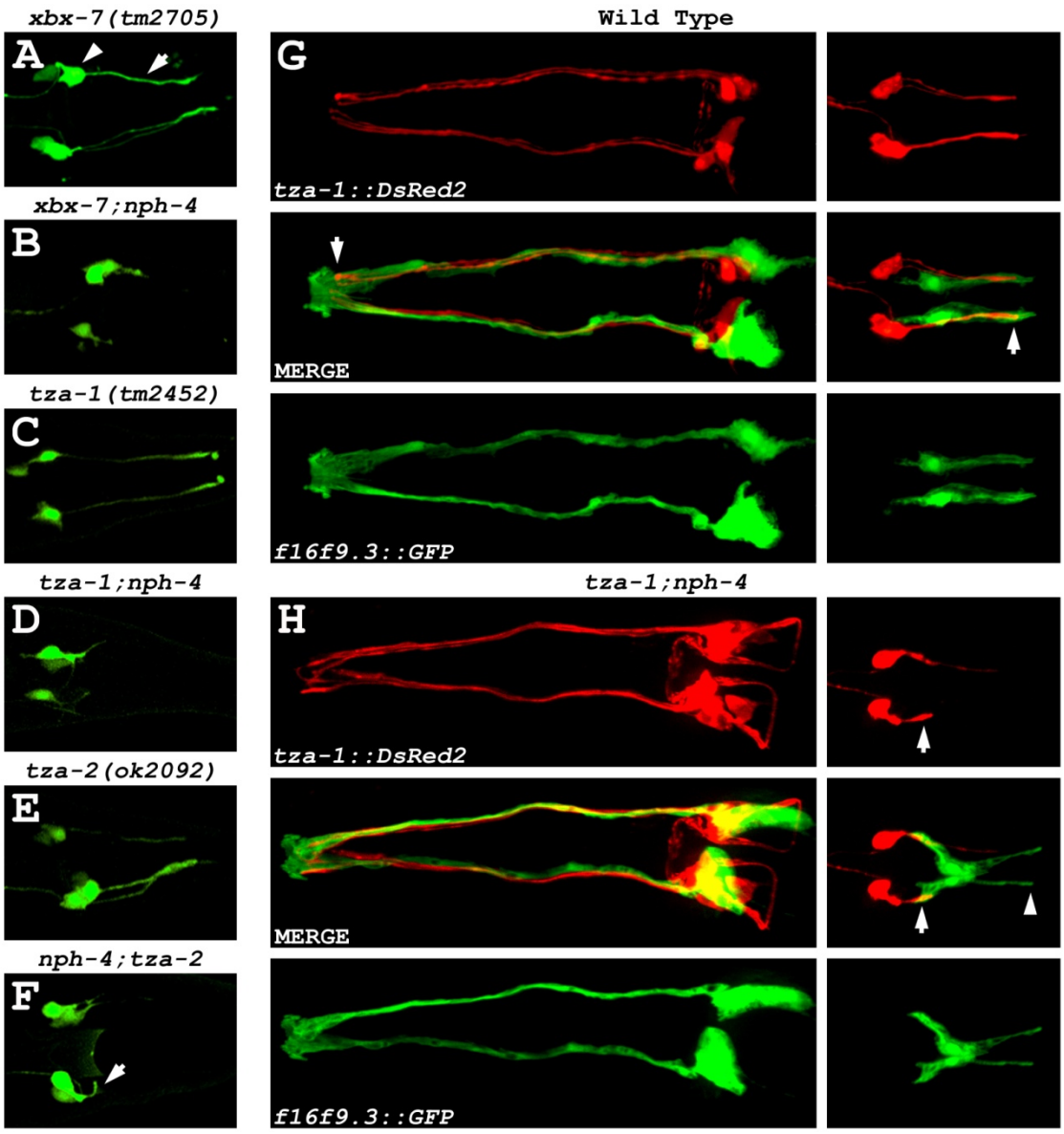

Figure 10. The dendrites of ciliated sensory neurons in *B9 gene;nph gene* double mutants are malformed although the surrounding sheath cells are intact.

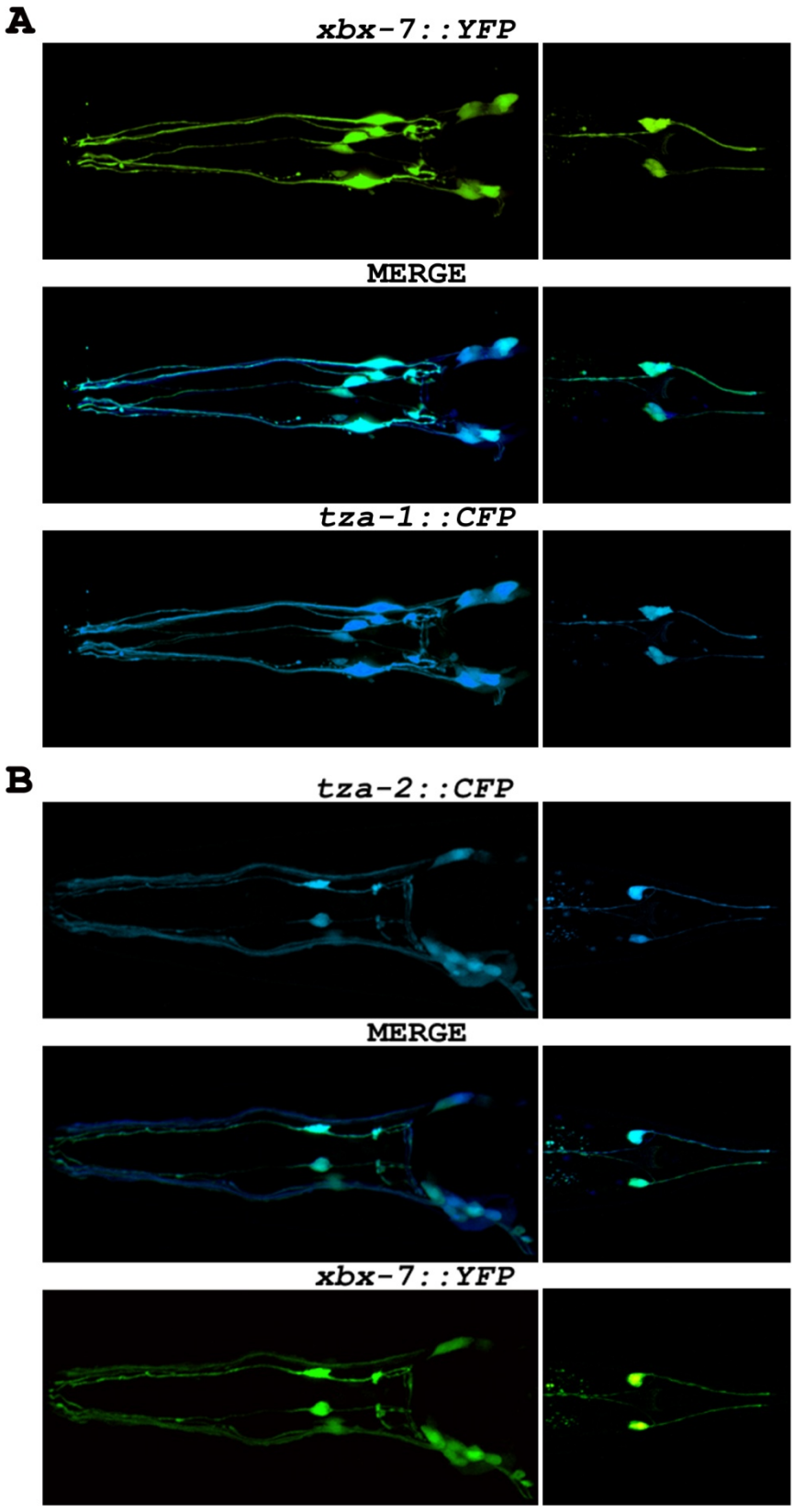

Supplementary Figure 1. Expression of *xbx-7*, *tza-1*, and *tza-2* in *C. elegans*.

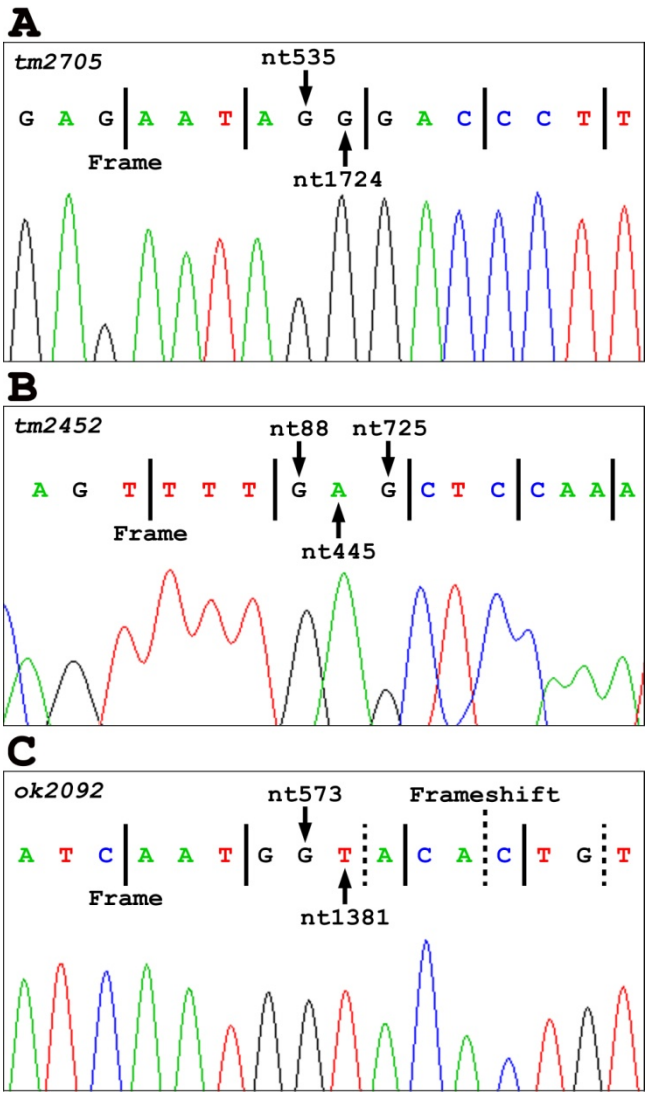

Supplementary Figure 2. Sequencing of the *tm2705*, *tm2452*, and *ok2092* mutant transcripts.

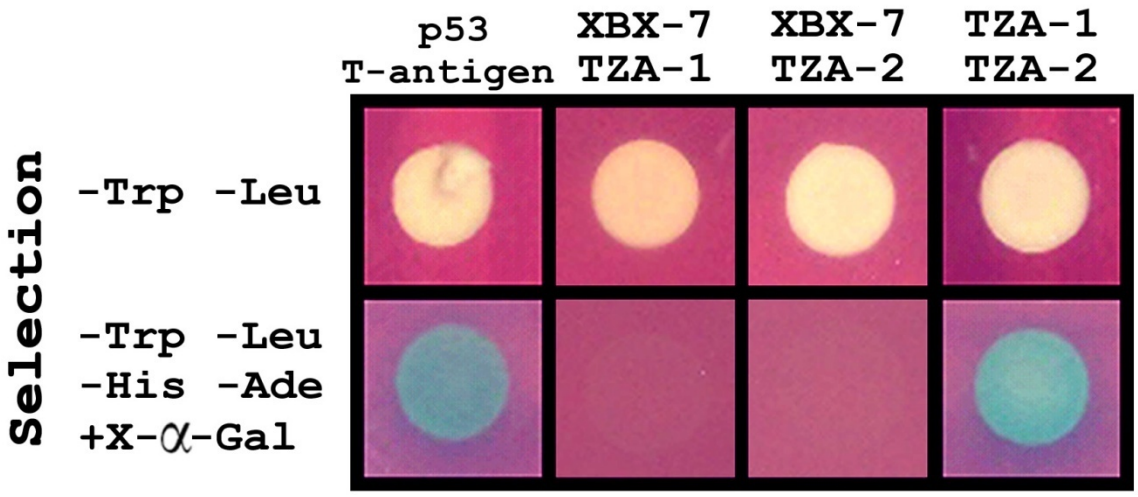

Supplementary Figure 3. Yeast two-hybrid analysis of possible interactions between the B9 proteins.

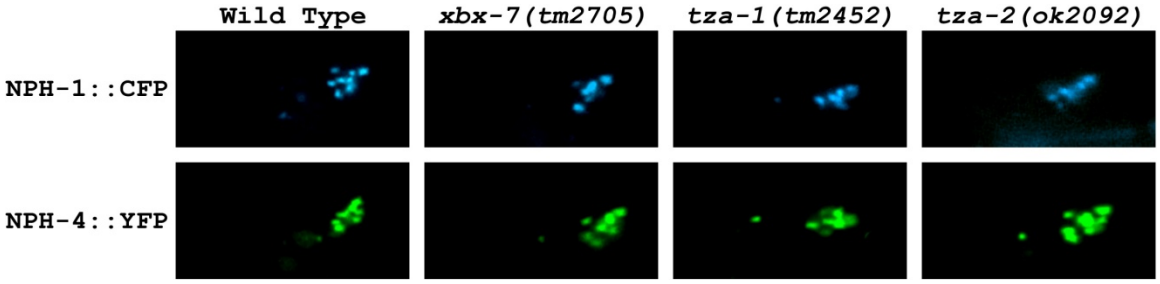

Supplementary Figure 4. NPH-1 and NPH-4 localization is not affected by mutations in the B9 genes.

REGULATION AND FUNCTION OF MKS-3 IN *CAENORHABDITIS ELEGANS*

COREY L. WILLIAMS, MARLENE E. WINKELBAUER, ELIZABETH SZTUL AND BRADLEY K. YODER

In preparation for *Journal of the American Society of Nephrology*

SUMMARY

Ciliopathies in humans include Nephronophthisis (NPHP), Meckel-Gruber Syndrome (MKS), Joubert Syndrome (JBTS) and Bardet-Biedl Syndrome (BBS). Combinations of single homozygous, compound heterozygous, and transheterozygous mutations in genes associated with these diseases contribute to the severity of a wide spectrum of renal (e.g. cystic disease) and extrarenal symptoms. "Cystoproteins" encoded by these disease genes most commonly localize to cilia and/or basal bodies, but their function is not understood. Herein, we report that the *C. elegans* homolog of the cystoprotein MKS3 (MKS-3) localizes specifically to the base of cilia. A large deletion in the *mks-3* gene does not inhibit ciliogenesis but instead results in a slight elongation of cilia. However, the combination this mutation in *mks-3* with a mutation in *nphp-4*, the homolog of the human disease gene *NPHP4*, leads to severe ciliogenesis defects. Our data indicate that *mks-3* is part of a genetic pathway that includes *mks-1*, the homolog of the human disease gene *MKS1*, and the two additional members of the *mks-1* gene family, which all encode B9 domain proteins. The B9 domain proteins TZA-1 and TZA-2 are necessary for restricting MKS-3 at the base of cilia and not allowing the protein to enter the cilium proper. TZA-1 is additionally required for restricting an unrelated transmembrane protein, TRAM-1, from ciliary entry. Because MKS-3 and TRAM-1 are allowed ciliary membrane access in the absence of the B9 proteins, we propose a general role of the B9 proteins in the process of regulating ciliary membrane composition. This is one of the first reports providing insight into this process.

INTRODUCTION

Cilia are microtubule-based organelles that extend from most cells in the mammalian body. Ciliopathies, or diseases involved in the disruption of cilia or basal body-localized proteins in humans, encompass a remarkably diverse array of developmental and clinical phenotypes. Meckel-Gruber Syndrome (MKS) is perhaps the most severe disease of cilia dysfunction as these patients present with renal cystic dysplasia, polydactyly, occipital encephalocele, and often die pre- or perinatally (Reviewed in Alexiev et al., 2006). MKS is an autosomal recessive and genetically heterogeneous disorder with six associated loci (*MKS1-6*). Five of these loci have been identified and linked to specific genes encoding cilia and/or basal body proteins (Baala et al., 2007a; Delous et al., 2007; Kyttala et al., 2006; Roume et al., 1998; Smith et al., 2006b; Tallila et al., 2008). Mutations in several of the MKS genes are also associated with phenotypes in other more mild forms of human ciliopathies such as Nephronophthisis (NPHP), Joubert Syndrome (JBTS), and Bardet-Biedl Syndrome (BBS). Examples of these multidisorder loci include *MKS1/BBS13*, *MKS3/JBTS6*, *MKS4/NPHP6/BBS14*, and *MKS5/NPHP8/JBTS7* (Arts et al., 2007; Baala et al., 2007b; Delous et al., 2007; Leitch et al., 2008; Sayer et al., 2006). These data suggest that MKS, NPHP, JBTS, and BBS represent a spectrum of phenotypes resulting from a common underlying ciliary dysfunction.

Proteins involved in MKS, NPHP, and BBS form distinct complexes at the base of the cilium; however, these complexes appear to be interconnected. For example, a complex containing several proteins involved in NPHP also includes CEP290 (MKS4), RPGRIP1L (MKS5), and Jouberin (JBTS1/AHI1) (Eley et al., 2008; Mollet et al., 2005; Roepman et al., 2005; Schafer et al., 2008b). MKS1 is believed to form a complex in *C.*

elegans that contains two B9 domain proteins, but it is not known whether these proteins are associated with other known complexes involved in human ciliopathies (Williams et al., 2008). However, this seems a possibility based on, first, the fact that some *MKS1* mutations can manifest BBS- and NPHP-like phenotypes, and second, the finding that MKS1 is in complex with MKS3, which is disrupted in some cases of JBTS (Badano et al., 2006a; Dawe et al., 2007b; Leitch et al., 2008).

The best characterized of the ciliopathy-associated complexes is the BBSome, which consist of at least seven BBS proteins (Nachury et al., 2007). The BBS complex is thought to regulate cilia membrane morphogenesis and to coordinate protein loading onto the Intraflagellar Transport (IFT) machinery (Blacque et al., 2004). Interestingly, it was shown that some G protein coupled receptors (GPCRs) fail to enter the cilium of cells with mutations in BBS proteins (Berbari et al., 2008). In contrast, the molecular roles of the NPHP and MKS complexes are poorly understood (Blacque et al., 2004).

Although proteins associated with human ciliopathies are found within the cilium, they are also often associated with the centrioles in dividing cells and then localize at the ciliary base when the centrioles have incorporated as basal bodies. Prior to ciliogenesis, the mother centriole associates with vesicles that form a phospholipid bubble over the growing axoneme of the cilium and later fuse with the plasma membrane, anchoring the centriole and cilium to the surface of the cell (Sorokin, 1968). During ciliogenesis the centriole functions as a nucleation site of the ciliary microtubule axoneme, facilitating the formation of the nine ciliary microtubule doublets from a template of nine microtubule triplets in the centriole/basal body (Snell, 1984). Additionally, basal bodies are thought to participate in the trafficking of materials into and out of the cilium, potentially func-

tioning as a docking or loading and unloading station for cilia and intraflagellar transport (IFT) proteins (Deane et al., 2001).

Analyses conducted in model organisms such as *Chlamydomonas reinhardtii* and *Caenorhabditis elegans* have been instrumental in developing our fundamental understanding of cilia biology and for identifying new genes involved in cilia function. In *C. elegans*, cilia are present on amphid/labial and phasmid sensory neurons in the head and tail of the animal, respectively. The cilia extend off the dendritic tips of these neurons and function as part of the main sensory machinery of the organism.

Ultrastructural data show these immotile cilia are comprised of three distinct regions of microtubule arrangement (Perkins et al., 1986). The first region is the distal tip of the cilium, which contains only singlet microtubules. The second region, known as the middle segment, contains the typical nine doublet microtubules in addition to seven or less inner singlet microtubules. The final proximal segment, which connects to the dendritic tip of the neuron, contains a transition zone and is comprised of nine doublet microtubules and seven inner singlets, but in this region the doublets and singlets are separated by an apical ring. Additionally, the doublets in the transition zone are anchored to the ciliary membrane. Transition fibers, which are thought to help regulate what proteins enter the cilium, are found immediately beneath the transition zone. In contrast to other organisms, in *C. elegans* there is no distinct centriole associated with these transition fibers. It has not been resolved whether the centriole is actually absent from the ciliary base or is present and simply not evident in the electron micrographs. Despite this difference, it is believed that the transition zone/ciliary base in *C. elegans* functions in similar manner to the basal bodies of other ciliated organisms. This is supported by the fact that

the *C. elegans* homologs of mammalian basal body proteins are similarly localized at the base of the cilium. These include NPH-1/NPHP-1 and NPH-4/NPHP-4, the *C. elegans* homologs of human NPHP1 (nephrocystin-1) and NPHP4 (nephrocystin-4), respectively, the three B9 domain-containing proteins MKS-1/XBX-7, TZA-2, and TZA-1 (human MKS1, B9D1 and B9D2, respectively), and multiple proteins involved in BBS (Blacque and Leroux, 2006; Williams et al., 2008; Winkelbauer et al., 2005) .

Multiple complexes containing proteins involved in human ciliopathies have now been identified that reside at the base of the cilium. *C. elegans* has been a good model system to assess the hierarchy of the interaction between proteins within a complex as well as to analyze potential functional interactions and redundancies between distinct basal body complexes. This has been done in the case of NPHP and MKS/B9 complexes, where it was shown that NPHP-1 requires NPHP-4 for its localization to the base of cilia, and with the B9 proteins, TZA-1 was needed for localization of TZA-2, which was in turn needed for localization of MKS-1. In contrast, mutations in *nphp-1* or *nphp-4* did not affect the B9 proteins nor did any mutation in the B9 genes affect localization of NPHP-1 or NPHP-4. In this manner, NPHP-1 and NPHP-4 were assigned to one protein complex group (NPHP complex) while MKS-1, TZA-2, and TZA-1 were assigned to another (MKS/B9 complex) (Williams et al., 2008; Winkelbauer et al., 2005). Although the MKS/B9 and NPHP complexes appear to be distinct, genetic analysis indicates there is a functional redundancy between these two complexes. Mutations in any of the genes encoding proteins of either complex alone (e.g. *nphp-1* or *mks-1*) or combined mutations in each of the genes encoding a specific complex of proteins (e.g. *nphp-1;nphp-4* double or *mks-1;tza-1;tza-2* triple mutants) were found to have minimal overt effects on cilia for-

mation (although some ciliary ultrastructural defects have been reported in *nphp* mutant worms) (Jauregui et al., 2008; Williams et al., 2008). In contrast, worms with a single mutation in an *nphp* gene along with a single mutation in any one of the B9 protein-encoding genes (e.g. *nphp-1;mks-1* double mutant) had severe defects in cilia formation, positioning, and orientation (Williams et al., 2008).

Herein, we demonstrate novel function of MKS-3 (F35D2.4), the homolog of human MKS3/tmem67/meckelin. MKS-3 unlike the other *B9* or *nphp* gene products conserved in *C. elegans*, is a transmembrane protein. We report that in *C. elegans,* MKS-3 localizes to two distinct domains, one at the distal end of the dendrite and the second at the base/proximal end of cilium. This localization partially overlaps that seen for other NPHP and MKS/B9 complex proteins. In contrast to the effect of knocking down MKS3 in mammalian cells where ciliogenesis was impaired, the *C. elegans mks-3* mutants exhibit a small but significant increase in cilia length. Similar to our results with the B9 protein-encoding genes, we demonstrate a genetic interaction of an *mks-3* mutation with a mutation in *nphp-4* that causes a severe cilia morphology defect. This is not seen in double mutations affecting *mks-3* and any of the other B9 protein-encoding genes. Together, the localization of MKS-3 and genetic interaction between the *mks-3* and *nphp-4* mutations indicate that MKS-3 can be functionally assigned to the MKS/B9 complex along with TZA-1, TZA-2, and MKS-1.

MATERIALS AND METHODS

General molecular biology methods

Molecular biology procedures were performed according to standard protocols (Sambrook et al., 1989). *C. elegans* genomic DNA, *C. elegans* cDNA, or cloned *C. elegans* DNA was used for PCR amplifications, for direct sequencing, or for subcloning (Sambrook *et al*., 1989). All PCR for cloning was performed with Phusion High-Fidelity DNA Polymerase (Finnzymes, Espoo, Finland). Clones, primer sequences, and PCR conditions are available upon request. DNA sequencing was performed by the University of Alabama at Birmingham Genomics Core Facility of the Heflin Center for Human Genetics.

DNA and protein sequence analyses

Genome sequence information was obtained from the National Center for Biotechnology Information (http://www.ncbi.nlm.nih.gov/). Gene and protein sequences were identified using the *C. elegans* database Wormbase and references therein (http://www.wormbase.org). BLAST searches to identify homologs in human, mouse, and *S. purpuratus* were performed using the National Center for Biotechnology Information (NCBI) BLAST service (http://www.ncbi.nlm.nih.gov/BLAST/). Protein sequence alignments were performed and conserved motifs were identified using Phobius (http://phobius.cbr.su.se/).

Strains

Worm strains were obtained from the *Caenorhabditis* Genetics Center, *C. elegans*

Knock-out Consortium, and National BioResource Project in Japan. Strains were grown using standard *C. elegans* growth methods (Brenner, 1974) at 22°C unless otherwise stated. The wild-type strain was N2 Bristol. The following mutations were used: RB743 *nphp-1(ok500)II*, JT6924 *daf-19(m86)II;daf-12(sa204)X*, FX2705 *mks-1(tm2705)III*, FX2452 *tza-1(tm2452)IV*, FX925 *nphp-4(tm925)V*, JT204 *daf-12(sa204)X*, RB1682 *tza-2(ok2092)X*, FX2547 *mks-3(tm2547)II*, YH499 *mks-3(tm2547)II;mks-1(tm2705)III*, YH576 *mks-3(tm2547)II;nphp-4(tm925)V*, and YH582 *mks-3(tm2547)II;tza-1(tm2452)IV*. RB743, FX2705, FX2547 FX2452, FX925, and RB1682 were outcrossed three times and genotyped by PCR prior to analysis.

Generation of constructs and strains

Vectors used for generating transcriptional and translational fusion constructs were modified from pPD95.81 (a gift from A. Fire). pCJF6 (CFP), pCJF7 (YFP), pCJ102 (DsRed2), pCJF36 (CHE-13::CFP), pCJF37 (CHE-13::YFP), pCJ146 (NPH-4::YFP), and pCJ148 (NPH-1::CFP) were generated as previously described (Winkelbauer *et al.*, 2005). pPD95.81::tdTomato was generously provided by M. Barr (Rutgers University). cGV1 (pPD95.81::Gateway::GFP) was generated by blunt cloning the Gateway cassette c.1 into pPD95.81 at SmaI (Invitrogen, Carlsbad, CA). pMW21.1 (P*osm-5*::tdTomato) was generated by subcloning the 350 bp *osm-5* promoter from pCJ5 to pPD95.81::tdTomato (Haycraft et al., 2001). p329.1 (*mks-3::GFP*) was generated by inserting pPD95.81 with a 300 bp promoter fragment amplified from N2 genomic DNA corresponding to the region immediately upstream and slightly downstream of the *mks-3* ATG,. p330.1 (MKS-3::GFP) was generated by amplifying the 300 bp promoter and en-

tire genomic region of *mks-3* from N2 genomic DNA and inserting the fragment into cGV1 via Gateway technology. p327.1 (MKS-1::tdTomato) was generated by subcloning the 3.2 kb *mks-1* genomic fragment from p318 to pPD95.81::tdTomato (Williams et al., 2008). p328.1 (P*osm-5*::XBX-1::tdTomato) was generated by subcloning the 700 bp tdTomato fragment from pPD95.81 to pCJF17.1 (P*osm-5*::XBX-1::YFP) (Schafer et al., 2003). p350 (P*osm-5*::TRAM-1a::tdTomato) was generated by amplifying the 1116 bp TRAM-1 transcript from N2 cDNA and inserting the fragment into pMW21.1. Transgenic worms were generated as previously described (Mello et al., 1991).

Imaging

Worms were anesthetized using 10 mM Levamisole and immobilized on 2% agar pads for imaging. Confocal analysis was performed on a Nikon 2000U inverted microscope (Melville, KY) outfitted with a PerkinElmer UltraVIEW ERS 6FE-US spinning disk laser apparatus (Shelton, CT). Confocal images were processed with Volocity 4 (Improvision Inc, Waltham, MA). Further processing of images was performed using Photoshop 7.0 (Adobe Systems, Inc., San Jose, CA, USA).

DAF-19 regulation

To asses DAF-19 regulation in vivo, the transgenic line YH588was generated by injection of *mks-3::GFP* into N2. This strain was then crossed to JT204 and subsequently to JT6924 to achieve *daf-19*(m86) background. The strain contained a mutation in *daf-12(sa204)X* to suppress the Daf-c phenotype of *daf-19(m86)II*. A backcross with JT204 was then used to assess *mks-3::GFP* expression in *daf-19(+/-)* background.

RT-PCR

RNA was isolated as described previously (Haycraft et al., 2003) from *mks-3(tm2547)* mutants. Reverse transcribed RNA was generated using Superscript II Reverse Transcriptase (Invitrogen, Carlsbad, CA, USA) using the manufacturer's instructions. Fragments spanning the deleted region of each respective gene were then amplified by PCR and sequenced.

Assays

Dye-filling using DiI (Molecular Probes, Carlsbad, CA, USA) was performed as described previously (Starich *et al*., 1995).

RESULTS

mks-3 Encodes a Predicted Seven Transmembrane-Spanning Protein

Recently, *tmem67* was identified as the gene responsible for the disease phenotypes in the Wistar Polycystic Kidney (*wpk*) rat and also the disease locus for human *MKS3* (Smith et al., 2006b). MKS3 is a predicted seven transmembrane-spanning protein that colocalizes with acetylated α-tubulin along the ciliary axoneme in mammalian inner medullar collecting duct cells (IMCD-3) cells (repeated in Adams et al., 2008; Dawe et al., 2007b). Data suggest based on *in vitro* siRNA knockdown approaches that MKS3 may have important roles in ciliogenesis, branching morphogenesis in the kidney, and centriole migration. The homolog of MKS3 in *C. elegans*, F35D2.4 (hereafter referred to as MKS-3), has not been described. BLAST analysis indicates that the nematode *mks-3* gene product is 30% identical and 46% similar to the human protein. Based on computational analysis, it also contains each of the seven transmembrane domains predicted in human MKS3, a cysteine-rich region near the N-terminus, and a highly conserved region in the C-terminal tail (Figure 1A and Supplementary Figure 1). The major difference between the nematode and mammalian protein is the lack of a predicted N-terminal signal peptide in the worm.

DAF-19 Regulates Expression of mks-3 in Ciliated Sensory Neurons

The *MKS3 C. elegans* homolog *mks-3* was first identified as a candidate ciliary gene in a computational search for X-box promoter elements, which are utilized by the ciliogenic RFX-type transcription factor DAF-19c to drive gene expression in ciliated sensory neurons (Efimenko et al., 2005; Senti and Swoboda, 2008; Swoboda et al., 2000).

A putative X-box motif was identified in the promoter of *mks-3* at position -159 relative to the predicted translational start. Efimenko *et al*. designed a transcriptional reporter containing about 2 kb of promoter plus a portion of the coding region of *mks-3* fused to GFP and expressed the construct in wild-type worms. They observed expression of the reporter specifically in ciliated sensory neurons, suggesting native expression of *mks-3* in these cells. We generated a similar but smaller *mks-3::GFP* reporter comprised of a 320 bp promoter segment and a portion of the first exon fused to GFP and used this construct to verify expression in the amphid and labial neurons in the head (Figure 2A) and phasmid neurons of the tail (data not shown). To determine if *mks-3* expression is regulated by DAF-19, we crossed transgenic wild-type worms expressing *mks-3::GFP* with *daf-19(m86)* mutant worms. We observed that *mks-3::GFP* expression was almost completely abolished in homozygous *daf-19* mutant background but could be restored by backcrossing with *daf-19(+/+)* worms (Figure 2B, C). This data suggests that *mks-3* is strongly regulated by the DAF-19 transcription factor.

MKS-3 Concentrates at the Base of the Cilium in C. elegans

The reported colocalization of human MKS3 with acetylated α-tubulin in IMCD-3 cells indicates that in mammals MKS3 is present along the ciliary axoneme (Dawe et al., 2007b). To determine if *C. elegans* MKS-3 also localizes to the cilium, we generated an MKS-3 translational fusion construct comprised of the 320-bp promoter and entire coding region of *mks-3* fused in frame with GFP (MKS-3::GFP). We coexpressed MKS-3::GFP in wild-type worms with XBX-1::tdTomato (dynein light intermediate chain involved in retrograde IFT) to compare MKS-3 localization with a known cilia protein. In

contrast to the data for mouse MKS3 in IMCD cells, we found *C. elegans* MKS-3::GFP was localized specifically to the base of cilia, and remarkably, not along the length of the cilium (Figure 3A, B). Upon closer inspection, we observed that MKS-3::GFP was diffusely localized in the dilated region of the dendritic tips of the ciliated sensory neurons where XBX-1::tdTomato strongly accumulated (Figure 3E, E'). Additionally, MSK-3 concentrated most heavily at the ciliary base (Figure 3E)..

Because mutations in *MKS1* and *MKS3* result in similar disease phenotypes in humans and the two associated proteins are found in complex together, we also compared localization of MKS-3::GFP with MKS-1::tdTomato. As shown previously, MKS1::tdTomato localization was tightly restricted to the base of the cilium in a domain that overlapped with MKS3::GFP (Figure 3F, G, G'). However, MKS1::tdTomato was not found in the dendritic tips (outside the cilium) where MKS-3::GFP diffusely accumulated (Figure 3F, G, G').

Bae et al. recently reported that the transmembrane protein PKD-2 (homolog of human transient receptor potential polycystin-2 channel) colocalized with translocating chain-associating membrane protein (TRAM-1) at the ER in cell bodies of ciliated sensory neurons and at the base of cilia as well (Bae et al., 2006). Because both PKD-2 and MKS-3 are transmembrane proteins that concentrate primarily at the base of cilia, we hypothesized that MKS-3 may similarly colocalize with TRAM-1. To address this possibility we coexpressed MKS-3::GFP and TRAM-1a::tdTomato in wild-type worms. In the cell bodies of ciliated sensory neurons, MKS-3::GFP overlapped TRAM-1a::tdTomato (Figure 4A). This data indicates MKS-3 is inserted into the ER membrane and is therefore likely to be trafficked to the base of cilia via vesicular transport. Near the base of

cilia, TRAM-1a::tdTomato colocalized with MKS-3::GFP only at the dendritic tips and not within the bases of cilia (Figure 4B). This suggests MKS-3 is sorted from vesicles into the cell membrane at the base of cilia.

Characterization of an mks-3 deletion allele

Previous experiments utilizing small interfering RNA (siRNA) against mammalian *MKS3* indicated MKS3 may function in ciliogenesis by controlling centriole movement to the apical membrane (Dawe et al., 2007b). To compare these results to *mks-3* gene function in *C. elegans*, we obtained a genetic mutant FX2547 *mks-3(tm2547)* from the National Bioresource Project (Japan). The *tm2547* allele contains a large internal genomic deletion of nucleotides 640-1588 (949 nt) that removes a region beginning in exon 4 spanning through a portion of exon 7. RT-PCR analysis of the mutant transcript revealed that the deletion fuses exons 4 and 7 and creates a translational frameshift (Figure 1B). The predicted amino acid chain continues only five residues past the frameshift before terminating at a premature stop. The *tm2547* allele would therefore encode a truncated protein of only 152 amino acids (compared to 897 amino acids in the full length protein). This truncated protein, if generated, lacks each of the predicted seven transmembrane domains. Thus *tm2547* likely represent a null allele (Figure 1B and C).

mks-3 is not required for C. elegans ciliogenesis

Multiple genes involved in cystic kidney disorders are involved in cilia formation. Using an siRNA-based knockdown approach, Dawe et al. targeted *MKS3* message and observed a disruption of cilia formation in IMCD-3 cells (Dawe et al., 2007b). To ana-

lyze whether cilia were present in homozygous *mks-3(tm2547)* null *C. elegans*, we utilized a dye-filling assay that measured the ability of worms to uptake fluorescent hydrophobic die (DiI) through the ciliary membrane (Starich et al., 1995). Properly formed cilia in *C. elegans* are projected from neurons through pores opening into the environment. This direct exposure allows cilia to contact and absorb DiI, which then spreads throughout the rest of the neuron. In contrast to siRNA data in mammalian cells, our dye-filling analysis using a genetic lesion in *C. elegans* revealed that *mks-3(tm2547)* null worms could normally uptake DiI, indicating that cilia are present in this mutant background (Figure 4B).

tza-1 and tza-2 are required to restrict MKS-3 to the base of cilia

In our previous work, we demonstrated that the B9 domain proteins (TZA-1, TZA-2, and MKS-1) function as part of a complex (MKS/B9 protein complex) at the base of the cilium in *C. elegans* (Williams et al., 2008). Within this complex, TZA-1 was needed for proper localization of TZA-2, which in turn was needed for localization of MKS-1. Furthermore, we observed with the NPHP complex, which is localized similarly at the base of cilia, that NPHP-4 is required for NPHP-1 localization. Because none of the B9 proteins nor the NPHP proteins were affected by the loss of any of the proteins in the other complex, we concluded that the NPHP and MKS/B9 complexes are distinct (Williams et al., 2008; Winkelbauer et al., 2005).

To begin evaluating if MKS-3 functions as part of one of these complexes, we analyzed whether NPHP or B9 proteins were needed to maintain MKS-3 localization or whether MKS-3 was needed to maintain NPHP or B9 proteins at the base of the cilium.

For this we first generated worms expressing MKS-3::GFP in the *mks-1(tm2705)*, *tza-1(tm2452)*, *tza-2(ok2092)* or *nphp-4*(*tm925*) mutant backgrounds. In *mks-1(tm2705)* mutants, MKS-3 localized normally (Figure 6B, Supplementary Figure 2A). In contrast, MKS-3 localization in *tza-1(tm2452)* and *tza-2(ok2092)* mutants was markedly altered (Figure 6C-F, Supplementary Figure 2B-E). In some of the *tza-1(tm2452)* and *tza-2(ok2092)* mutants, expression of MKS-3::GFP was undetectable. However, in most cases, MKS-3::GFP was found to extend past its normal restriction at the dendritic tip and ciliary base and accumulate in the cilium axoneme, This was never observed in the context of a wild type control (Figure 6A, and Supplementary Figure 2F and G). In addition, the localization of MKS3::GFP was not the altered in *nph-4(tm925)* mutants. Together, these data suggest that MKS3 may function as part of the MKS/B9 complex and importantly indicate that TZA-1 and TZA-2 function to restrict entry of MKS-3 to the cilium.

To further evaluate a potential interaction between MKS-3 and the NPHP and MKS/B9 complexes, we generated *mks-3(tm2547)* mutant worms coexpressing MKS-1::YFP and CHE-13::CFP as well as *mks-3(tm2547)* mutants coexpressing NPHP-1::CFP and CHE-13::YFP. CHE-13 is an IFT complex B protein (IFT57) and served as a cilia marker. In *mks-3(tm2547)* mutant background, both MKS-1 and NPHP-1 were evident at the base of cilia and did not appear different than in the wild-type control (Supplementary Figure 3). Because previous hierarchal analysis indicates that MKS-1 and NPHP-1 are dependant on TZA-1/TZA-2 and NPHP-4 for their normal localization, respectively, then these results suggest those proteins will also be correctly localized in the *mks-3(tm2547)* mutants, although this has not been directly analyzed.

tza-1 is required to restrict TRAM-1 from the cilium

Because MKS-3::GFP freely localized along the length of cilia in *tza-1(tm2452)* and *tza-2(ok2092)* mutants, we speculated that the B9 proteins may restrict other transmembrane proteins from the cilium. To test this possibility, we analyzed transgenic *tza-1(tm2452)* mutants coexpressing TRAM-1a::tdTomato (a transmembrane protein that accumulates at the base of but not within the cilium) and MKS-3::GFP. Similar to the altered localization of MKS-3, we readily observed TRAM-1 along the ciliary axonemes of *tza-1(tm2452)* mutants (Figure 7). This intriguing result suggests that B9 proteins may function in a general manner to regulate ciliary membrane composition by restricting the access of transmembrane proteins into the cilium.

MKS-3 functions as part of the MKS/B9 complex

Recent data indicate that while the MKS/B9 and NPHP protein complexes are not dependent on each other for proper localization to the base of the cilium, they are functionally connected. *C. elegans* with disruptions in multiple proteins within one complex were found to have no overt effects on cilia formation; however, compound mutants consisting of a disruption in one protein from each complex caused severe cilia phenotypes. Such phenotypes included shortened cilia in disorganized non-fasciculated bundles, improperly oriented cilia, and malformed neuronal dendrites. These data indicate that there is a functional redundancy between the NPHP and MKS/B9 complexes that is needed for normal ciliogenesis and cilia positioning (Williams et al., 2008).

To address whether there is a functional interaction between MKS-3 and the NPHP and/or MKS/B9 proteins, we analyzed *mks-3;tza-1* and *mks-3;nphp-4* double mutant worms for potential defects in ciliogenesis using transgenic lines expressing the IFT complex B protein CHE-13::YFP (IFT57) as a cilia marker. We included transgenic wild-type controls and *mks-3(tm2547)* single mutants in this analysis. We observed no overt cilia morphology defects in *mks-3;tza-1* double mutants (Figure 8A and B). In contrast, severe cilia and dendrite abnormalities were apparent in the *mks-3;nphp-4* double mutants (Figure 8C). Similar to defects caused by simultaneous disruption of both an MKS/B9 and an NPHP complex protein, defects in *mks-3;nphp-4* double mutants included the loss of tight fasciculation of the amphid cilia in the head and shortened cilia projecting from malformed phasmid dendrites in the tail (Figure 8C). Quantification of phasmid cilia length confirmed that *mks-3;nphp-4* double mutants had significantly shorter cilia than wild-type worms and *mks-3(tm2547)* single mutants (Figure 8D). Interestingly, as part of this analysis we uncovered that the phasmid cilia in *mks-3(tm2547)* single mutants were slightly, but significantly, longer than wild-type worms. Overall, the genetic interactions between *mks-3* and *nphp-4* with regards to cilia assembly are identical to that obtained when we conducted similar analysis with the B9 protein- encoding genes and *nphp-4* (we did not attempt to generate *mks-3;nphp-1* double mutants because both genes are closely linked in the genome). These data along with the effects of B9 protein disruptions on the localization of MKS-3 strongly support the idea that MKS-3 functions as additional member of the MKS/B9 protein complex.

DISCUSSION

Since the discovery of polycystins in the cilium, nearly every gene identified in association with inherited cystic kidney disease has proven to encode a ciliary- and/or basal body-localized protein. While the number of identified cystic kidney disease genes has rapidly increased over the past few years, development of our basic understanding of the associated proteins has lagged. In particular, function of the proteins affected in MKS patients has not been extensively analyzed. Studies with siRNA knockdown of *MKS1* in mammalian renal epithelium uncovered potential roles of this protein in centriole migration and ciliogenesis (Dawe et al., 2007b). However, an in-frame deletion mutation in *C. elegans mks-1* did not confer an alteration in cilia morphology (Williams et al., 2008). This discrepancy was partially reconciled with our finding that ciliogenesis defects did occur when an *nphp-1* or *nphp-4* mutation was combined with the *mks-1* mutation, suggesting that genetic background may influence the severity of ciliary phenotypes (Williams et al., 2008). This is reminiscent of a theme emerging in human disease families in which heterozygous mutations in one disease-related gene can enhance the severity of disease caused by a separate homozygous mutation in the same individual. Additionally, morpholino knockdown of multiple disease genes in zebrafish can have synergistic effects on cilia-related developmental phenotypes such as the formation of renal cysts (Leitch et al., 2008).

Like *MKS1*, knockdown of *MKS3* in cell culture by siRNA can inhibit ciliogenesis, but again, genetic mutations in *MKS3* have not caused ciliogenesis defects *in vivo*. This was first observed with a missense mutation in rodent *MKS3* that did not confer any reported alterations in cilia morphology but did cause cystic kidney disease and other

MKS-like phenotypes (Gattone et al., 2004; Smith et al., 2006b). Similarly, we demonstrated here that a truncation mutation in *C. elegans mks-3* did not did not affect ciliogenesis. In contrast, this mutation actually conferred a slight increase in cilia length. This finding is not without precedent, as *Nphp3*$^{pcy/ko}$ mice have elongated renal epithelial cilia as well as cystic kidneys (Bergmann et al., 2008). Additionally, elongation of male-specific CEM cilia in *nphp-1* and *nphp-4* mutant *C. elegans* is sometimes observed (Jauregui et al., 2008). Only when we combined the *mks-3(tm2547)* mutation with the *nphp-4(tm925)* mutation did cilia morphology defects arise. Because of this finding and our observation that no defects were observed when *mks-3* was disrupted in conjunction with mutations in any of the three B9 protein-encoding genes, we conclude that MKS-3 is likely an additional component of the MKS/B9 protein complex (Figure 9A).

We found MKS-3::GFP specifically at the tips of dendrites and concentrated at the base of cilia in wild-type worms and not present along ciliary axonemes. This observation conflicts with previous reports of mouse MKS3 localizing throughout cilia in cell culture (Adams et al., 2008; Dawe et al., 2007b). Similar discrepancies have been reported between the localization of *C. elegans* versus mammalian NPHP1 and NPHP4. Whereas these two proteins specifically localize to the base of cilia in *C. elegans*, mammalian NPHP1 localizes to the ciliary base and to focal adhesions while mammalian NPHP4 is found along the ciliary axoneme in addition to concentrating at the ciliary base (Donaldson et al., 2002; Mollet et al., 2005). We demonstrated here that MKS-3::GFP freely entered the cilia only when expressed in *tza-1(tm2452)* or *tza-2(ok2092)* mutant background. This may allude to a molecular mechanism in which MKS-3 entry into the cilium is directly or indirectly regulated by B9 proteins at the ciliary base (Figure 9B).

Despite data indicating that mammalian MKS1 and MKS3 are part of the same protein complex, we saw no dependency between *C. elegans* MKS-1 and MKS-3 for localization to the base of cilia. Because *mks-3(tm2547)* is a deletion mutation that results in the truncation of all seven MKS-3 transmembrane domains, we considered the allele to be a null mutation. MKS-1 localized normally in this mutant background, strongly suggesting MKS-3 does not participate in the anchoring of MKS-1 at the base of cilia. Likewise, MKS-3 localized normally in *mks-1(tm2705)* mutant background. However, *mks-1(tm2705)* is an in-frame deletion mutation to disrupts only a small segment in the N-terminal region of MKS-1 (Williams et al., 2008). Because this mutation is possibly hypomorphic, we cannot formally rule out the possibility that MKS-1 may regulate MKS-3 at the base of cilia in a fashion similar to TZA-1 and TZA-2.

Because the transmembrane protein MKS-3 was allowed ciliary entry in *tza-1(tm2452)* and *tza-2(ok2092)* mutant worms, we extended our analysis of these mutants to include an additional transmembrane protein concentrated at the base of cilia. One such protein is TRAM-1, which in mammals is a core component of the translocon. Mammalian TRAM is found primarily in the ER but can also "escape" from the ER membrane and reside in post-ER compartments (Greenfield and High, 1999). In *C. elegans*, TRAM-1 concentrates most heavily in the ER but is also observed moving in particles along the dendrites of ciliated sensory neurons. TRAM-1 additionally accumulates at the dendritic tips of these neurons where MKS-3 also diffusely localized (Bae et al., 2006 and Figure 4). The function of TRAM-1 at the dendritic tips has not been described, and we did not perform that analysis here. However, when we expressed TRAM-1::tdTomato in *tza-1(tm2452)* mutants, TRAM-1 freely accessed the cilium simi-

lar to MKS-3 ciliary access in this genetic background. It was not determined whether TRAM-1 (or MKS-3) were inserted into the plasma membrane prior to accessing the cilium or if vesicles containing these proteins were instead leaking into the cilium. Overall, our data suggest that the B9 protein-encoding genes (at least *tza-1*) are required not only for the specific restriction of MKS-3 at the base of cilia, but may also be required in a general capacity to globally regulate ciliary membrane access.

Analysis of genes associated with inherited cystic kidney disease is essential to the understanding of renal and extrarenal pathologies arising in afflicted families. This analysis should include the determination of how genetic modifiers can influence disease severity. Herein, we demonstrated a redundant requirement of *mks-3* and *nphp-4* in ciliogenesis and dendrite morphology and uncovered a potential role of the MKS/B9 protein complex in regulating the ciliary access of MKS-3 and other transmembrane proteins. Understanding how the *C. elegans* B9 proteins function in this capacity may provide insight into why their disruption results in systemic developmental abnormalities in higher organisms.

AKNOWLEDGEMENTS

We thank M. Croyle, V. Roper, and E. Hamby for technical assistance. The *C. elegans* Genome Sequencing Consortium provided sequence information, and the *Caenorhabditis* Genetics Center, which is funded by the National Institutes of Health, provided some of the C. elegans strains used in this study. We thank the National BioResource Project in Japan for the *mks-3(tm2547)* deletion mutants. This work was supported by NIH R01 DK065655 to B.K.Y. Additional support was provided by the P30 DK074038 UAB Recessive Polycystic Kidney Disease Research and Translational Core Center.

REFERENCES

Adams, M, Smith, UM, Logan, CV & Johnson, CA: Recent advances in the molecular pathology, cell biology and genetics of ciliopathies. *J Med Genet,* 45**:**257-67, 2008.

Alexiev, BA, Lin, X, Sun, CC & Brenner, DS: Meckel-Gruber syndrome: pathologic manifestations, minimal diagnostic criteria, and differential diagnosis. *Arch Pathol Lab Med,* 130**:**1236-8, 2006.

Arts, HH, Doherty, D, van Beersum, SE, Parisi, MA, Letteboer, SJ, Gorden, NT, Peters, TA, Marker, T, Voesenek, K, Kartono, A, Ozyurek, H, Farin, FM, Kroes, HY, Wolfrum, U, Brunner, HG, Cremers, FP, Glass, IA, Knoers, NV & Roepman, R: Mutations in the gene encoding the basal body protein RPGRIP1L, a nephrocystin-4 interactor, cause Joubert syndrome. *Nat Genet,* 39**:**882-8, 2007.

Baala, L, Audollent, S, Martinovic, J, Ozilou, C, Babron, MC, Sivanandamoorthy, S, Saunier, S, Salomon, R, Gonzales, M, Rattenberry, E, Esculpavit, C, Toutain, A, Moraine, C, Parent, P, Marcorelles, P, Dauge, MC, Roume, J, Le Merrer, M, Meiner, V, Meir, K, Menez, F, Beaufrere, AM, Francannet, C, Tantau, J, Sinico, M, Dumez, Y, MacDonald, F, Munnich, A, Lyonnet, S, Gubler, MC, Genin, E, Johnson, CA, Vekemans, M, Encha-Razavi, F & Attie-Bitach, T: Pleiotropic effects of CEP290 (NPHP6) mutations extend to Meckel syndrome. *Am J Hum Genet,* 81**:**170-9, 2007.

Baala, L, Romano, S, Khaddour, R, Saunier, S, Smith, UM, Audollent, S, Ozilou, C, Faivre, L, Laurent, N, Foliguet, B, Munnich, A, Lyonnet, S, Salomon, R, Encha-Razavi, F, Gubler, MC, Boddaert, N, de Lonlay, P, Johnson, CA, Vekemans, M, Antignac, C & Attie-Bitach, T: The Meckel-Gruber syndrome gene, MKS3, is mutated in Joubert syndrome. *Am J Hum Genet,* 80**:**186-94, 2007.

Badano, JL, Leitch, CC, Ansley, SJ, May-Simera, H, Lawson, S, Lewis, RA, Beales, PL, Dietz, HC, Fisher, S & Katsanis, N: Dissection of epistasis in oligogenic Bardet-Biedl syndrome. *Nature,* 439**:**326-30, 2006.

Bae, YK, Qin, H, Knobel, KM, Hu, J, Rosenbaum, JL & Barr, MM: General and cell-type specific mechanisms target TRPP2/PKD-2 to cilia. *Development,* 133**:**3859-70, 2006.

Berbari, NF, Lewis, JS, Bishop, GA, Askwith, CC & Mykytyn, K: Bardet-Biedl syndrome proteins are required for the localization of G protein-coupled receptors to primary cilia. *Proc Natl Acad Sci U S A,* 105**:**4242-6, 2008.

Bergmann, C, Fliegauf, M, Bruchle, NO, Frank, V, Olbrich, H, Kirschner, J, Schermer, B, Schmedding, I, Kispert, A, Kranzlin, B, Nurnberg, G, Becker, C, Grimm, T, Girschick, G, Lynch, SA, Kelehan, P, Senderek, J, Neuhaus, TJ, Stallmach, T, Zentgraf, H, Nurnberg, P, Gretz, N, Lo, C, Lienkamp, S, Schafer, T, Walz, G, Benzing, T, Zerres, K & Omran, H: Loss of nephrocystin-3 function can cause embryonic lethality, Meckel-Gruber-like syndrome, situs inversus, and renal-hepatic-pancreatic dysplasia. *Am J Hum Genet,* 82**:**959-70, 2008.

Blacque, OE & Leroux, MR: Bardet-Biedl syndrome: an emerging pathomechanism of intracellular transport. *Cell Mol Life Sci,* 63**:**2145-61, 2006.

Blacque, OE, Reardon, MJ, Li, C, McCarthy, J, Mahjoub, MR, Ansley, SJ, Badano, JL, Mah, AK, Beales, PL, Davidson, WS, Johnsen, RC, Audeh, M, Plasterk, RH,

Baillie, DL, Katsanis, N, Quarmby, LM, Wicks, SR & Leroux, MR: Loss of C. elegans BBS-7 and BBS-8 protein function results in cilia defects and compromised intraflagellar transport. *Genes Dev,* 18**:**1630-42, 2004.

Brenner, S: The genetics of Caenorhabditis elegans. *Genetics,* 77**:**71-94, 1974.

Dawe, HR, Smith, UM, Cullinane, AR, Gerrelli, D, Cox, P, Badano, JL, Blair-Reid, S, Sriram, N, Katsanis, N, Attie-Bitach, T, Afford, SC, Copp, AJ, Kelly, DA, Gull, K & Johnson, CA: The Meckel-Gruber Syndrome proteins MKS1 and meckelin interact and are required for primary cilium formation. *Hum Mol Genet,* 16**:**173-86, 2007.

Deane, JA, Cole, DG, Seeley, ES, Diener, DR & Rosenbaum, JL: Localization of intraflagellar transport protein IFT52 identifies basal body transitional fibers as the docking site for IFT particles. *Current Biology,* 11**:**1586-90, 2001.

Delous, M, Baala, L, Salomon, R, Laclef, C, Vierkotten, J, Tory, K, Golzio, C, Lacoste, T, Besse, L, Ozilou, C, Moutkine, I, Hellman, NE, Anselme, I, Silbermann, F, Vesque, C, Gerhardt, C, Rattenberry, E, Wolf, MT, Gubler, MC, Martinovic, J, Encha-Razavi, F, Boddaert, N, Gonzales, M, Macher, MA, Nivet, H, Champion, G, Bertheleme, JP, Niaudet, P, McDonald, F, Hildebrandt, F, Johnson, CA, Vekemans, M, Antignac, C, Ruther, U, Schneider-Maunoury, S, Attie-Bitach, T & Saunier, S: The ciliary gene RPGRIP1L is mutated in cerebello-oculo-renal syndrome (Joubert syndrome type B) and Meckel syndrome. *Nat Genet,* 39**:**875-81, 2007.

Donaldson, JC, Dise, RS, Ritchie, MD & Hanks, SK: Nephrocystin-conserved domains involved in targeting to epithelial cell-cell junctions, interaction with filamins, and establishing cell polarity. *J Biol Chem,* 277**:**29028-35, 2002.

Efimenko, E, Bubb, K, Mak, HY, Holzman, T, Leroux, MR, Ruvkun, G, Thomas, JH & Swoboda, P: Analysis of xbx genes in C. elegans. *Development,* 132**:**1923-34, 2005.

Eley, L, Gabrielides, C, Adams, M, Johnson, CA, Hildebrandt, F & Sayer, JA: Jouberin localizes to collecting ducts and interacts with nephrocystin-1. *Kidney Int*, 2008.

Gattone, VH, 2nd, Tourkow, BA, Trambaugh, CM, Yu, AC, Whelan, S, Phillips, CL, Harris, PC & Peterson, RG: Development of multiorgan pathology in the wpk rat model of polycystic kidney disease. *Anat Rec A Discov Mol Cell Evol Biol,* 277**:**384-95, 2004.

Greenfield, JJ & High, S: The Sec61 complex is located in both the ER and the ER-Golgi intermediate compartment. *J Cell Sci,* 112 (Pt 10)**:**1477-86, 1999.

Haycraft, CJ, Schafer, JC, Zhang, Q, Taulman, PD & Yoder, BK: Identification of CHE-13, a novel intraflagellar transport protein required for cilia formation. *Exp Cell Res,* 284**:**251-63, 2003.

Haycraft, CJ, Swoboda, P, Taulman, PD, Thomas, JH & Yoder, BK: The C. elegans homolog of the murine cystic kidney disease gene Tg737 functions in a ciliogenic pathway and is disrupted in osm-5 mutant worms. *Development,* 128**:**1493-1505, 2001.

Jauregui, AR, Nguyen, KC, Hall, DH & Barr, MM: The Caenorhabditis elegans nephrocystins act as global modifiers of cilium structure. *J Cell Biol,* 180**:**973-88, 2008.

Kyttala, M, Tallila, J, Salonen, R, Kopra, O, Kohlschmidt, N, Paavola-Sakki, P, Peltonen, L & Kestila, M: MKS1, encoding a component of the flagellar apparatus basal body proteome, is mutated in Meckel syndrome. *Nat Genet,* 38**:**155-7, 2006.

Leitch, CC, Zaghloul, NA, Davis, EE, Stoetzel, C, Diaz-Font, A, Rix, S, Alfadhel, M, Lewis, RA, Eyaid, W, Banin, E, Dollfus, H, Beales, PL, Badano, JL & Katsanis, N: Hypomorphic mutations in syndromic encephalocele genes are associated with Bardet-Biedl syndrome. *Nat Genet,* 40**:**443-8, 2008.

Mello, CC, Kramer, JM, Stinchcomb, D & Ambros, V: Efficient gene transfer in C.elegans: extrachromosomal maintenance and integration of transforming sequences. *EMBO Journal,* 10**:**3959-70, 1991.

Mollet, G, Silbermann, F, Delous, M, Salomon, R, Antignac, C & Saunier, S: Characterization of the nephrocystin/nephrocystin-4 complex and subcellular localization of nephrocystin-4 to primary cilia and centrosomes. *Hum Mol Genet,* 14**:**645-56, 2005.

Nachury, MV, Loktev, AV, Zhang, Q, Westlake, CJ, Peranen, J, Merdes, A, Slusarski, DC, Scheller, RH, Bazan, JF, Sheffield, VC & Jackson, PK: A core complex of BBS proteins cooperates with the GTPase Rab8 to promote ciliary membrane biogenesis. *Cell,* 129**:**1201-13, 2007.

Perkins, LA, Hedgecock, EM, Thomson, JN & Culotti, JG: Mutant sensory cilia in the nematode Caenorhabditis elegans. *Developmental Biology,* 117**:**456-87, 1986.

Roepman, R, Letteboer, SJ, Arts, HH, van Beersum, SE, Lu, X, Krieger, E, Ferreira, PA & Cremers, FP: Interaction of nephrocystin-4 and RPGRIP1 is disrupted by nephronophthisis or Leber congenital amaurosis-associated mutations. *Proc Natl Acad Sci U S A,* 102**:**18520-5, 2005.

Roume, J, Genin, E, Cormier-Daire, V, Ma, HW, Mehaye, B, Attie, T, Razavi-Encha, F, Fallet-Bianco, C, Buenerd, A, Clerget-Darpoux, F, Munnich, A & Le Merrer, M: A gene for Meckel syndrome maps to chromosome 11q13. *Am J Hum Genet,* 63**:**1095-101, 1998.

Sambrook, J, Fritsch, EF & Maniatis, T: *Molecular Cloning: A Laboratory Manual,* Cold Spring Harbor, NY, Cold Spring Harbor Laboratory 1989.

Sayer, JA, Otto, EA, O'Toole, JF, Nurnberg, G, Kennedy, MA, Becker, C, Hennies, HC, Helou, J, Attanasio, M, Fausett, BV, Utsch, B, Khanna, H, Liu, Y, Drummond, I, Kawakami, I, Kusakabe, T, Tsuda, M, Ma, L, Lee, H, Larson, RG, Allen, SJ, Wilkinson, CJ, Nigg, EA, Shou, C, Lillo, C, Williams, DS, Hoppe, B, Kemper, MJ, Neuhaus, T, Parisi, MA, Glass, IA, Petry, M, Kispert, A, Gloy, J, Ganner, A, Walz, G, Zhu, X, Goldman, D, Nurnberg, P, Swaroop, A, Leroux, MR & Hildebrandt, F: The centrosomal protein nephrocystin-6 is mutated in Joubert syndrome and activates transcription factor ATF4. *Nat Genet,* 38**:**674-81, 2006.

Schafer, JC, Haycraft, CJ, Thomas, JH, Yoder, BK & Swoboda, P: XBX-1 encodes a dynein light intermediate chain required for retrograde intraflagellar transport and cilia assembly in Caenorhabditis elegans. *Mol Biol Cell,* 14**:**2057-70, 2003.

Schafer, T, Putz, M, Lienkamp, S, Ganner, A, Bergbreiter, A, Ramachandran, H, Gieloff, V, Gerner, M, Mattonet, C, Czarnecki, PG, Sayer, JA, Otto, EA, Hildebrandt, F, Kramer-Zucker, A & Walz, G: Genetic and physical interaction between the NPHP5 and NPHP6 gene products. *Hum Mol Genet*, 2008.

Senti, G & Swoboda, P: Distinct isoforms of the RFX transcription factor DAF-19 regulate ciliogenesis and maintenance of synaptic activity. *Mol Biol Cell,* 19**:**5517-28, 2008.

Smith, UM, Consugar, M, Tee, LJ, McKee, BM, Maina, EN, Whelan, S, Morgan, NV, Goranson, E, Gissen, P, Lilliquist, S, Aligianis, IA, Ward, CJ, Pasha, S, Punyashthiti, R, Malik Sharif, S, Batman, PA, Bennett, CP, Woods, CG, McKeown, C, Bucourt, M, Miller, CA, Cox, P, Algazali, L, Trembath, RC, Torres, VE, Attie-Bitach, T, Kelly, DA, Maher, ER, Gattone, VH, 2nd, Harris, PC & Johnson, CA: The transmembrane protein meckelin (MKS3) is mutated in Meckel-Gruber syndrome and the wpk rat. *Nat Genet,* 38**:**191-6, 2006.

Snell, WJ: The role of cilia and flagella in cell interactions. *Journal of Protozoology,* 31**:**12-6, 1984.

Sorokin, SP: Reconstructions of centriole formation and ciliogenesis in mammalian lungs. *Journal of Cell Science,* 3**:**207-30, 1968.

Starich, TA, Herman, RK, Kari, CK, Yeh, WH, Schackwitz, WS, Schuyler, MW, Collet, J, Thomas, JH & Riddle, DL: Mutations affecting the chemosensory neurons of Caenorhabditis elegans. *Genetics,* 139**:**171-88, 1995.

Swoboda, P, Adler, HT & Thomas, JH: The RFX-type transcription factor DAF-19 regulates sensory neuron cilium formation in C.elegans. *Mol. Cell,* 5**:**411-421, 2000.

Tallila, J, Jakkula, E, Peltonen, L, Salonen, R & Kestila, M: Identification of CC2D2A as a Meckel syndrome gene adds an important piece to the ciliopathy puzzle. *Am J Hum Genet,* 82**:**1361-7, 2008.

Williams, CL, Winkelbauer, ME, Schafer, JC, Michaud, EJ & Yoder, BK: Functional Redundancy of the B9 Proteins and Nephrocystins in Caenorhabditis elegans Ciliogenesis. *Mol Biol Cell,* 19**:**2154-2168, 2008.

Winkelbauer, ME, Schafer, JC, Haycraft, CJ, Swoboda, P & Yoder, BK: The C. elegans homologs of nephrocystin-1 and nephrocystin-4 are cilia transition zone proteins involved in chemosensory perception. *J Cell Sci,* 118**:**5575-87, 2005.

FIGURE LEGENDS

Figure 1. *mks-3* encodes a predicted seven transmembrane-spanning protein. (A) Illustration of *C. elegans* MKS-3 structure, demonstrating an N-terminal cysteine-rich region and seven membrane-bound motifs. (B) Sequence of the *tm2547* deletion allele, showing a frameshift that results in a premature stop. (C) Illustration of the predicted protein encoded by *mks-3(tm2547)* mutants. The truncated protein would lack all seven transmembrane domains.

Figure 2. Expression and DAF-19 regulation of *mks-3*. (A-C) Confocal fluorescence images of worms coexpressing *mks-3::GFP* (top) and *tza-1::DsRed2* (bottom) as a control marker of ciliated sensory neurons. (A) Compared to the expression of *tza-1::DsRed2*, *mks-3::GFP* was strongly expressed in amphid (arrowhead) and labial (arrow) sets of neurons of the head, which both extend dendritic processes to the (double arrowhead) anterior of the worm where they project sensory cilia. *tza-1::DsRed2* expression in labial neurons was not strong. (B) *mks-3* and *tza-1* transgene expression was almost completely abolished in worms crossed into *daf-19(m86)* mutant background. *mks-3::GFP* was faintly detected only in labial neurons (arrow). (C) Outcrossing transgenic worms from *daf-19(m86)* to *daf-19(+)* restored expression of both *mks-3::GFP* and *tza-1::DsRed2*.

Figure 3. MKS-3 concentrates at the base of cilia in *C. elegans*. (A) An illustration depicting the anatomical positions of (left) amphid cilia bundles in the head and (right)

phasmid cilia bundles in the tail with respect to (middle) a DIC image of the full body of an adult hermaphrodite worm. Red represents the ciliary axoneme, green represents the ciliary base, and blue represents the dendritic processes from which the cilia project. Short labial cilia surrounding the distal region of the amphid bundles and the degenerate PQR cilium near the phasmid bundles are not shown. (B-E) Confocal fluorescence images of wild-type transgenic worms coexpressing MKS-3::GFP (driven by its endogenous promoter) and XBX-1/dynein light intermediate chain::tdTomato (driven by the *osm-5* promoter). With respect to XBX-1, which freely entered the cilia (arrowheads), MKS-3 concentrated specifically at the base of cilia (arrows) on (B and D, left) sensory neurons in the head and (C and D, right) sensory neurons in the tail. (E) Increased magnification of a phasmid cilia pair marked with MKS-3::GFP and XBX-1::tdTomato. MKS-3 localized diffusely in the distal tips of the dendritic processes (arrow) and concentrated heavily at the proximal end of the cilia (double arrowhead), just beyond a region where XBX-1 intensely marked (arrowhead). (E') Numbered cross sections cut through a 3D projection of the top cilium in (E) corresponding to the anatomical positions marked. Depending upon the position along the dendritic tip and proximal end of the cilium, MKS-3 localized alone (1), partially overlapped XBX-1 (2), completely overlapped XBX-1, or localized separate from XBX-1 (4). (F and G) Confocal fluorescence images of wild-type transgenic worms coexpressing MKS-3::GFP and MKS-1::tdTomato (driven by its endogenous promoter). With respect to MKS-3, MKS-1 localized only to the proximal end of cilia where MKS-3 concentrated most intensely (arrows). (G') In cross sections cut through the anatomical positions marked in (G), MKS-3 fully overlapped MKS-1 wherever both markers were detected. Scale, 5μm (D and F); 2.5μm (E and G).

Figure 4. MKS-3 localizes to ER and post-ER compartments. (A and B) Confocal fluorescence images of wild-type transgenic worms coexpressing MKS-3::GFP (driven by its endogenous promoter) and TRAM1a::tdTomato (driven by the *osm-5* promoter). (A) In phasmid neuron cell bodies MKS-3::GFP localization overlapped the localization of TRAM1a::tdTomato, which marks the ER and post-ER compartments. (B) At phasmid ciliated endings, TRAM1a::tdTomato overlapped the localization of MKS-3::GFP only at the dendritic tips (arrowheads) and not at the bases of cilia where MKS-3::GFP concentrated most heavily (arrows). Scale, 2.5μm.

Figure 5. *mks-3(tm2547)* mutants dye-fill normally. The ability to uptake DiI was examined in wild-type worms and *mks-3(tm2547)* mutants. Inverted DIC images overlaid with confocal fluorescence of DiI staining are shown. (A and B) Wild-type and *mks-3(tm2547)* worms consistently absorbed DiI into ciliated sensory neurons in the head (arrows) and tail (arrowheads), indicative of properly formed cilia.

Figure 6. MKS-3 aberrantly localizes along the cilium axoneme in *tza-1(tm2452)* and *tza-2(ok2092)* mutants. MKS-3 localization was analyzed in confocal fluorescence images of wild-type, *mks-1(tm2705)*, *tza-1(tm2452)*, and *tza-2(ok2092)* strains coexpressing MKS-3::GFP (left) and XBX-1::tdTomato (right). One pair of phasmid cilia is shown in each panel. Cartoons illustrating MKS-3 localization are on the far right. Similar to (A) wild type, MKS-3 expressed in (B) *mks-1(tm2705)* mutants localized diffusely at the dendritic tips (arrow) and concentrated at the proximal end of the cilium (arrowhead). In

contrast, MKS-3 in (C) *tza-1(tm2452)* mutants did not concentrate at the proximal end of the cilium (arrowhead) but instead localized along the axoneme (double arrowhead) and accumulated at the dendritic tip (arrow). (D) MKS-3 was not detected in 22% of *tza-1(tm2452)* mutants (n=64). Similar to *tza-1(tm2452)* mutants, MKS-3 localized along the axoneme (double arrowhead) and accumulated at the dendritic tip (arrow) in (E) *tza-2(ok2092)* mutants. (F) Likewise, MKS-3 was not detected in 18% of *tza-2(ok2092)* mutants (n=57). Scale, 2.5µm.

Figure 7. TRAM-1 aberrantly localizes along the cilium axoneme in *tza-1(tm2452)* mutants. TRAM-1 localization was analyzed in confocal fluorescence images of *tza-1(tm2452)* strains coexpressing MKS-3::GFP (left) and P*osm-5*::TRAM-1a::tdTomato (right). One pair of phasmid cilia is shown. Cartoons illustrating TRAM-1 localization are on the far right. Compared to wild type (see Figure 4B), TRAM-1 in *tza-1(tm2452)* mutants was clearly detected along ciliary axonemes, similar to the mislocalization of MKS-3. Scale, 2.5µm.

Figure 8. *mks-3;nph-4* double mutants have short and incorrectly positioned cilia. Cilia morphology was analyzed in confocal fluorescence images of wild-type, *mks-3(tm2547)*, *mks-3;mks-1*, and *mks-3;nph-4* worms expressing the transgenic IFT particle B protein CHE-13::YFP. (A and B) Cilia morphology appeared overtly normal in wild-type (top), *mks-3(tm2547)* (middle), and *mks-3;tza-1* (bottom) strains. Arrowheads, proximal ends of cilia; double arrowheads, distal tips of cilia. (A) Representative pairs of amphid cilia bundles in the head. (A'and C') 1.66X magnification of amphid bundles in A and C, re-

spectively, and (A''and C'') 3D projections of the bundles rotated 90° along the x-axis, viewed from the proximal end. From this angle, the amphid cilia appeared tightly bundled. Arrows indicate the shorter labial cilia that are not part of the amphid organ. (B) Representative sets of phasmid neurons in the tail. Compared to wild type (top), mutant strains *mks-3(tm2547)* and *mks-3;tza-1* exhibited no abnormalities in the extension of dendrites (dotted lines) from the phasmid cell bodies (arrows) nor in the projection of full-length cilia (double-headed arrow) from the distal tips of the dendrites. (C) Amphid and (D) phasmid cilia arrangement and morphology was abnormal in *mks-3;nph-4* double mutants. Compared to wild type, some amphid cilia were positioned posterior with the respect to the rest of the sensory organ (C', arrowhead), and other amphid cilia often altogether lacked axonemes (arrow). (C'') Viewing the amphid organ down the axis of the axonemes indicated the cilia were not tightly bundled. (D) Phasmid dendrites often failed to properly extend from the cell bodies and projected stunted cilia. Scale, 5μm. (E) Measurements of phasmid cilia length in wild-type, *mks-3(tm2547)*, *mks-3;tza-1*, and *mks-3;nph-4* worms expressing CHE-13::YFP. Compared to wild type, *mks-3(tm2547)* mutants exhibited slightly longer phasmid cilia. In contrast, *mks-3;nph-4* double mutant phasmid cilia were only about half the length of wild-type cilia. Error bars, SEM. *$p < 0.05$; **$p < 0.0001$, compared with wild type. [a] Values are mean ± SEM.

Figure 9. *mks* and *nphp* genetic pathways and model of B9 protein-mediated sorting of membrane proteins at the ciliary base. (A) *mks-1* and *mks-3* lie downstream of *tza-1* and *tza-2* in a pathway involved in the formation of dendrites and cilia. *nphp-4* and *nphp-1* are in a separate pathway also involved in the formation of dendrites and cilia. Disrup-

tion of one pathway does not have a dramatic effect, but the loss of both pathways confers severe defects in dendrite and cilia morphology. (B) Vesicles fuse with the plasma membrane at the dendritic tip to deposit proteins at the base of cilia. The B9 proteins TZA-1 and TZA-2 participate in (1) holding membrane proteins such as MKS-3 at the base of cilia and (2) restricting other membrane proteins such as TRAM-1 from freely accessing the cilium. It is unclear whether the B9 proteins perform these functions directly or through intermediaries.

Supplementary Figure 1. Protein sequence alignment of MKS3 from *Homo sapiens (Hs)*, *Mus musculus (Ms)*, *Caenorhabditis elegans (Ce)*, and *Paramecium tetraurelia (Pt)*. Consensus residues and residues with positive Blosum62 scores are marked as indicated. The cysteine rich region is marked. Seven transmembrane domains (boxed) were identified in each sequence with the combined transmembrane topology and signal peptide predictor, Phobius (http://phobius.cbr.su.se/). An N-terminal cleavable signal peptide upstream of the cysteine rich region was identified in *Homo sapiens* and *Mus musculus* but not in *Caenorhabditis elegans* or *Paramecium tetraurelia* (not marked). The location of the *tm2547* frameshift (arrowhead) is shown.

Supplementary Figure 2. Localization of B9 proteins and Nephrocystins is unaffected in *mks-3(tm2547)* mutants. Confocal fluorescence images of worms coexpressing MKS-1::YFP and CHE-13::CFP (A and B) or NPH-1::CFP and CHE-13::YFP (C and D) are shown. Compared to (A) wild type, MKS-1 localized normally to the proximal end of

cilia in (B) *mks-3(tm2547)* mutants. Compared to (C) wild type, NPH-1 localized normally to the proximal end of cilia in (D) *mks-3(tm2547)*.

Supplementary Figure 3. Localization of MKS-3::GFP in *mks-1(tm2705)*, *tza-1(tm2452)*, *tza-2(ok2092)*, and *nph-4(tm925)* mutants. Confocal fluorescence images of worms coexpressing MKS-3::GFP (top) and XBX-1::tdTomato (bottom) in the head (A-F) and tail (G). (A) MKS-3 localized normally to the proximal ends of amphid cilia in *mks-1(tm2705)* mutants. In contrast, MKS-3 localized either predominantly to dendritic tips of amphid neurons (arrowhead) in (B) *tza-1(tm2452)* mutants or was not detected (C). Similarly, MKS-3 localized either predominantly to dendritic tips of amphid neurons (arrowhead) in (D) *tza-2(ok2092)* mutants or was not detected (E). (F and G) MKS-3 normally localized to the dendritic tips and proximal ends of amphid and phasmid cilia in *nph-4(tm925)* mutants. Scale, 5μm.

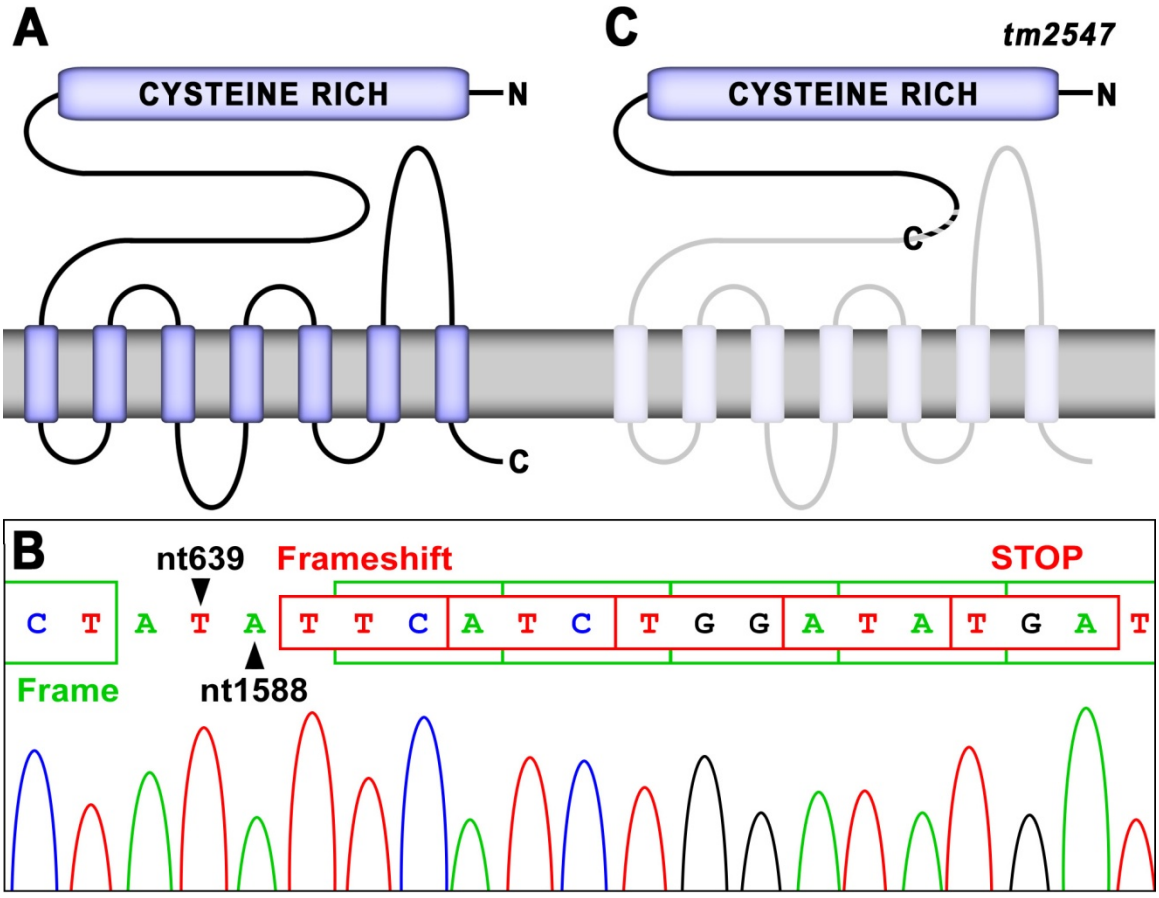

Figure 1. *mks-3* encodes a predicted seven transmembrane-spanning protein.

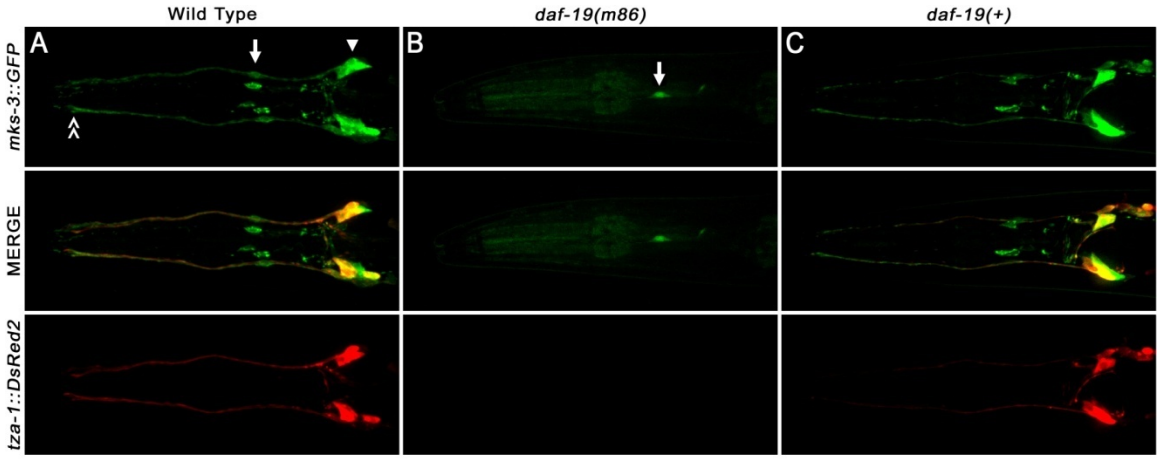

Figure 2. Expression and DAF-19 regulation of *mks-3*.

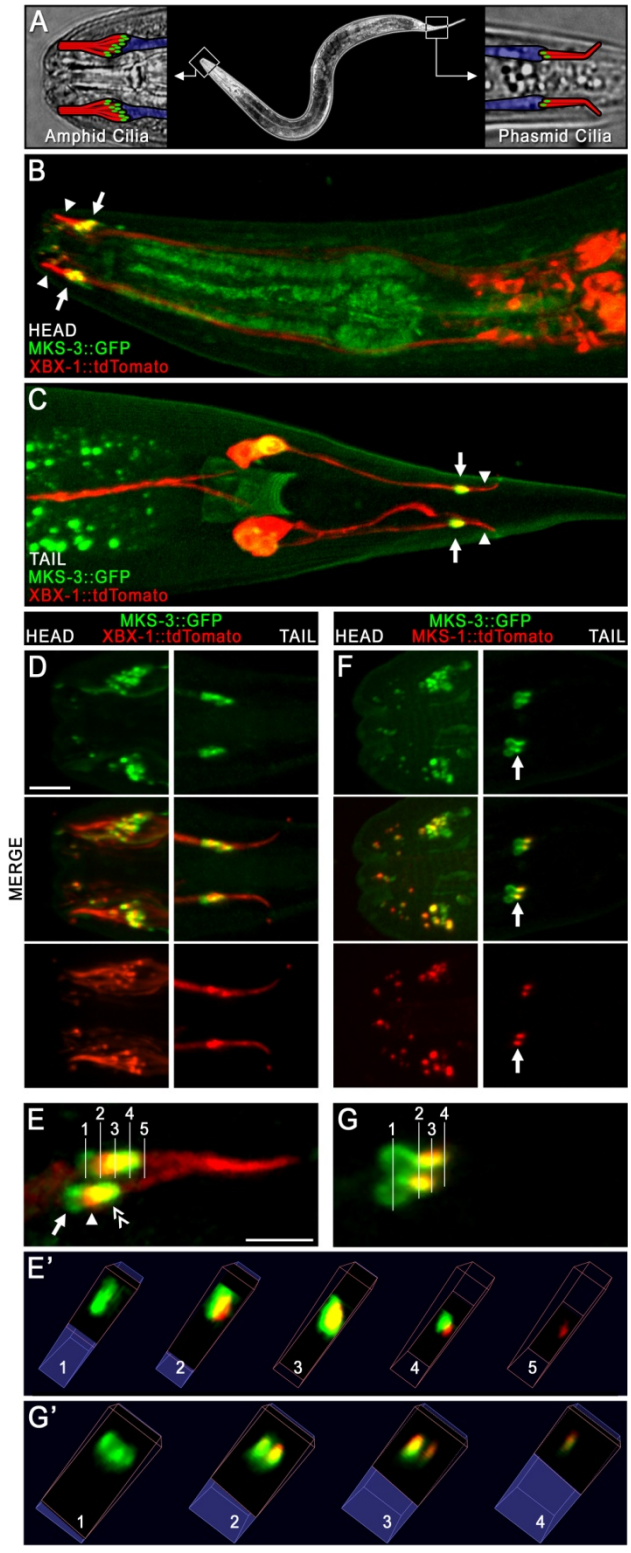

Figure 3. MKS-3 concentrates at the base of cilia in *C. elegans*.

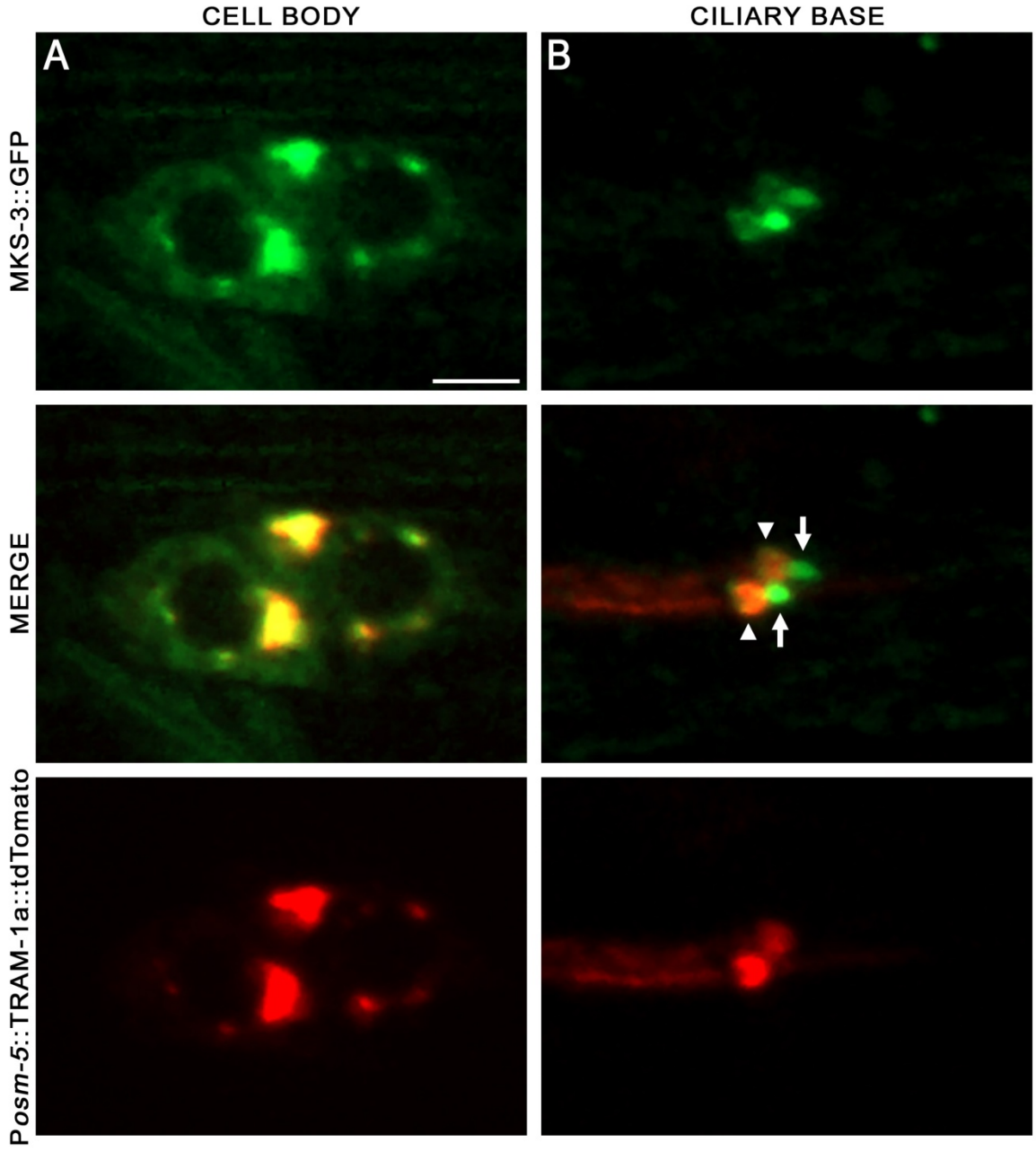

Figure 4. MKS-3 localizes to ER and post-ER compartments.

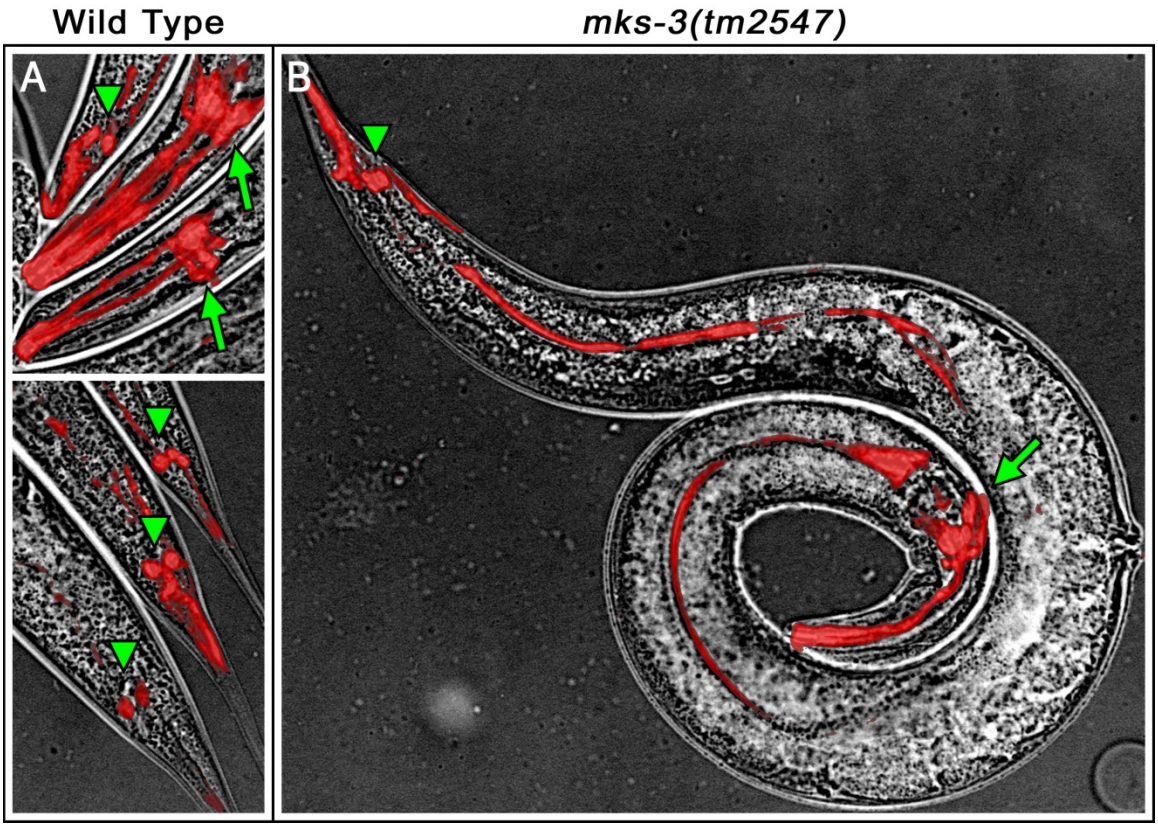

Figure 5. *mks-3(tm2547)* mutants dye-fill normally.

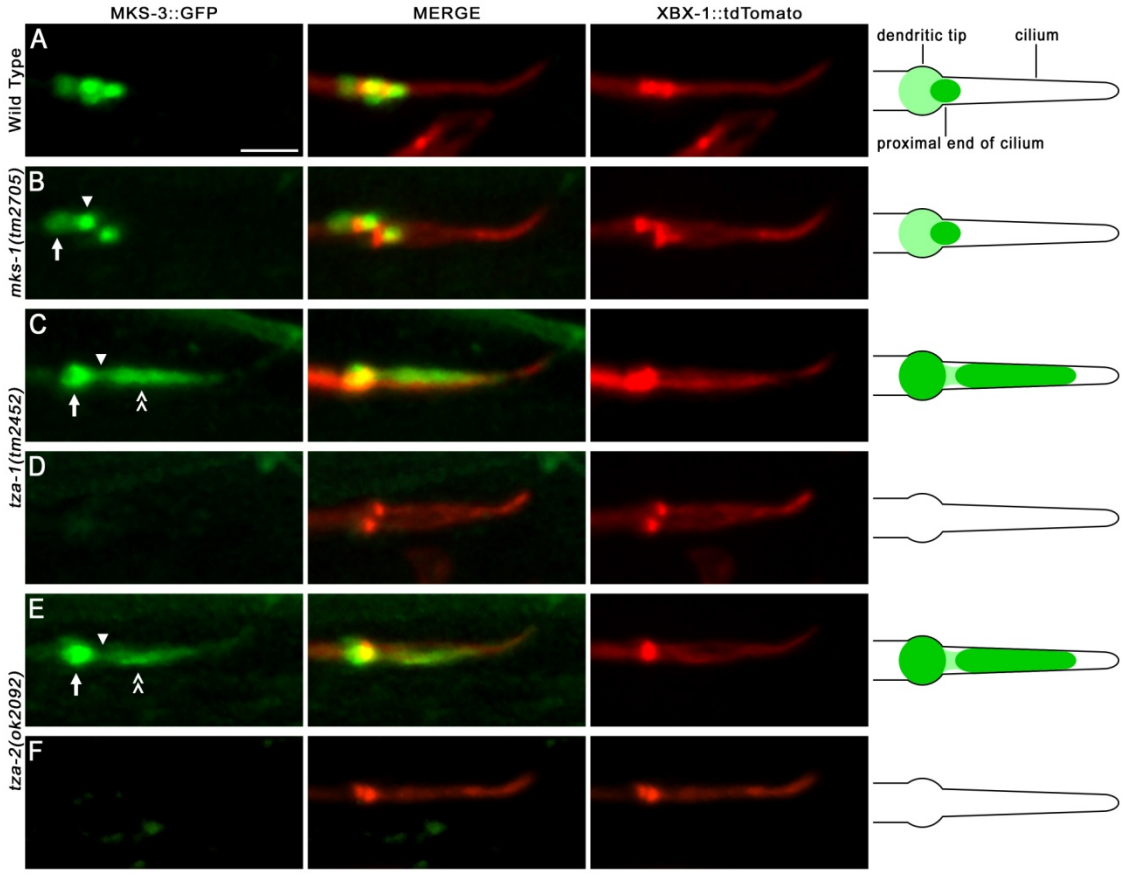

Figure 6. MKS-3 aberrantly localizes along the cilium axoneme in *tza-1(tm2452)* and *tza-2(ok2092)* mutants.

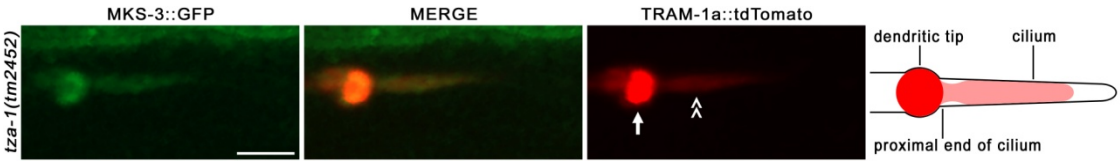

Figure 7. TRAM-1 aberrantly localizes along the cilium axoneme in *tza-1(tm2452)* mutants.

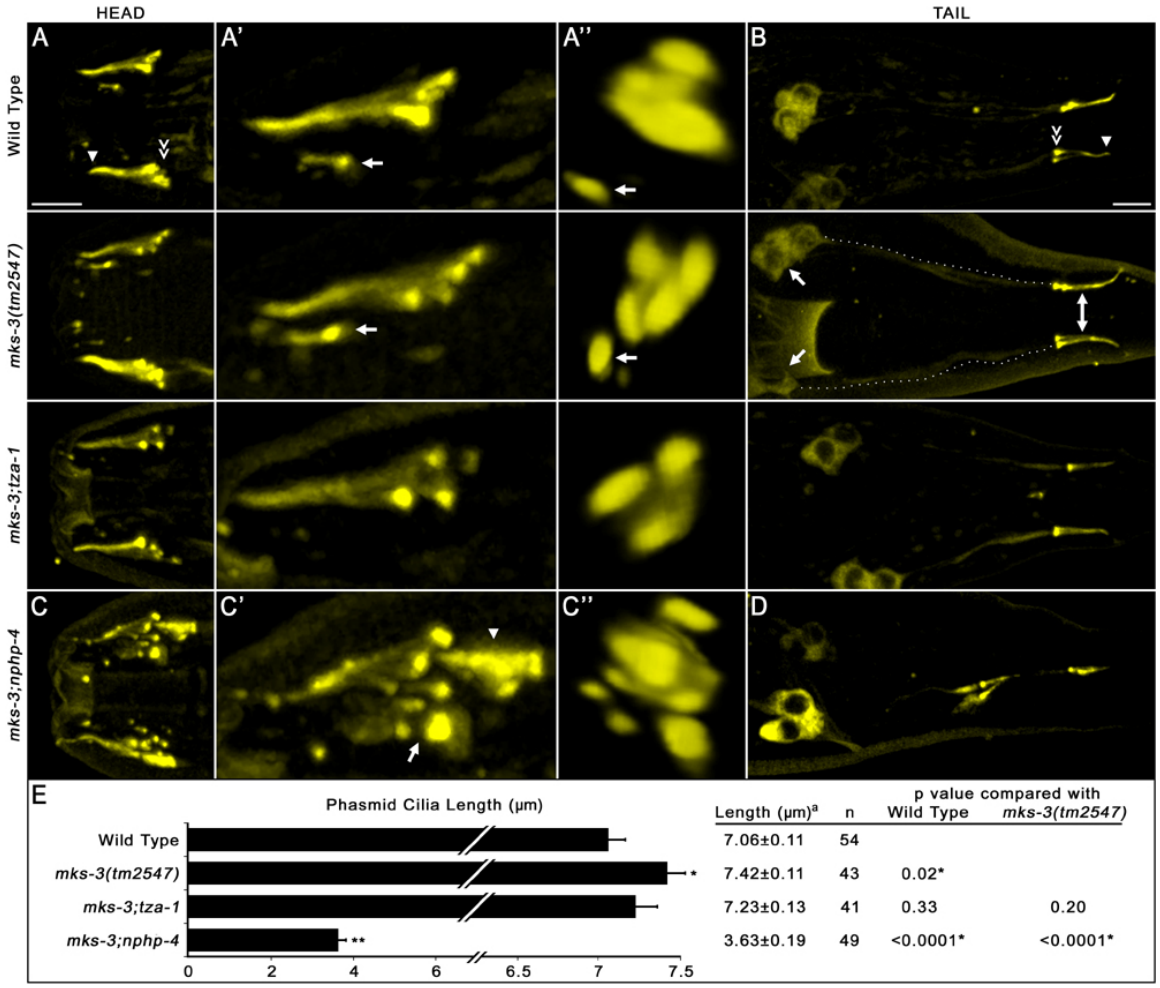

Figure 8. *mks-3;nph-4* double mutants have short and incorrectly positioned cilia.

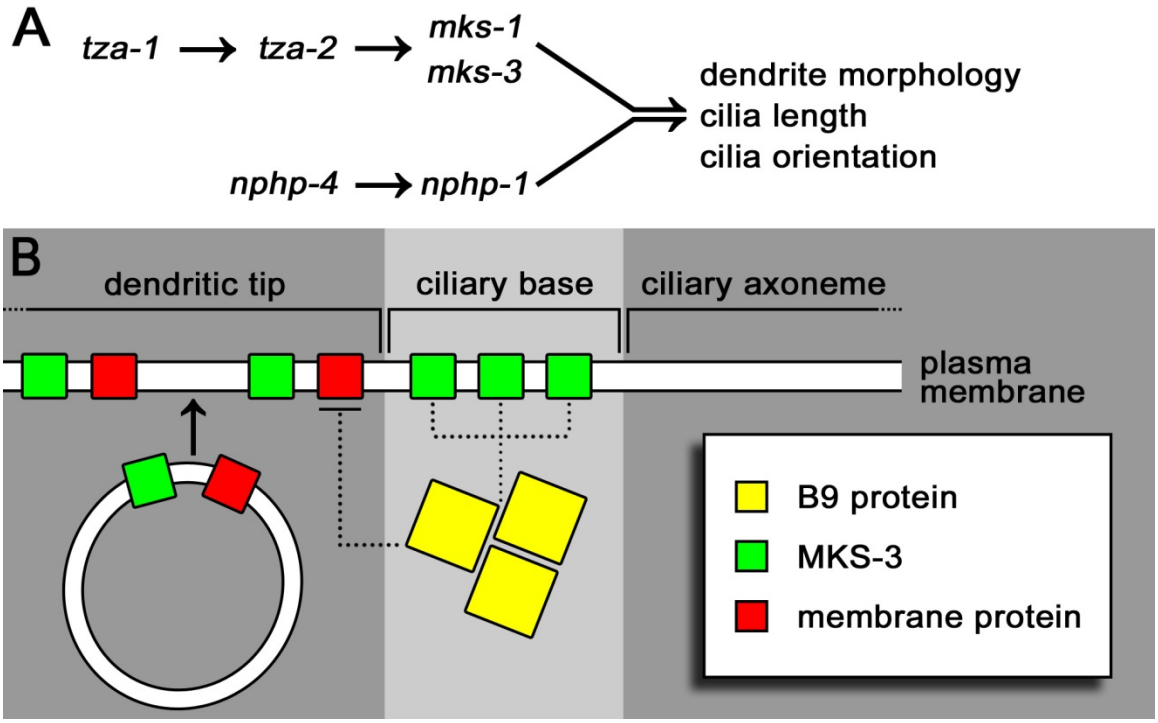

Figure 9. *mks* and *nphp* genetic pathways and model of B9 protein-mediated sorting of membrane proteins at the ciliary base.

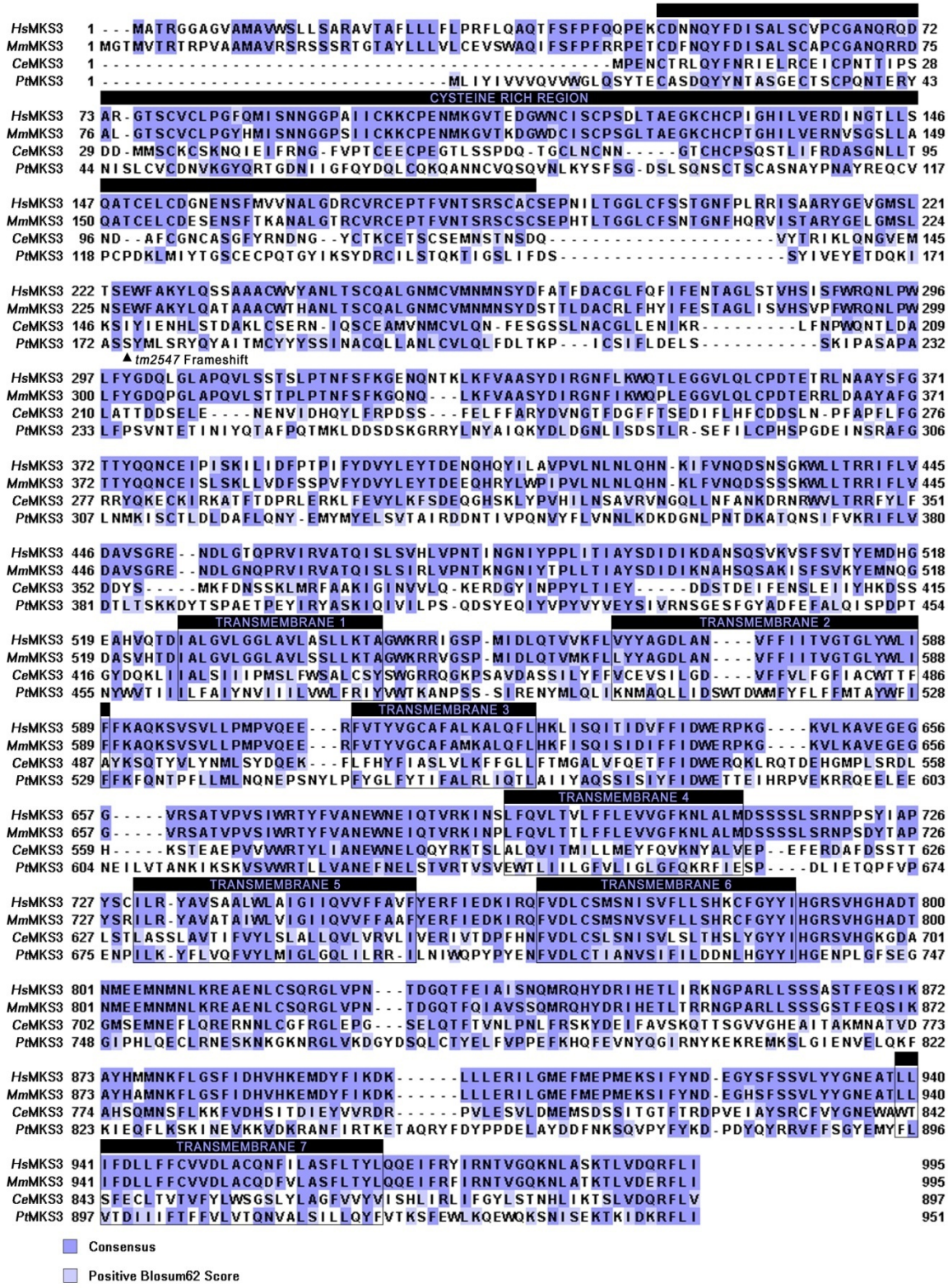

Supplementary Figure 1. Protein sequence alignment of MKS3 from *Homo sapiens (Hs)*, *Mus musculus (Ms)*, *Caenorhabditis elegans (Ce)*, and *Paramecium tetraurelia (Pt)*.

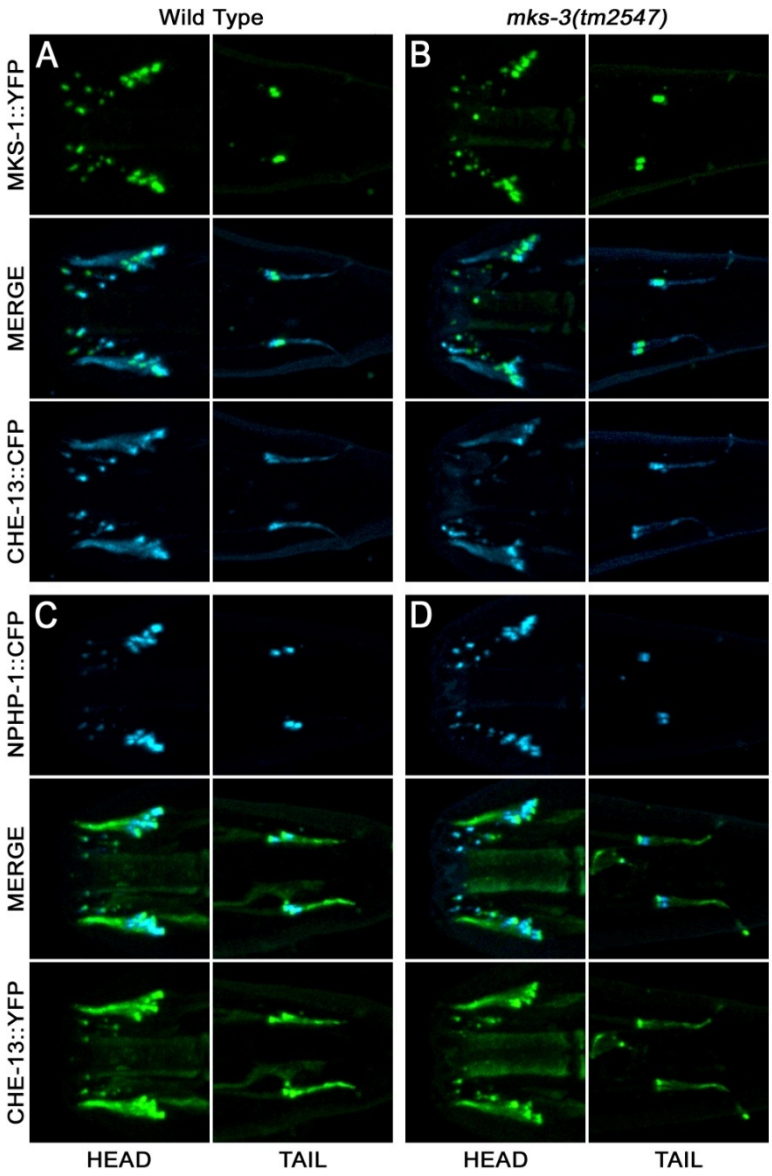

Supplementary Figure 2. Localization of B9 proteins and Nephrocystins is unaffected in *mks-3(tm2547)* mutants.

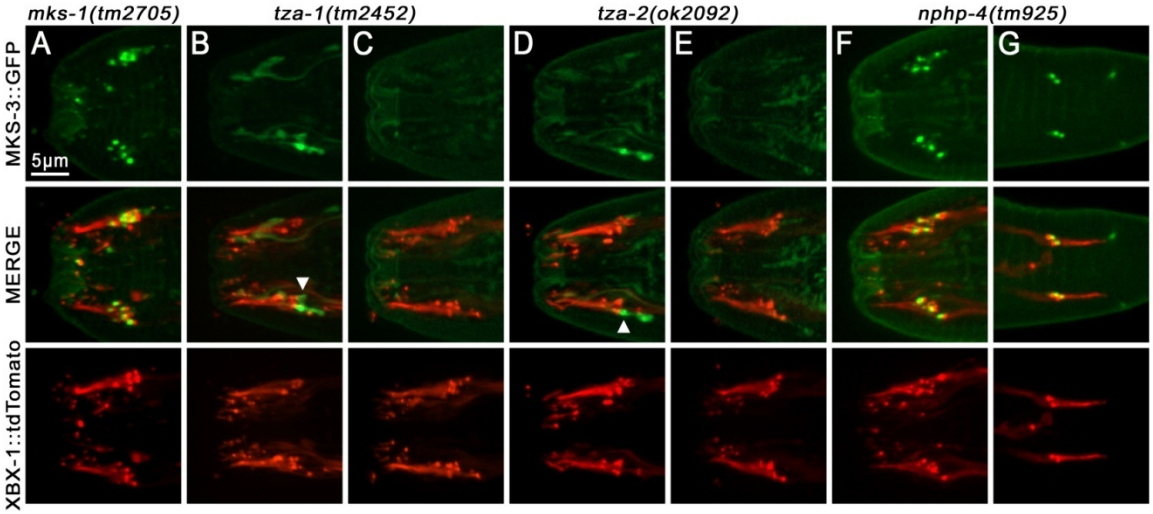

Supplementary Figure 3. Localization of MKS-3::GFP in *mks-1(tm2705)*, *tza-1(tm2452)*, *tza-2(ok2092)*, and *nph-4(tm925)* mutants.

SUMMARY

Modeling MKS protein function in C. elegans

Despite a noticeable absence of kidneys in *C. elegans*, this microscopic organism is credited with providing the very first evidence of a direct link between cilia and cystic kidney disease. A decade ago, Maureen Barr and Paul Sternberg observed the localization of *C. elegans* polycystin-1 and polycystin-2 at the ciliated endings of sensory neurons, thus opening up a can of worms in the field of inherited cystic kidney disease research (Barr and Sternberg, 1999). In short order, the ciliary theory of cystic kidney disease was firmly established. Striking evidence in support of this new theory was provided by concurrent reports that identified mutations in *C. elegans osm-5*, the homolog of the gene disrupted in the Oak Ridge Polycystic Kidney (ORPK) mouse, as causing severe defects in the formation of cilia (Haycraft et al., 2001; Qin et al., 2001).

More recently, *C. elegans* has been employed by us and others to examine genes linked to human renal cystic disorders such as NPHP and BBS. These analyses have been vital for the understanding of NPHP and BBS protein function. At the initiation of this project none of the MKS loci were completely mapped, and we had simply set forth with the intention to utilize *C. elegans* for the analysis of a novel conserved family of predicted ciliary proteins, the three B9 domain-containing proteins. Not until mutations in one of the B9 protein-encoding genes (*MKS1*) were identified in some MKS families was it realized we were already modeling MKS in *C. elegans* (Kyttala et al., 2006). On the very same day, mutations in *TMEM67/MKS3* were reported as causing some cases of MKS, and we therefore added the *C. elegans* homolog of *MKS3* (*mks-3*) to our analyses (Smith et al., 2006b).

Multiple genetic pathways influence cilia morphology

The heterogeneity of the genetic causes of ADPKD, NPHP, MKS, JBTS, BBS and other ciliopathic disorders underlies the notion that there are multiple manners in which cilia function can be compromised. In the case of ADPKD, ciliary signaling is disrupted by the loss of calcium channel functionality. In BBS patients, deregulation of IFT and the loss of some ciliary receptor localization may be responsible for disease symptoms (Berbari et al., 2008; Blacque et al., 2004). Elongation of cilia and ciliary/basal body protein delocalization and/or abnormal accumulation is associated with the disruption of some NPHP genes (Bergmann et al., 2008; McEwen et al., 2007; Smith et al., 2006a; Winkelbauer et al., 2005). In the case of MKS, improperly formed cilia were directly observed in some afflicted fetuses (Tallila et al., 2008). With so many factors and phenotypes involved, it should therefore not come as a surprise that simultaneous disruption of more than one disease-related gene in an individual can result in synergistic effects on phenotype severity in humans as well as model organisms (Leitch et al., 2008). We were able to demonstrate this in *C. elegans* with the analysis of MKS- and NPHP-related genes. Mutations in either or both *nphp-1* and *nphp-4* were not sufficient to confer noticeable cilia morphology defects. Similarly, mutations in *mks-1*, *mks-3*, *tza-1*, and *tza-2* alone or together did not inhibit cilia formation (although *mks-3* mutants had slightly elongated cilia). Only when combinations of *nphp* and *mks/tza* mutations were made did severe cilia morphology defects emerge. This indicates the *nphp* and *mks/tza* genes affect cilia biology in distinct but perhaps functionally similar pathways.

In the future, we hope to utilize the distinction between the *nphp* and *mks/tza* genetic pathways to identify novel genes involved in coordinated regulation of cilia homeostasis. To accomplish this, we propose a pair of EMS mutagenesis screens. Because mutations in both an *nphp* gene and an *mks/tza* gene result in a dye-filling defective (Dyf) phenotype whereas a mutation in any of these genes alone does not, we hypothesize that by inducing mutations via EMS in worms carrying a single *nphp* pathway mutation (e.g. *nphp-4(tm925)* alone), we can identify worms with the Dyf phenotype that have a mutation in a novel gene of the *mks/tza* pathway or a functionally equivalent pathway. The reciprocal mutagenesis screen is also possible such that induction of mutations in the background of an *mks/tza* mutation would lead to the identification of novel genes in the *nphp* pathway or a functionally equivalent pathway.

A caveat in this screen is the likelihood of mutating genes that when disrupted alone can confer dye-filling defects independent of the *nphp* or *mks/tza* gene mutations (i.e. many of the IFT genes such as *osm-5* and a host of other genes already associated with abnormal dye-filling) (Perkins et al., 1986). Two strategies can be employed to select against mutations in such genes. First, we can directly observe cilia morphology in Dyf worms identified in the screen by introducing a transgenic cilia marker protein such as CHE-13::YFP. This could be accomplished either by injection of the cilia marker construct following the mutagenesis or by performing the mutagenesis in transgenic worms already expressing the marker. Because disruption of either anterograde or retrograde IFT results in cilia morphology defects that are distinct from the cilia morphology defects in *nphp;mks/tza* compound mutants, we should be able to eliminate IFT mutants by this method. However, the cilia structure phenotype in *nphp;mks/tza* compound mutants

closely resembles that observed in other single mutants such as *mec-8(e398)*, indicating that these mutants would not be selected against via this method. A second approach to eliminating unrelated Dyf mutations would be to simply outcross Dyf worms identified in the screen and select for the Dyf phenotype over several generations. If the initial mutation (i.e. *nphp-4(tm925)*) is required, then all Dyf worms following the outcross should remain homozygous for that mutation. If the initial mutation is not required, then we should observe a mix of wild-type and mutant alleles for the original gene in Dyf worms after the outcross. By this method, we should be able to firmly establish whether the new mutations are genetically interacting with the original mutation.

We would then attempt to establish proof of principle by performing allelic non-complementation assays between the Dyf mutants and our stock of pathway mutants, with the intent to identify novel mutations in the known pathway genes. For example, a Dyf mutant from a screen performed in *nphp-4* mutant background would be crossed with *mks-1;nphp-4*, *tza-1;nphp-4*, *nphp-4;tza-2*, and *mks-3;nphp-4* double mutant strains. If the new mutant allele is in the same gene that is mutated in the double mutant mating partner (i.e. *mks-1(new allele);nphp-4(tm925)* crossed with *mks-1(tm2705);nphp-4(tm925)*), then allelic non-complementation between the two *mks-1* alleles will occur, and offspring from the mating will remain Dyf. If the new mutant allele is in a novel gene (i.e. *novel(new allele);nphp-4(tm925)* crossed with *mks-1(tm2705);nphp-4(tm925)*), then complementation will occur when the new mutant worm provides a wild-type *mks-1* allele and the *mks-1(tm2705);nphp-4(tm925)* worm provides a wild-type allele for the novel gene in the mating, thereby conferring a non-Dyf phenotype in the offspring. By this method, we would identify which Dyf worms have novel mutations in known path-

way genes and which Dyf worms have mutations in novel genes. Mapping analyses of these novel genes would then follow.

We recently initiated a large scale EMS mutagenesis screen for Dyf worms arising in the *nphp-4(tm925)* mutant background. We initially isolated 167 Dyf or partially Dyf worms in the F2 generation (where P0 worms were mutagenized and F1 worms were their progeny). Of these 167 strains, most failed to pass the Dyf phenotype to subsequent generations. Those with a stable Dyf phenotype were outcrossed with wild type and genotyped for *nphp-4(tm925)* homozygosity. At the time of this writing, 25 strains remained homozygous for *nphp-4(tm925)* after one or more outcrosses, indicating a requirement of *nphp-4(tm925)* in conferring the Dyf phenotype. We plan to begin non-complementation and mapping analyses with these novel mutations shortly.

This type of powerful screen, for which *C. elegans* is so amenable, should eventually identify strong candidate genes for sequencing in MKS, NPHP, JBTS, or even BBS families in which a genetic lesion has not been identified. Identifying such candidates is important since it is currently impractical to sequence every gene in these patients that encodes a cilia or basal body proteome protein. Additionally, identification of novel members in the *nphp* and *mks/tza* pathways (or altogether new, functionally redundant pathways) will provide more insight into the function of these pathways and how they coordinately control cilia homeostasis.

Factors affecting ciliary membrane composition

The ciliary membrane is a tightly regulated region with a molecular composition which is distinct from the rest of the cell. Some membrane proteins accumulate specifi-

cally in the cilium while many others are excluded. How this sorting occurs is unknown. Multiple steps are involved in the transport of a ciliary membrane protein from its point of origin to its final destination, the cilium. In the sensory neurons of *C. elegans*, ciliary membrane proteins could either be trafficked though the dendrites to the base of cilia via vesicular transport or enter the cell membrane at an earlier point and migrate down the length of the dendrite to reach the base of the cilia. The transmembrane protein PKD-2 is observed moving in particles along the dendrites, suggestive of vesicular transport (Barr et al., 2001). No matter how these proteins arrive at the base of cilia, once there they must be selectively sorted away from membrane proteins not destined for the ciliary membrane. Evidence suggests different gatekeeper functionalities are involved with particular proteins or groups of proteins in gaining ciliary access. For example, a mutation in *BBS4* disrupted ciliary localization of some G protein coupled receptors but not the ciliary membrane protein ACIII (Berbari et al., 2008). Conversely, some factors are involved in regulating the levels of membrane proteins within the cilium. This is seen in the case of *jck/NPHP9* mutant mice, which exhibit increased abundance of polycystin-1 and polycystin-2 within cilia (Smith et al., 2006a).

In our analyses of the B9 proteins, we observed a requirement of TZA-1 for the localization of TZA-2 to the base of cilia and a requirement of TZA-2 for the localization of MKS-1. In conjunction, we showed a binding interaction between TZA-1 and TZA-2. These results along with our grouping of *mks-1*, *tza-1*, and *tza-2* into the same genetic pathway (in terms of functional redundancy with the *nphp* genetic pathway) led us to conclude that the B9 proteins function together as part of a protein complex at the base of cilia. Because the transmembrane protein MKS3 was identified in complex with MKS1

in mice, we predicted *C. elegans* MKS-3 would also function as part of the B9 protein complex (Dawe et al., 2007b). Two pieces of evidence confirmed this. First, *mks-3* exhibited a genetic interaction with *nphp-4* in terms of ciliogenesis in cilia positioning. Second, MKS-3 localization was dependent on the presence of TZA-1 and TZA-2. Similar to the localization of the three B9 proteins, we observed *C. elegans* MKS-3::GFP primarily at the ciliary base and diffusely localized in the adjacent dendritic tip. However, when we expressed MKS-3::GFP in the background of *tza-1(tm2452)* and *tza-2(ok2092)* mutants, MKS-3 was detectable within cilia and completely delocalized from the ciliary base (although the protein still accumulated at the dendritic tips). Because of this abnormal ciliary accumulation and our data suggesting *mks-3* is part of the *mks/tza* genetic pathway, we speculated that the B9 proteins (at least TZA-1 and TZA-2) are involved specifically in the restriction of MKS-3 ciliary access and are therefore necessary for regulating at least some of the proteins that comprise the ciliary membrane.

Our additional observation that a presumably unrelated transmembrane protein TRAM-1 also entered the cilium in the absence of TZA-1 and TZA-2 indicates that these proteins may also function in a general manner to regulate ciliary membrane access. Because the TRAM-1 protein accesses the cilium when the B9 proteins are disrupted, we could speculate that these proteins function not as a gatekeeper that chooses what proteins gain entry but instead as the gate itself, which when lacking, would allow free entry regardless of the gatekeeper. The possibility exists that MKS-3 is part of this gate, held in place by the B9 proteins, and perhaps functioning as a barrier in the membrane at the base of cilia. However, we currently have no data that conclusively demonstrates this role for the B9 proteins.

Further analyses are necessary for determining the actual mechanisms by which the B9 proteins are influencing ciliary membrane composition. Only two transmembrane proteins were examined here, partly because few transmembrane proteins are known to localize only at the base of cilia and not along the axonemes. Two additional transmembrane proteins that conconcentrate at the base of cilia in *C. elegans* are the homologs of human polycystin-1 and polycystin-2. Although these proteins also localize diffusely along the length of cilia, it would be of interest to determine whether disruption of the B9 proteins or MKS-3 can influence the degree to which the polycystins accumulate inside the cilium. In a recent EMS mutagenesis screen for genes affecting the localization of PKD-2 (polycystin-2), Maureen Barr and colleagues identified several mutations that resulted in increased levels of PKD-2 in the ciliary membrane (Bae et al., 2008). It will be interesting to see what genes are affected by these mutations and to evaluate how they might relate to the B9 complex proteins. A similar genetic screen could be utilized to identify additional genes involved in restricting MKS-3 or TRAM-1 from entering the ciliary membrane.

Final remarks

The cilium is a complex organelle with a myriad of vital functions in most eukaryotic organisms. The analyses described in this dissertation have provided important insight into the functions of the *C. elegans* NPHP and MKS/TZA proteins in ciliary biology. Hopefully, some of this insight can be applied to further the understanding of what mechanisms contribute to the spectrum of human ciliopathic disease. Our contribution here puts but a few pieces into the puzzle of cilia function and regulation. However, fur-

ther analysis of cilia in *C. elegans* should continue to provide interesting and possibly surprising answers to pertinent questions in cell biology.

GENERAL LIST OF REFERENCES

Adams, M., Smith, U. M., Logan, C. V. and Johnson, C. A. (2008). Recent advances in the molecular pathology, cell biology and genetics of ciliopathies. *J Med Genet* **45**, 257-67.

Alexiev, B. A., Lin, X., Sun, C. C. and Brenner, D. S. (2006). Meckel-Gruber syndrome: pathologic manifestations, minimal diagnostic criteria, and differential diagnosis. *Arch Pathol Lab Med* **130**, 1236-8.

Apfeld, J. and Kenyon, C. (1999). Regulation of lifespan by sensory perception in Caenorhabditis elegans. *Nature* **402**, 804-9.

Arts, H. H., Doherty, D., van Beersum, S. E., Parisi, M. A., Letteboer, S. J., Gorden, N. T., Peters, T. A., Marker, T., Voesenek, K., Kartono, A. et al. (2007). Mutations in the gene encoding the basal body protein RPGRIP1L, a nephrocystin-4 interactor, cause Joubert syndrome. *Nat Genet* **39**, 882-8.

Attanasio, M., Uhlenhaut, N. H., Sousa, V. H., O'Toole, J. F., Otto, E., Anlag, K., Klugmann, C., Treier, A. C., Helou, J., Sayer, J. A. et al. (2007). Loss of GLIS2 causes nephronophthisis in humans and mice by increased apoptosis and fibrosis. *Nat Genet* **39**, 1018-24.

Baala, L., Audollent, S., Martinovic, J., Ozilou, C., Babron, M. C., Sivanandamoorthy, S., Saunier, S., Salomon, R., Gonzales, M., Rattenberry, E. et al. (2007a). Pleiotropic effects of CEP290 (NPHP6) mutations extend to Meckel syndrome. *Am J Hum Genet* **81**, 170-9.

Baala, L., Romano, S., Khaddour, R., Saunier, S., Smith, U. M., Audollent, S., Ozilou, C., Faivre, L., Laurent, N., Foliguet, B. et al. (2007b). The Meckel-Gruber syndrome gene, MKS3, is mutated in Joubert syndrome. *Am J Hum Genet* **80**, 186-94.

Badano, J. L., Leitch, C. C., Ansley, S. J., May-Simera, H., Lawson, S., Lewis, R. A., Beales, P. L., Dietz, H. C., Fisher, S. and Katsanis, N. (2006a). Dissection of epistasis in oligogenic Bardet-Biedl syndrome. *Nature* **439**, 326-30.

Badano, J. L., Mitsuma, N., Beales, P. L. and Katsanis, N. (2006b). The Ciliopathies: An Emerging Class of Human Genetic Disorders. *Annu Rev Genomics Hum Genet* **7**, 125-148.

Bae, Y. K., Lyman-Gingerich, J., Barr, M. M. and Knobel, K. M. (2008). Identification of genes involved in the ciliary trafficking of C. elegans PKD-2. *Dev Dyn* **237**, 2021-9.

Bae, Y. K., Qin, H., Knobel, K. M., Hu, J., Rosenbaum, J. L. and Barr, M. M. (2006). General and cell-type specific mechanisms target TRPP2/PKD-2 to cilia. *Development* **133**, 3859-70.

Barr, M. M., DeModena, J., Braun, D., Nguyen, C. Q., Hall, D. H. and Sternberg, P. W. (2001). The Caenorhabditis elegans autosomal dominant polycystic kidney disease gene homologs lov-1 and pkd-2 act in the same pathway. *Curr Biol* **11**, 1341-6.

Barr, M. M. and Sternberg, P. W. (1999). A polycystic kidney-disease gene homologue required for male mating behaviour in C. elegans. *Nature* **401**, 386-9.

Beales, P. L., Bland, E., Tobin, J. L., Bacchelli, C., Tuysuz, B., Hill, J., Rix, S., Pearson, C. G., Kai, M., Hartley, J. et al. (2007). IFT80, which encodes a conserved intraflagellar transport protein, is mutated in Jeune asphyxiating thoracic dystrophy. *Nat Genet* **39**, 727-9.

Bell, L. R., Stone, S., Yochem, J., Shaw, J. E. and Herman, R. K. (2006). The molecular identities of the Caenorhabditis elegans intraflagellar transport genes dyf-6, daf-10 and osm-1. *Genetics* **173**, 1275-86.

Benzing, T., Gerke, P., Hopker, K., Hildebrandt, F., Kim, E. and Walz, G. (2001). Nephrocystin interacts with Pyk2, p130(Cas), and tensin and triggers phosphorylation of Pyk2. *Proc Natl Acad Sci U S A* **98**, 9784-9.

Berbari, N. F., Lewis, J. S., Bishop, G. A., Askwith, C. C. and Mykytyn, K. (2008). Bardet-Biedl syndrome proteins are required for the localization of G protein-coupled receptors to primary cilia. *Proc Natl Acad Sci U S A* **105**, 4242-6.

Bergmann, C., Fliegauf, M., Bruchle, N. O., Frank, V., Olbrich, H., Kirschner, J., Schermer, B., Schmedding, I., Kispert, A., Kranzlin, B. et al. (2008). Loss of nephrocystin-3 function can cause embryonic lethality, Meckel-Gruber-like syndrome, situs inversus, and renal-hepatic-pancreatic dysplasia. *Am J Hum Genet* **82**, 959-70.

Blacque, O. E. and Leroux, M. R. (2006). Bardet-Biedl syndrome: an emerging pathomechanism of intracellular transport. *Cell Mol Life Sci* **63**, 2145-61.

Blacque, O. E., Li, C., Inglis, P. N., Esmail, M. A., Ou, G., Mah, A. K., Baillie, D. L., Scholey, J. M. and Leroux, M. R. (2006). The WD repeat-containing protein IFTA-1 is required for retrograde intraflagellar transport. *Mol Biol Cell* **17**, 5053-62.

Blacque, O. E., Perens, E. A., Boroevich, K. A., Inglis, P. N., Li, C., Warner, A., Khattra, J., Holt, R. A., Ou, G., Mah, A. K. et al. (2005). Functional genomics of the cilium, a sensory organelle. *Curr Biol* **15**, 935-41.

Blacque, O. E., Reardon, M. J., Li, C., McCarthy, J., Mahjoub, M. R., Ansley, S. J., Badano, J. L., Mah, A. K., Beales, P. L., Davidson, W. S. et al. (2004). Loss of C. elegans BBS-7 and BBS-8 protein function results in cilia defects and compromised intraflagellar transport. *Genes Dev* **18**, 1630-42.

Brancati, F., Iannicelli, M., Travaglini, L., Mazzotta, A., Bertini, E., Boltshauser, E., D'Arrigo, S., Emma, F., Fazzi, E., Gallizzi, R. et al. (2008). MKS3/TMEM67 mutations are a major cause of COACH Syndrome, a Joubert syndrome related disorder with liver involvement. *Hum Mutat*.

Brenner, S. (1974). The genetics of Caenorhabditis elegans. *Genetics* **77**, 71-94.

Burghoorn, J., Dekkers, M. P., Rademakers, S., de Jong, T., Willemsen, R. and Jansen, G. (2007). Mutation of the MAP kinase DYF-5 affects docking and undocking of kinesin-2 motors and reduces their speed in the cilia of Caenorhabditis elegans. *Proc Natl Acad Sci U S A* **104**, 7157-62.

Cantagrel, V., Silhavy, J. L., Bielas, S. L., Swistun, D., Marsh, S. E., Bertrand, J. Y., Audollent, S., Attie-Bitach, T., Holden, K. R., Dobyns, W. B. et al. (2008). Mutations in the cilia gene ARL13B lead to the classical form of Joubert syndrome. *Am J Hum Genet* **83**, 170-9.

Caridi, G., Murer, L., Bellantuono, R., Sorino, P., Caringella, D. A., Gusmano, R. and Ghiggeri, G. M. (1998). Renal-retinal syndromes: association of retinal anomalies and recessive nephronophthisis in patients with homozygous deletion of the NPH1 locus. *Am J Kidney Dis* **32**, 1059-62.

Chang, B., Khanna, H., Hawes, N., Jimeno, D., He, S., Lillo, C., Parapuram, S. K., Cheng, H., Scott, A., Hurd, R. E. et al. (2006). In-frame deletion in a novel centrosomal/ciliary protein CEP290/NPHP6 perturbs its interaction with RPGR and results in early-onset retinal degeneration in the rd16 mouse. *Hum Mol Genet* **15**, 1847-57.

Chapman, A. B. (2007). Autosomal dominant polycystic kidney disease: time for a change? *J Am Soc Nephrol* **18**, 1399-407.

Chen, C. P. (2007). Meckel syndrome: genetics, perinatal findings, and differential diagnosis. *Taiwan J Obstet Gynecol* **46**, 9-14.

Cole, D. G., Diener, D. R., Himelblau, A. L., Beech, P. L., Fuster, J. C. and Rosenbaum, J. L. (1998). Chlamydomonas kinesin-II-dependent intraflagellar transport (IFT): IFT particles contain proteins required for ciliary assembly in Caenorhabditis elegans sensory neurons. *Journal of Cell Biology* **141**, 993-1008.

Collet, J., Spike, C. A., Lundquist, E. A., Shaw, J. E. and Herman, R. K. (1998). Analysis of osm-6, a gene that affects sensory cilium structure and sensory neuron function in Caenorhabditis elegans. *Genetics* **148**, 187-200.

Consugar, M. B., Kubly, V. J., Lager, D. J., Hommerding, C. J., Wong, W. C., Bakker, E., Gattone, V. H., 2nd, Torres, V. E., Breuning, M. H. and Harris, P. C. (2007). Molecular diagnostics of Meckel-Gruber syndrome highlights phenotypic differences between MKS1 and MKS3. *Hum Genet* **121**, 591-9.

Culotti, J. G. and Russell, R. L. (1978). Osmotic avoidance defective mutants of the nematode Caenorhabditis elegans. *Genetics* **90**, 243-56.

Davenport, J. R., Watts, A. J., Roper, V. C., Croyle, M. J., van Groen, T., Wyss, J. M., Nagy, T. R., Kesterson, R. A. and Yoder, B. K. (2007). Disruption of intraflagellar transport in adult mice leads to obesity and slow-onset cystic kidney disease. *Curr Biol* **17**, 1586-94.

Dawe, H. R., Farr, H. and Gull, K. (2007a). Centriole/basal body morphogenesis and migration during ciliogenesis in animal cells. *J Cell Sci* **120**, 7-15.

Dawe, H. R., Smith, U. M., Cullinane, A. R., Gerrelli, D., Cox, P., Badano, J. L., Blair-Reid, S., Sriram, N., Katsanis, N., Attie-Bitach, T. et al. (2007b). The Meckel-Gruber Syndrome proteins MKS1 and meckelin interact and are required for primary cilium formation. *Hum Mol Genet* **16**, 173-86.

De Riso, L., Ristoratore, F., Sebastiano, M. and Bazzicalupo, P. (1994). Amphid defective mutant of Caenorhabditis elegans. *Genetica* **94**, 195-202.

Deane, J. A., Cole, D. G., Seeley, E. S., Diener, D. R. and Rosenbaum, J. L. (2001). Localization of intraflagellar transport protein IFT52 identifies basal body transitional fibers as the docking site for IFT particles. *Current Biology* **11**, 1586-90.

Delous, M., Baala, L., Salomon, R., Laclef, C., Vierkotten, J., Tory, K., Golzio, C., Lacoste, T., Besse, L., Ozilou, C. et al. (2007). The ciliary gene RPGRIP1L is mutated in cerebello-oculo-renal syndrome (Joubert syndrome type B) and Meckel syndrome. *Nat Genet* **39**, 875-81.

Doering, J. E., Kane, K., Hsiao, Y. C., Yao, C., Shi, B., Slowik, A. D., Dhagat, B., Scott, D. D., Ault, J. G., Page-McCaw, P. S. et al. (2008). Species differences in the expression of Ahi1, a protein implicated in the neurodevelopmental disorder Joubert syndrome, with preferential accumulation to stigmoid bodies. *J Comp Neurol* **511**, 238-56.

Donaldson, J. C., Dempsey, P. J., Reddy, S., Bouton, A. H., Coffey, R. J. and Hanks, S. K. (2000). Crk-associated substrate p130(Cas) interacts with nephrocystin and both proteins localize to cell-cell contacts of polarized epithelial cells. *Exp Cell Res* **256**, 168-78.

Donaldson, J. C., Dise, R. S., Ritchie, M. D. and Hanks, S. K. (2002). Nephrocystin-conserved domains involved in targeting to epithelial cell-cell junctions, interaction with filamins, and establishing cell polarity. *J Biol Chem* **277**, 29028-35.

Dusenbery, D. B., Sheridan, R. E. and Russell, R. L. (1975). Chemotaxis-defective mutants of the nematode Caenorhabditis elegans. *Genetics* **80**, 297-309.

Efimenko, E., Blacque, O. E., Ou, G., Haycraft, C. J., Yoder, B. K., Scholey, J. M., Leroux, M. R. and Swoboda, P. (2006). Caenorhabditis elegans DYF-2, an orthologue of human WDR19, is a component of the intraflagellar transport machinery in sensory cilia. *Mol Biol Cell* **17**, 4801-11.

Efimenko, E., Bubb, K., Mak, H. Y., Holzman, T., Leroux, M. R., Ruvkun, G., Thomas, J. H. and Swoboda, P. (2005). Analysis of xbx genes in C. elegans. *Development* **132**, 1923-34.

Eley, L., Gabrielides, C., Adams, M., Johnson, C. A., Hildebrandt, F. and Sayer, J. A. (2008). Jouberin localizes to collecting ducts and interacts with nephrocystin-1. *Kidney Int*.

Fath, M. A., Mullins, R. F., Searby, C., Nishimura, D. Y., Wei, J., Rahmouni, K., Davis, R. E., Tayeh, M. K., Andrews, M., Yang, B. et al. (2005). Mkks-null mice have a phenotype resembling Bardet-Biedl syndrome. *Hum Mol Genet* **14**, 1109-18.

Ferland, R. J., Eyaid, W., Collura, R. V., Tully, L. D., Hill, R. S., Al-Nouri, D., Al-Rumayyan, A., Topcu, M., Gascon, G., Bodell, A. et al. (2004). Abnormal cerebellar development and axonal decussation due to mutations in AHI1 in Joubert syndrome. *Nat Genet* **36**, 1008-13.

Fliegauf, M., Horvath, J., von Schnakenburg, C., Olbrich, H., Muller, D., Thumfart, J., Schermer, B., Pazour, G. J., Neumann, H. P., Zentgraf, H. et al. (2006). Nephrocystin specifically localizes to the transition zone of renal and respiratory cilia and photoreceptor connecting cilia. *J Am Soc Nephrol* **17**, 2424-33.

Frank, V., den Hollander, A. I., Bruchle, N. O., Zonneveld, M. N., Nurnberg, G., Becker, C., Du Bois, G., Kendziorra, H., Roosing, S., Senderek, J. et al. (2008). Mutations of the CEP290 gene encoding a centrosomal protein cause Meckel-Gruber syndrome. *Hum Mutat* **29**, 45-52.

Frank, V., Ortiz Bruchle, N., Mager, S., Frints, S. G., Bohring, A., du Bois, G., Debatin, I., Seidel, H., Senderek, J., Besbas, N. et al. (2007). Aberrant splicing is a common mutational mechanism in MKS1, a key player in Meckel-Gruber syndrome. *Hum Mutat* **28**, 638-9.

Fujiwara, M., Ishihara, T. and Katsura, I. (1999). A novel WD40 protein, CHE-2, acts cell-autonomously in the formation of C. elegans sensory cilia. *Development* **126**, 4839-48.

Fujiwara, M., Sengupta, P. and McIntire, S. L. (2002). Regulation of body size and behavioral state of C. elegans by sensory perception and the EGL-4 cGMP-dependent protein kinase. *Neuron* **36**, 1091-102.

Gattone, V. H., 2nd, Tourkow, B. A., Trambaugh, C. M., Yu, A. C., Whelan, S., Phillips, C. L., Harris, P. C. and Peterson, R. G. (2004). Development of multiorgan pathology in the wpk rat model of polycystic kidney disease. *Anat Rec A Discov Mol Cell Evol Biol* **277**, 384-95.

Gherman, A., Davis, E. E. and Katsanis, N. (2006). The ciliary proteome database: an integrated community resource for the genetic and functional dissection of cilia. *Nat Genet* **38**, 961-2.

Gorden, N. T., Arts, H. H., Parisi, M. A., Coene, K. L., Letteboer, S. J., van Beersum, S. E., Mans, D. A., Hikida, A., Eckert, M., Knutzen, D. et al. (2008). CC2D2A is mutated in Joubert syndrome and interacts with the ciliopathy-associated basal body protein CEP290. *Am J Hum Genet* **83**, 559-71.

Green, J. S., Parfrey, P. S., Harnett, J. D., Farid, N. R., Cramer, B. C., Johnson, G., Heath, O., McManamon, P. J., O'Leary, E. and Pryse-Phillips, W. (1989). The cardinal manifestations of Bardet-Biedl syndrome, a form of Laurence-Moon-Biedl syndrome. *N Engl J Med* **321**, 1002-9.

Greenfield, J. J. and High, S. (1999). The Sec61 complex is located in both the ER and the ER-Golgi intermediate compartment. *J Cell Sci* **112 (Pt 10)**, 1477-86.

Haycraft, C. J., Banizs, B., Aydin-Son, Y., Zhang, Q., Michaud, E. J. and Yoder, B. K. (2005). Gli2 and Gli3 localize to cilia and require the intraflagellar transport protein polaris for processing and function. *PLoS Genet* **1**, e53.

Haycraft, C. J., Schafer, J. C., Zhang, Q., Taulman, P. D. and Yoder, B. K. (2003). Identification of CHE-13, a novel intraflagellar transport protein required for cilia formation. *Exp Cell Res* **284**, 251-63.

Haycraft, C. J., Swoboda, P., Taulman, P. D., Thomas, J. H. and Yoder, B. K. (2001). The C. elegans homolog of the murine cystic kidney disease gene Tg737 functions in a ciliogenic pathway and is disrupted in osm-5 mutant worms. *Development* **128**, 1493-1505.

Hildebrandt, F. and Omram, H. (2001). New insights: nephronophthisis-medullary cystic kidney disease. *Pediatr Nephrol* **16**, 168-76.

Hildebrandt, F. and Otto, E. (2000). Molecular genetics of nephronophthisis and medullary cystic kidney disease. *J Am Soc Nephrol* **11**, 1753-61.

Hildebrandt, F. and Otto, E. (2005). Cilia and centrosomes: a unifying pathogenic concept for cystic kidney disease? *Nat Rev Genet* **6**, 928-40.

Hildebrandt, F. and Zhou, W. (2007). Nephronophthisis-associated ciliopathies. *J Am Soc Nephrol* **18**, 1855-71.

Hori, Y., Kobayashi, T., Kikko, Y., Kontani, K. and Katada, T. (2008). Domain architecture of the atypical Arf-family GTPase Arl13b involved in cilia formation. *Biochem Biophys Res Commun* **373**, 119-24.

Hosking, C. R., Ulloa, F., Hogan, C., Ferber, E. C., Figueroa, A., Gevaert, K., Birchmeier, W., Briscoe, J. and Fujita, Y. (2007). The transcriptional repressor Glis2 is a novel binding partner for p120 catenin. *Mol Biol Cell* **18**, 1918-27.

Hou, X., Mrug, M., Yoder, B. K., Lefkowitz, E. J., Kremmidiotis, G., D'Eustachio, P., Beier, D. R. and Guay-Woodford, L. M. (2002). Cystin, a novel cilia-associated protein, is disrupted in the cpk mouse model of polycystic kidney disease. *J Clin Invest* **109**, 533-40.

Hu, J., Wittekind, S. G. and Barr, M. M. (2007). STAM and Hrs down-regulate ciliary TRP receptors. *Mol Biol Cell* **18**, 3277-89.

Jauregui, A. R. and Barr, M. M. (2005). Functional characterization of the C. elegans nephrocystins NPHP-1 and NPHP-4 and their role in cilia and male sensory behaviors. *Exp Cell Res* **305**, 333-42.

Jauregui, A. R., Nguyen, K. C., Hall, D. H. and Barr, M. M. (2008). The Caenorhabditis elegans nephrocystins act as global modifiers of cilium structure. *J Cell Biol* **180**, 973-88.

Jauregui, A. R., Nguyen, K. C. Q., Hall, D. H. and Barr, M. M. (*in press* 2008). The C. elegans nephrocystins act as global modifiers of cilium structure. *Journal of Cell Biology*.

Keeler, L. C., Marsh, S. E., Leeflang, E. P., Woods, C. G., Sztriha, L., Al-Gazali, L., Gururaj, A. and Gleeson, J. G. (2003). Linkage analysis in families with Joubert syndrome plus oculo-renal involvement identifies the CORS2 locus on chromosome 11p12-q13.3. *Am J Hum Genet* **73**, 656-62.

Khaddour, R., Smith, U., Baala, L., Martinovic, J., Clavering, D., Shaffiq, R., Ozilou, C., Cullinane, A., Kyttala, M., Shalev, S. et al. (2007). Spectrum of MKS1 and MKS3 mutations in Meckel syndrome: a genotype-phenotype correlation. Mutation in brief #960. Online. *Hum Mutat* **28**, 523-4.

Kim, J., Krishnaswami, S. R. and Gleeson, J. G. (2008). CEP290 interacts with the centriolar satellite component PCM-1 and is required for Rab8 localization to the primary cilium. *Hum Mol Genet* **17**, 3796-805.

Kim, Y. S., Kang, H. S. and Jetten, A. M. (2007). The Kruppel-like zinc finger protein Glis2 functions as a negative modulator of the Wnt/beta-catenin signaling pathway. *FEBS Lett* **581**, 858-64.

Kobayashi, T., Gengyo-Ando, K., Ishihara, T., Katsura, I. and Mitani, S. (2007). IFT-81 and IFT-74 are required for intraflagellar transport in C. elegans. *Genes Cells* **12**, 593-602.

Kozminski, K. G., Johnson, K. A., Forscher, P. and Rosenbaum, J. L. (1993). A motility in the eukaryotic flagellum unrelated to flagellar beating. *Proceedings of the National Academy of Sciences of the United States of America* **90**, 5519-23.

Kulaga, H. M., Leitch, C. C., Eichers, E. R., Badano, J. L., Lesemann, A., Hoskins, B. E., Lupski, J. R., Beales, P. L., Reed, R. R. and Katsanis, N. (2004). Loss of BBS proteins causes anosmia in humans and defects in olfactory cilia structure and function in the mouse. *Nat Genet* **36**, 994-8.

Kyttala, M., Tallila, J., Salonen, R., Kopra, O., Kohlschmidt, N., Paavola-Sakki, P., Peltonen, L. and Kestila, M. (2006). MKS1, encoding a component of the flagellar apparatus basal body proteome, is mutated in Meckel syndrome. *Nat Genet* **38**, 155-7.

Leitch, C. C., Zaghloul, N. A., Davis, E. E., Stoetzel, C., Diaz-Font, A., Rix, S., Alfadhel, M., Lewis, R. A., Eyaid, W., Banin, E. et al. (2008). Hypomorphic mutations in syndromic encephalocele genes are associated with Bardet-Biedl syndrome. *Nat Genet* **40**, 443-8.

Lewis, J. A. and Hodgkin, J. A. (1977). Specific neuroanatomical changes in chemosensory mutants of the nematode Caenorhabditis elegans. *J Comp Neurol* **172**, 489-510.

Li, S., Armstrong, C. M., Bertin, N., Ge, H., Milstein, S., Boxem, M., Vidalain, P. O., Han, J. D., Chesneau, A., Hao, T. et al. (2004). A map of the interactome network of the metazoan C. elegans. *Science* **303**, 540-3.

Liu, K. S. and Sternberg, P. W. (1995). Sensory regulation of male mating behavior in Caenorhabditis elegans. *Neuron* **14**, 79-89.

Liu, S., Lu, W., Obara, T., Kuida, S., Lehoczky, J., Dewar, K., Drummond, I. A. and Beier, D. R. (2002). A defect in a novel Nek-family kinase causes cystic kidney disease in the mouse and in zebrafish. *Development* **129**, 5839-46.

Low, S. H., Vasanth, S., Larson, C. H., Mukherjee, S., Sharma, N., Kinter, M. T., Kane, M. E., Obara, T. and Weimbs, T. (2006). Polycystin-1, STAT6, and P100 function in a pathway that transduces ciliary mechanosensation and is activated in polycystic kidney disease. *Dev Cell* **10**, 57-69.

Lu, W., Shen, X., Pavlova, A., Lakkis, M., Ward, C. J., Pritchard, L., Harris, P. C., Genest, D. R., Perez-Atayde, A. R. and Zhou, J. (2001). Comparison of Pkd1-targeted mutants reveals that loss of polycystin-1 causes cystogenesis and bone defects. *Hum Mol Genet* **10**, 2385-96.

Marshall, W. F. (2007). What is the function of centrioles? *J Cell Biochem* **100**, 916-22.

McEwen, D. P., Koenekoop, R. K., Khanna, H., Jenkins, P. M., Lopez, I., Swaroop, A. and Martens, J. R. (2007). Hypomorphic CEP290/NPHP6 mutations result in anosmia caused by the selective loss of G proteins in cilia of olfactory sensory neurons. *Proc Natl Acad Sci U S A* **104**, 15917-22.

Mello, C. C., Kramer, J. M., Stinchcomb, D. and Ambros, V. (1991). Efficient gene transfer in C.elegans: extrachromosomal maintenance and integration of transforming sequences. *EMBO Journal* **10**, 3959-70.

Mochizuki, T., Saijoh, Y., Tsuchiya, K., Shirayoshi, Y., Takai, S., Taya, C., Yonekawa, H., Yamada, K., Nihei, H., Nakatsuji, N. et al. (1998). Cloning of inv, a gene that controls left/right asymmetry and kidney development. *Nature* **395**, 177-81.

Mollet, G., Salomon, R., Gribouval, O., Silbermann, F., Bacq, D., Landthaler, G., Milford, D., Nayir, A., Rizzoni, G., Antignac, C. et al. (2002). The gene mutated in juvenile nephronophthisis type 4 encodes a novel protein that interacts with nephrocystin. *Nat Genet* **32**, 300-5.

Mollet, G., Silbermann, F., Delous, M., Salomon, R., Antignac, C. and Saunier, S. (2005). Characterization of the nephrocystin/nephrocystin-4 complex and subcellular localization of nephrocystin-4 to primary cilia and centrosomes. *Hum Mol Genet* **14**, 645-56.

Morgan, D., Eley, L., Sayer, J., Strachan, T., Yates, L. M., Craighead, A. S. and Goodship, J. A. (2002). Expression analyses and interaction with the anaphase promoting complex protein Apc2 suggest a role for inversin in primary cilia and involvement in the cell cycle. *Hum Mol Genet* **11**, 3345-50.

Moyer, J. H., Lee-Tischler, M. J., Kwon, H. Y., Schrick, J. J., Avner, E. D., Sweeney, W. E., Godfrey, V. L., Cacheiro, N. L., Wilkinson, J. E. and Woychik, R. P. (1994). Candidate gene associated with a mutation causing recessive polycystic kidney disease in mice. *Science* **264**, 1329-33.

Mukhopadhyay, S., Lu, Y., Qin, H., Lanjuin, A., Shaham, S. and Sengupta, P. (2007). Distinct IFT mechanisms contribute to the generation of ciliary structural diversity in C. elegans. *Embo J* **26**, 2966-80.

Murayama, T., Toh, Y., Ohshima, Y. and Koga, M. (2005). The dyf-3 gene encodes a novel protein required for sensory cilium formation in Caenorhabditis elegans. *J Mol Biol* **346**, 677-87.

Murcia, N. S., Richards, W. G., Yoder, B. K., Mucenski, M. L., Dunlap, J. R. and Woychik, R. P. (2000). The Oak Ridge Polycystic Kidney (orpk) disease gene is required for left-right axis determination. *Development* **127**, 2347-55.

Mykytyn, K., Mullins, R. F., Andrews, M., Chiang, A. P., Swiderski, R. E., Yang, B., Braun, T., Casavant, T., Stone, E. M. and Sheffield, V. C. (2004). Bardet-Biedl syndrome type 4 (BBS4)-null mice implicate Bbs4 in flagella formation but not global cilia assembly. *Proc Natl Acad Sci U S A* **101**, 8664-9.

Nachury, M. V., Loktev, A. V., Zhang, Q., Westlake, C. J., Peranen, J., Merdes, A., Slusarski, D. C., Scheller, R. H., Bazan, J. F., Sheffield, V. C. et al. (2007). A Core Complex of BBS Proteins Cooperates with the GTPase Rab8 to Promote Ciliary Membrane Biogenesis. *Cell* **129**, 1201-13.

Nagao, S., Watanabe, T., Ogiso, N., Marunouchi, T. and Takahashi, H. (1995). Genetic mapping of the polycystic kidney gene, pcy, on mouse chromosome 9. *Biochemical Genetics* **33**, 401-12.

Nauta, J., Goedbloed, M. A., Herck, H. V., Hesselink, D. A., Visser, P., Willemsen, R., Dokkum, R. P., Wright, C. J. and Guay-Woodford, L. M. (2000). New rat model that phenotypically resembles autosomal recessive polycystic kidney disease. *Journalof the American Society of Nephrology* **11**, 2272-84.

Nishimura, D. Y., Fath, M., Mullins, R. F., Searby, C., Andrews, M., Davis, R., Andorf, J. L., Mykytyn, K., Swiderski, R. E., Yang, B. et al. (2004). Bbs2-null mice have neurosensory deficits, a defect in social dominance, and retinopathy associated with mislocalization of rhodopsin. *Proc Natl Acad Sci U S A* **101**, 16588-93.

Nonaka, S., Tanaka, Y., Okada, Y., Takeda, S., Harada, A., Kanai, Y., Kido, M. and Hirokawa, N. (1998). Randomization of left-right asymmetry due to loss of nodal cilia generating leftward flow of extraembryonic fluid in mice lacking KIF3B motor protein. *Cell* **95**, 829-37.

Noor, A., Windpassinger, C., Patel, M., Stachowiak, B., Mikhailov, A., Azam, M., Irfan, M., Siddiqui, Z. K., Naeem, F., Paterson, A. D. et al. (2008). CC2D2A, encoding a coiled-coil and C2 domain protein, causes autosomal-recessive mental retardation with retinitis pigmentosa. *Am J Hum Genet* **82**, 1011-8.

Olbrich, H., Fliegauf, M., Hoefele, J., Kispert, A., Otto, E., Volz, A., Wolf, M. T., Sasmaz, G., Trauer, U., Reinhardt, R. et al. (2003). Mutations in a novel gene, NPHP3, cause adolescent nephronophthisis, tapeto-retinal degeneration and hepatic fibrosis. *Nat Genet* **34**, 455-9.

Omran, H., Haffner, K., Burth, S., Fernandez, C., Fargier, B., Villaquiran, A., Nothwang, H. G., Schnittger, S., Lehrach, H., Woo, D. et al. (2001). Human adolescent nephronophthisis: gene locus synteny with polycystic kidney disease in pcy mice. *J Am Soc Nephrol* **12**, 107-13.

Orozco, J. T., Wedaman, K. P., Signor, D., Brown, H., Rose, L. and Scholey, J. M. (1999). Movement of motor and cargo along cilia. *Nature* **398**, 674.

Otto, E., Hoefele, J., Ruf, R., Mueller, A. M., Hiller, K. S., Wolf, M. T., Schuermann, M. J., Becker, A., Birkenhager, R., Sudbrak, R. et al. (2002). A gene mutated in nephronophthisis and retinitis pigmentosa encodes a novel protein, nephroretinin, conserved in evolution. *Am J Hum Genet* **71**, 1161-7.

Otto, E., Kispert, A., Schatzle, Lescher, B., Rensing, C. and Hildebrandt, F. (2000). Nephrocystin: gene expression and sequence conservation between human, mouse, and Caenorhabditis elegans. *J Am Soc Nephrol* **11**, 270-82.

Otto, E. A., Loeys, B., Khanna, H., Hellemans, J., Sudbrak, R., Fan, S., Muerb, U., O'Toole, J. F., Helou, J., Attanasio, M. et al. (2005). Nephrocystin-5, a ciliary IQ domain protein, is mutated in Senior-Loken syndrome and interacts with RPGR and calmodulin. *Nat Genet* **37**, 282-8.

Otto, E. A., Schermer, B., Obara, T., O'Toole, J. F., Hiller, K. S., Mueller, A. M., Ruf, R. G., Hoefele, J., Beekmann, F., Landau, D. et al. (2003). Mutations in INVS encoding inversin cause nephronophthisis type 2, linking renal cystic disease to the function of primary cilia and left-right axis determination. *Nat Genet* **34**, 413-20.

Otto, E. A., Trapp, M. L., Schultheiss, U. T., Helou, J., Quarmby, L. M. and Hildebrandt, F. (2008). NEK8 mutations affect ciliary and centrosomal localization and may cause nephronophthisis. *J Am Soc Nephrol* **19**, 587-92.

Ou, G., Blacque, O. E., Snow, J. J., Leroux, M. R. and Scholey, J. M. (2005). Functional coordination of intraflagellar transport motors. *Nature* **436**, 583-7.

Ou, G., Koga, M., Blacque, O. E., Murayama, T., Ohshima, Y., Schafer, J. C., Li, C., Yoder, B. K., Leroux, M. R. and Scholey, J. M. (2007). Sensory ciliogenesis in Caenorhabditis elegans: assignment of IFT components into distinct modules based on transport and phenotypic profiles. *Mol Biol Cell* **18**, 1554-69.

Parisi, M. A., Bennett, C. L., Eckert, M. L., Dobyns, W. B., Gleeson, J. G., Shaw, D. W., McDonald, R., Eddy, A., Chance, P. F. and Glass, I. A. (2004). The NPHP1 gene deletion associated with juvenile nephronophthisis is present in a subset of individuals with Joubert syndrome. *Am J Hum Genet* **75**, 82-91.

Pazour, G. J., Dickert, B. L., Vucica, Y., Seeley, E. S., Rosenbaum, J. L., Witman, G. B. and Cole, D. G. (2000). Chlamydomonas IFT88 and its mouse homologue, polycystic kidney disease gene Tg737, are required for assembly of cilia and flagella. *Journal of Cell Biology* **151**, 709-18.

Perkins, L. A., Hedgecock, E. M., Thomson, J. N. and Culotti, J. G. (1986). Mutant sensory cilia in the nematode Caenorhabditis elegans. *Developmental Biology* **117**, 456-87.

Piperno, G., Siuda, E., Henderson, S., Segil, M., Vaananen, H. and Sassaroli, M. (1998). Distinct mutants of retrograde intraflagellar transport (IFT) share similar morphological and molecular defects. *Journal of Cell Biology* **143**, 1591-601.

Ponsard, C., Skowron-Zwarg, M., Seltzer, V., Perret, E., Gallinger, J., Fisch, C., Dupuis-Williams, P., Caruso, N., Middendorp, S. and Tournier, F. (2007). Identification of ICIS-1, a new protein involved in cilia stability. *Front Biosci* **12**, 1661-9.

Porter, M. E., Bower, R., Knott, J. A., Byrd, P. and Dentler, W. (1999). Cytoplasmic dynein heavy chain 1b is required for flagellar assembly in Chlamydomonas. *Mol Biol Cell* **10**, 693-712.

Qian, F., Germino, F. J., Cai, Y. Q., Zhang, X. B., Somlo, S. and Germino, G. G. (1997). Pkd1 Interacts With Pkd2 Through a Probable Coiled-Coil Domain. *Nature Genetics* **16**, 179-183.

Qin, H. M., Rosenbaum, J. L. and Barr, M. M. (2001). An autosomal recessive polycystic kidney disease gene homolog is involved in intraflagellar transport in C-elegans ciliated sensory neurons. *Current Biology* **11**, 457-461.

Riddle, D. L., Swanson, M. M. and Albert, P. S. (1981). Interacting genes in nematode dauer larva formation. *Nature* **290**, 668-71.

Roepman, R., Letteboer, S. J., Arts, H. H., van Beersum, S. E., Lu, X., Krieger, E., Ferreira, P. A. and Cremers, F. P. (2005). Interaction of nephrocystin-4 and RPGRIP1 is disrupted by nephronophthisis or Leber congenital amaurosis-associated mutations. *Proc Natl Acad Sci U S A* **102**, 18520-5.

Rosenbaum, J. and Witman, G. (2002). Intraflagellar transport. *Nat Rev Mol Cell Biol* **3**, 813-25.

Ross, A. J., May-Simera, H., Eichers, E. R., Kai, M., Hill, J., Jagger, D. J., Leitch, C. C., Chapple, J. P., Munro, P. M., Fisher, S. et al. (2005). Disruption of Bardet-Biedl syndrome ciliary proteins perturbs planar cell polarity in vertebrates. *Nat Genet* **37**, 1135-40.

Roume, J., Genin, E., Cormier-Daire, V., Ma, H. W., Mehaye, B., Attie, T., Razavi-Encha, F., Fallet-Bianco, C., Buenerd, A., Clerget-Darpoux, F. et al. (1998). A gene for Meckel syndrome maps to chromosome 11q13. *Am J Hum Genet* **63**, 1095-101.

Saar, K., Al-Gazali, L., Sztriha, L., Rueschendorf, F., Nur, E. K. M., Reis, A. and Bayoumi, R. (1999). Homozygosity mapping in families with Joubert syndrome identifies a locus on chromosome 9q34.3 and evidence for genetic heterogeneity. *Am J Hum Genet* **65**, 1666-71.

Sambrook, J., Fritsch, E. F. and Maniatis, T. (1989). *Molecular Cloning: A Laboratory Manual*. Cold Spring Harbor, NY: Cold Spring Harbor Laboratory.

Sayer, J. A., Otto, E. A., O'Toole, J. F., Nurnberg, G., Kennedy, M. A., Becker, C., Hennies, H. C., Helou, J., Attanasio, M., Fausett, B. V. et al. (2006). The centrosomal protein nephrocystin-6 is mutated in Joubert syndrome and activates transcription factor ATF4. *Nat Genet* **38**, 674-81.

Schafer, J. C., Haycraft, C. J., Thomas, J. H., Yoder, B. K. and Swoboda, P. (2003). XBX-1 encodes a dynein light intermediate chain required for retrograde intraflagellar transport and cilia assembly in Caenorhabditis elegans. *Mol Biol Cell* **14**, 2057-70.

Schafer, T., Putz, M., Lienkamp, S., Ganner, A., Bergbreiter, A., Ramachandran, H., Gieloff, V., Gerner, M., Mattonet, C., Czarnecki, P. G. et al. (2008a). Genetic and physical interaction between the NPHP5 and NPHP6 gene products. *Hum Mol Genet* **17**, 3655-62.

Schafer, T., Putz, M., Lienkamp, S., Ganner, A., Bergbreiter, A., Ramachandran, H., Gieloff, V., Gerner, M., Mattonet, C., Czarnecki, P. G. et al. (2008b). Genetic and physical interaction between the NPHP5 and NPHP6 gene products. *Hum Mol Genet*.

Schermer, B., Hopker, K., Omran, H., Ghenoiu, C., Fliegauf, M., Fekete, A., Horvath, J., Kottgen, M., Hackl, M., Zschiedrich, S. et al. (2005). Phosphorylation by casein kinase 2 induces PACS-1 binding of nephrocystin and targeting to cilia. *Embo J* **24**, 4415-24.

Scholey, J. M. (2003). Intraflagellar transport. *Annu Rev Cell Dev Biol* **19**, 423-43.

Scholey, J. M., Ou, G., Snow, J. and Gunnarson, A. (2004). Intraflagellar transport motors in Caenorhabditis elegans neurons. *Biochem Soc Trans* **32**, 682-4.

Senti, G. and Swoboda, P. (2008). Distinct isoforms of the RFX transcription factor DAF-19 regulate ciliogenesis and maintenance of synaptic activity. *Mol Biol Cell* **19**, 5517-28.

Sepulveda, W., Sebire, N. J., Souka, A., Snijders, R. J. and Nicolaides, K. H. (1997). Diagnosis of the Meckel-Gruber syndrome at eleven to fourteen weeks' gestation. *Am J Obstet Gynecol* **176**, 316-9.

Shillingford, J. M., Murcia, N. S., Larson, C. H., Low, S. H., Hedgepeth, R., Brown, N., Flask, C. A., Novick, A. C., Goldfarb, D. A., Kramer-Zucker, A. et al. (2006). The mTOR pathway is regulated by polycystin-1, and its inhibition reverses renal cystogenesis in polycystic kidney disease. *Proc Natl Acad Sci U S A* **103**, 5466-71.

Signor, D., Wedaman, K. P., Rose, L. S. and Scholey, J. M. (1999). Two heteromeric kinesin complexes in chemosensory neurons and sensory cilia of Caenorhabditis elegans. *Molecular Biology of the Cell* **10**, 345-60.

Simons, M., Gloy, J., Ganner, A., Bullerkotte, A., Bashkurov, M., Kronig, C., Schermer, B., Benzing, T., Cabello, O. A., Jenny, A. et al. (2005). Inversin, the gene product mutated in nephronophthisis type II, functions as a molecular switch between Wnt signaling pathways. *Nat Genet* **37**, 537-43.

Smith, L. A., Bukanov, N. O., Husson, H., Russo, R. J., Barry, T. C., Taylor, A. L., Beier, D. R. and Ibraghimov-Beskrovnaya, O. (2006a). Development of polycystic kidney disease in juvenile cystic kidney mice: insights into pathogenesis, ciliary abnormalities, and common features with human disease. *J Am Soc Nephrol* **17**, 2821-31.

Smith, U. M., Consugar, M., Tee, L. J., McKee, B. M., Maina, E. N., Whelan, S., Morgan, N. V., Goranson, E., Gissen, P., Lilliquist, S. et al. (2006b). The transmembrane protein meckelin (MKS3) is mutated in Meckel-Gruber syndrome and the wpk rat. *Nat Genet* **38**, 191-6.

Snell, W. J. (1984). The role of cilia and flagella in cell interactions. *Journal of Protozoology* **31**, 12-6.

Sohara, E., Luo, Y., Zhang, J., Manning, D. K., Beier, D. R. and Zhou, J. (2008). Nek8 regulates the expression and localization of polycystin-1 and polycystin-2. *J Am Soc Nephrol* **19**, 469-76.

Sorokin, S. P. (1968). Reconstructions of centriole formation and ciliogenesis in mammalian lungs. *Journal of Cell Science* **3**, 207-30.

Starich, T. A., Herman, R. K., Kari, C. K., Yeh, W. H., Schackwitz, W. S., Schuyler, M. W., Collet, J., Thomas, J. H. and Riddle, D. L. (1995). Mutations affecting the chemosensory neurons of Caenorhabditis elegans. *Genetics* **139**, 171-88.

Stoetzel, C., Muller, J., Laurier, V., Davis, E. E., Zaghloul, N. A., Vicaire, S., Jacquelin, C., Plewniak, F., Leitch, C. C., Sarda, P. et al. (2007). Identification of a novel BBS gene (BBS12) highlights the major role of a vertebrate-specific branch of chaperonin-related proteins in Bardet-Biedl syndrome. *Am J Hum Genet* **80**, 1-11.

Swoboda, P., Adler, H. T. and Thomas, J. H. (2000). The RFX-type transcription factor DAF-19 regulates sensory neuron cilium formation in C.elegans. *Mol. Cell* **5**, 411-421.

Takahashi, H., Ueyama, Y., Hibino, T., Kuwahara, Y., Suzuki, S., Hioki, K. and Tamaoki, N. (1986). A new mouse model of genetically transmitted polycystic kidney disease. *Journal of Urology* **135**, 1280-3.

Tallila, J., Jakkula, E., Peltonen, L., Salonen, R. and Kestila, M. (2008). Identification of CC2D2A as a Meckel syndrome gene adds an important piece to the ciliopathy puzzle. *Am J Hum Genet* **82**, 1361-7.

Taulman, P. D., Haycraft, C. J., Balkovetz, D. F. and Yoder, B. K. (2001). Polaris, a protein involved in left-right axis patterning, localizes to basal bodies and cilia. *Molecular Biology of the Cell* **12**, 589-99.

Tobin, J. L. and Beales, P. L. (2007). Bardet-Biedl syndrome: beyond the cilium. *Pediatr Nephrol* **22**, 926-36.

Torres, V. E., Harris, P. C. and Pirson, Y. (2007). Autosomal dominant polycystic kidney disease. *Lancet* **369**, 1287-301.

Town, T., Breunig, J. J., Sarkisian, M. R., Spilianakis, C., Ayoub, A. E., Liu, X., Ferrandino, A. F., Gallagher, A. R., Li, M. O., Rakic, P. et al. (2008). The stumpy gene is required for mammalian ciliogenesis. *Proceedings of the National Academy of Sciences* **105**, 2853-2858.

Trapp, M. L., Galtseva, A., Manning, D. K., Beier, D. R., Rosenblum, N. D. and Quarmby, L. M. (2008). Defects in ciliary localization of Nek8 is associated with cystogenesis. *Pediatr Nephrol* **23**, 377-87.

Tsiokas, L., Kim, E., Arnould, T., Sukhatme, V. P. and Walz, G. (1997). Homo- and heterodimeric interactions between the gene products of PKD1 and PKD2. *Proceedings of the National Academy of Sciences of the United States of America* **94**, 6965-70.

Wang, Q., Pan, J. and Snell, W. J. (2006). Intraflagellar transport particles participate directly in cilium-generated signaling in Chlamydomonas. *Cell* **125**, 549-62.

Ward, S., Thomson, N., White, J. G. and Brenner, S. (1975). Electron microscopical reconstruction of the anterior sensory anatomy of the nematode Caenorhabditis elegans. *Journal of Comparative Neurology* **160**, 313-37.

Ware R., W., Clark, D., Crossland, K. and Russell, R., L. (1975). The nerve ring of the neamtode Caenorhabditis elegans: sensory input and motor out. *Journal of Comparative Neurology* **162**, 71-110.

Wicks, S. R., de Vries, C. J., van Luenen, H. G. and Plasterk, R. H. (2000). CHE-3, a cytosolic dynein heavy chain, is required for sensory cilia structure and function in Caenorhabditis elegans. *Dev Biol* **221**, 295-307.

Williams, C. L., Winkelbauer, M. E., Schafer, J. C., Michaud, E. J. and Yoder, B. K. (2008). Functional Redundancy of the B9 Proteins and Nephrocystins in Caenorhabditis elegans Ciliogenesis. *Mol Biol Cell* **19**, 2154-2168.

Wilson, P. D. (2004). Polycystic kidney disease. *N Engl J Med* **350**, 151-64.

Winkelbauer, M. E., Schafer, J. C., Haycraft, C. J., Swoboda, P. and Yoder, B. K. (2005). The C. elegans homologs of nephrocystin-1 and nephrocystin-4 are cilia transition zone proteins involved in chemosensory perception. *J Cell Sci* **118**, 5575-87.

Wu, G., V, D. A., Cai, Y., Markowitz, G., Park, J. H., Reynolds, D. M., Maeda, Y., Le, T. C., Hou, H., Jr., Kucherlapati, R. et al. (1998). Somatic inactivation of Pkd2 results in polycystic kidney disease. *Cell* **93**, 177-88.

Yoder, B. K., Hou, X. and Guay-Woodford, L. M. (2002). The polycystic kidney disease proteins, polycystin-1, polycystin-2, polaris, and cystin, are co-localized in renal cilia. *J Am Soc Nephrol* **13**, 2508-16.

Yoder, B. K., Richards, W. G., Sweeney, W. E., Wilkinson, J. E., Avener, E. D. and Woychik, R. P. (1995). Insertional mutagenesis and molecular analysis of a new gene associated with polycystic kidney disease. *Proceedings of the Association of American Physicians* **107**, 314-23.

Zhang, F., Nakanishi, G., Kurebayashi, S., Yoshino, K., Perantoni, A., Kim, Y. S. and Jetten, A. M. (2002). Characterization of Glis2, a novel gene encoding a Gli-related, Kruppel-like transcription factor with transactivation and repressor functions. Roles in kidney development and neurogenesis. *J Biol Chem* **277**, 10139-49.